EVALUATING SHEAR MOBILIZATION IN ROCKFILL COLUMNS USED FOR RIVERBANK STABILIZATION

by

CHANG SEOK KIM

A Thesis
Submitted to the Faculty of Graduate Studies
in Partial Fulfillment of the Requirements for the Degree of

MASTER OF SCIENCE

Department of Civil Engineering
University of Manitoba
Winnipeg, Manitoba

June, 2007

THE UNIVERSITY OF MANITOBA

FACULTY OF GRADUATE STUDIES

*****

COPYRIGHT PERMISSION

EVALUATING SHEAR MOBILIZATION IN ROCKFILL COLUMNS USED FOR RIVERBANK STABILIZATION

BY

CHANG SEOK KIM

A Thesis/Practicum submitted to the Faculty of Graduate Studies of The University of Manitoba in partial fulfillment of the requirement of the degree

MASTER OF SCIENCE

ABSTRACT

The City of Winnipeg has four primary rivers with over 240 km of waterfront property. The rivers are founded in the historic glacial Lake Agassiz clay and silt sediments that are relatively weak with low shear strength. As such, riverbank instabilities are a common issue along many stretches of the major rivers within the City. The use of rockfill columns has become an increasingly utilized approach for stabilizing failing banks.

Recent cases in Winnipeg have shown that movements can occur following installation of rockfill columns. Uncertainty regarding the magnitude of these movements required to mobilize shearing resistance in the rockfill columns has resulted in situations where stability of riverbanks following remediation has been questioned. This has provided a need to improve our understanding about how much movement a stabilized slope must undergo before sufficient shear resistance of the rockfill column will be mobilized.

Large-scale direct shear tests have been conducted on rockfill materials, undisturbed clays, and rockfill-clay composite soil samples to investigate the mobilization of shear resistance of rockfill column materials. The effects of cemented rockfill materials and various area replacement ratios were investigated in laboratory tests. Rockfill columns in group were conducted with different spacing patterns, and the results were compared with those from shear key and ribbed type layouts.

The results from large-scale direct shear tests were used to develop a numerical model using commercially available computer software FLAC (Fast Lagrangian Analysis of Continua) as the modelling platform. The numerical model was then used to study the performance of a riverbank with and without rockfill columns. Factors of safety were

calculated using the FLAC program and compared with those obtained from GeoStudio 2004 and Phase2.0.

This document presents results of experimental testing carried out to assess the shear mobilization of rockfill column materials using a large-scale direct shear test apparatus. Results from large-scale direct shear tests present understanding of the stress-strain characteristics of native soil, rockfill material, and the rockfill-clay composite to be able to provide appropriate analysis, design, and construction methods for stabilizing riverbanks using rockfill columns. Results from numerical simulations show that for a natural riverbank the factor of safety is close to unity from FLAC, GeoStudio 2004 and Phase2.0 computer programs. For a stabilized riverbank, by increasing vertical displacement at the crest or at the toe up to 5 cm the mobilized shear resistance of rockfill material increases the mobilized factor of safety and reduces the deformations of the stabilized riverbank.

ACKNOWLEDGEMENT

I would like to thank my supervisor, Dr. Marolo C. Alfaro who has provided me with valuable supervision and encouragement. His advice and suggestions have been very helpful for the project.

I wish to acknowledge Dr. James Blatz for helping me in all aspects. I would like to thank all graduate students and staffs in our geotechnical group. In particular, I would like to thank Deni G. Priyanto and Michael Van Helden for their help in my early numerical modelling. Special thanks are extended to my best friends in Winnipeg.

Financial and logistical supports were provided by the City of Winnipeg, KGS Group, AMEC, UMA, Subterranean Ltd., and NSERC.

Most importantly, I would like to express sincere thanks and love to my parents and all other family members for their love, encouragement, interest, and support. All that I have achieved is truly because of them.

TABLE OF CONTENTS

NOTATIONS

A_c	Horizontal area of clayey ground surrounding the pile
A_s	Horizontal area of a granular pile
a_s	Area replacement ratio
B_g	Breakage factor
c^{trial}	Trial cohesion
D	Diameter
D_{50}	Average particle diameter
D_e	Effective diameter
E	Modulus of elasticity
e	Void ratio
FS	Factor of safety
F^{trial}	Trial factor of safety
FS_{mob}	Mobilized factor of safety
G	Shear modulus
G_s	Specific gravity
LI	Liquidity index
LL	Liquid limit
LVDT	Linear variable displacement transducer
N	Normal load
n	Porosity
PI	Plasticity index
PL	Plastic limit
S	Spacing of granular piles

s_u	Undrained shear strength
T	Shear load
δ_{he}	Horizontal strain at the edge of circular cross section
δ_{hm}	Horizontal strain in the middle of circular cross section
δl	Shear displacement
ε_s	Horizontal shear strain
ε_v	Volumetric strain
ϕ'	Generic friction angle
ϕ'_{cs}	Critical state friction angle
ϕ'_{mob}	Mobilized friction angle
ϕ'_p	Peak friction angle
ϕ'_r	Residual friction angle
$\phi'_{transition}$	Transition friction angle
ϕ^{trial}	Trial friction angle
γ_{zx}	Shear strain
μ_s	Ratio of vertical stresses in the rockfill column to the average stress over the tributary area
μ_c	Ratio of vertical stresses in the clay to the average stress over the tributary area
ν	Poisson ratio
ρ^{wet}	Wet in-situ density of a soil
ρ_w	Water density
σ	Normal stress

σ_c	Stress in the surrounding soil
σ_s	Stress in the granular pile
τ	Shear stress
τ_{av}	Average shear strength
τ_{cs}	Critical state shear strength
τ_f	Shear strength at failure
τ_p	Peak shear strength
$\tau_{i,mob}$	Mobilized shear stress at an i location
$\tau_{i,app}$	Applied or driving shear stress at an i location

LIST OF FIGURES

LIST OF COPYRIGHTED MATERIAL WITH PERMISSION

UNIVERSITY of MANITOBA

Faculty of Graduate Studies
500 University Centre
Winnipeg, Manitoba R3T 2N2

PERMISSION TO USE COPYRIGHTED MATERIAL

Date: April 13, 2007

Student Name: CHANG SEOK KIM

Student Address: 436-99 DALHOUSIE DRIVE

WINNIPEG, MB. R3T 3M2

I, CHANG SEOK KIM , a graduate student at The University of Manitoba, request permission to quote/reproduce the material listed below in preparation of my thesis/practicum for the degree of MASTER OF SCIENCE .

My thesis/practicum will be microfiched by Library and Archives Canada (LAC). A microfiche copy of the theses/practicum will be available for loan from LAC, and will be reproduced and sold in various formats through LAC's agent, University Microfilms International (UMI). My thesis/practicum may also be submitted in an electronic format to The University of Manitoba, and be accessible to a worldwide audience from both the University of Manitoba's and LAC's Theses Canada (www.collectionscanada.ca/thesescanada) websites. I would be very grateful for your favourable consideration of this request.

Title of article / book: Landslide problems in Winnipeg

Page numbers: 391

Title and number of image: Identified active and inactive slide locations along Winnipeg riverbanks

Publisher and year: 1981

Journal name, issue number: Canadian Geotechnical Journal, No.3

Authorization is granted to the above named graduate student, The University of Manitoba and Library and Archives Canada and their associates to reproduce excerpts from the following in their thesis /practicum:

Signature of author or copyright holder(s): _____

_____

Please print name(s): Please see the attached paper

Title (s):

Date:

Please return this signed form to the address noted above.

Chang Seok Kim

From: Landriault, Roxanne [Roxanne.Landriault@nrc-cnrc.gc.ca] on behalf of CISTI, Research Press Business [ResearchPressBusiness.CISTI@nrc-cnrc.gc.ca]
Sent: April 13, 2007 2:09 PM
To: corechang@hotmail.com
Cc: Landriault, Roxanne
Subject: RE: Permission to Reproduce Article

Permission is granted for use of the material, as described below, provided that acknowledgement is given to the source.

Sincerely

Mike Boroczki

Business Manager

NRC Research Press

Tel: 613-993-9108

Fax: 613-952-7656

-----Original Message-----
From: rp.business@nrc.ca [mailto:rp.business@nrc.ca]
Sent: 04/13/2007 12:29 PM
To: CISTI, Research Press Business
Subject: Permission to Reproduce Article

Below is the result of your feedback form. It was submitted by
(rp.business@nrc.ca) on Friday, April 13, 2007 at 12:28:49

LIST OF TABLES

CHAPTER 1

INTRODUCTION

1.1 INTRODUCTION

It has been observed that failure geometry of riverbanks incorporates a long flat horizontal portion, parallel to the bedding, in a weak clay stratum above the hard stratum. These riverbank failures occur generally in the layer of brown and grey plastic clays, which are deep-seated extending 12 to 15 metres below the ground surface. Clay banks will typically move to achieve overall gradients in the order 6H:1V to 9H:1V when, at that stage a state of quasi-equilibrium established (Baracos and Graham 1981). Figure 1.1 shows identified active and inactive slide locations along Winnipeg riverbanks. A number of factors can reactivate these previously unstable banks, thereby triggering more extensive movements. The principal factors controlling riverbank failure include groundwater conditions in the clay and independent underlying till, river hydraulics and progressive soil weakening.

Rockfill columns, also known as stone columns or rock caissons, have become an established technique for riverbank stabilization in the City of Winnipeg for the past 10 years (City of Winnipeg 2000, Yarechewski and Tallin 2003). Rockfill columns are large diameter holes drilled through the clay into the underlying till and filled with crushed rocks or stones. The rockfill columns are generally located in the mid bank or lower bank area of unstable riverbanks. Studies by Goughnour et al. (1991), Yarechewski and Tallin

(2003) have shown the successful use of rockfill columns for both stabilization of natural slopes and decrease of displacement rate.

In spite of cases reporting relatively successful stabilization of slopes, they have shown that movements generally occurred following installation of rockfill columns. This post-construction movement is expected to mobilize the shear resistance in the rockfill. Uncertainty regarding the magnitude of movements required to mobilize shearing resistance in rockfill columns has resulted in situations where stability of riverbanks and slopes following remediation has been questioned. This has provided a need to improve understanding regarding anticipated displacements of remediated slopes to develop sufficient shear resistance in rockfill columns. Additionally, understanding shear mobilization of the rockfill provides a basis of how to improve material specifications and installation procedures to minimize post-construction displacements.

The mobilization of shear resistance for granular materials such as crushed rocks is highly dependent on the shear displacement and applied normal stress at the location of the failure plane. A proper evaluation of the shear resistance mobilization in the rockfill columns and the rockfill-clay composite soil will improve the assessment of rockfill column performance. In addition to the physical requirement for movement to mobilize shearing resistance in rockfill columns, the method of installation can also impact the compliance of the system and therefore the movements required for shear mobilization. These questions are the basis of the objectives of this research.

1.2 OBJECTIVES OF RESEARCH

The objectives of the research include the following:

1. To assess the displacements required to mobilize shear resistance in rockfill columns.
2. To assess the mobilization of shear resistance of the rockfill column in rockfill-clay composite soil.
3. To compare the performance between rockfill columns and cemented rockfill columns for riverbank stabilization.
4. To compare the influence of different spacing of rockfill columns in a group.
5. To compare numerical simulations with results of laboratory experiments and to assess the performance of the riverbank stabilized with rockfill columns.

These objectives require three major tasks. The first task is to conduct comprehensive laboratory tests using large scale direct shear apparatus and determine the mobilized shear resistance of rockfill columns in rockfill-large undisturbed clay composite soil samples. The second task is to develop and simulate a numerical model of shear mobilization for rockfill materials, clay, and rockfill-clay composites. The final task is to evaluate the performance of typical Winnipeg riverbanks before and after installation of rockfill columns.

1.3 ORGANIZATION OF THESIS

This thesis consists of total 7 Chapters. After the introduction in Chapter 1, Chapter 2 presents a literature review of properties of Winnipeg soil units, slope stability problems in Lake Agassiz clays, rockfill columns or stone columns as a ground improvement technique, and numerical methods of slope stability analysis. Chapter 3 explains laboratory testing programs undertaken in this research. Details of testing materials and procedures with various testing conditions are discussed. Results and discussion are presented in Chapter 4. Stress-strain characteristics of rockfill, native clay, rockfill-clay composite soils, cemented rockfill columns, and rockfill columns in groups are presented and discussed. Chapter 5 presents procedures and results of numerical simulation of direct shear tests. The numerical results are compared with the experimental results. In Chapter 6, slope stability analyses for a typical Winnipeg riverbank with and without rockfill columns are discussed. Finally, Chapter 7 provides conclusions of the research program from both experiments and numerical analyses and recommendations for further studies.

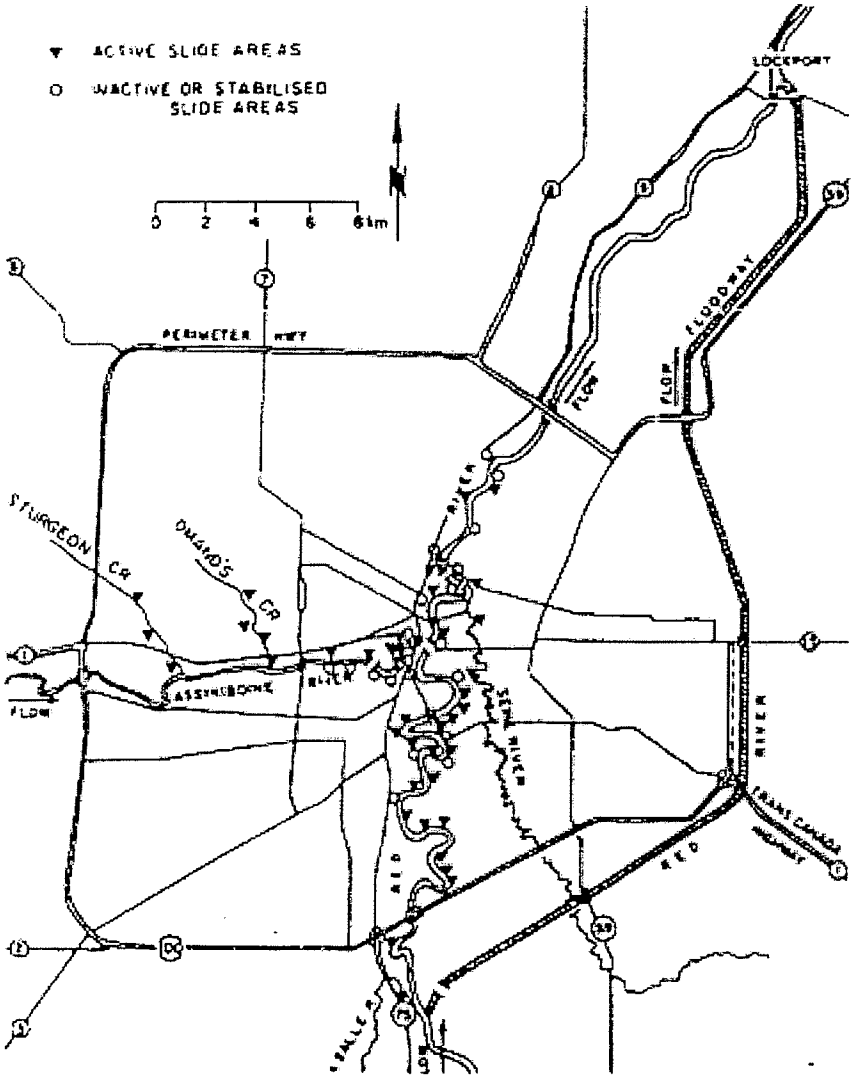

Figure 1.1 Identified active and inactive slide locations along Winnipeg riverbanks (Baracos and Graham, 1981)

*Permission for reuse granted, see List of Copyrighted Materials for which Permission was Obtained

CHAPTER 2

LITERATURE REVIEW

2.1 INTRODUCTION

Riverbank instabilities along the rivers have been the major issue within the City of Winnipeg since the 1950 flood. Slope instability problems are associated with the properties of the lacustrine clays underlying Winnipeg. A number of researchers have studied the properties of the lacustrine clays and slope instability problems. These include Baracos et al. (1983), Baracos (1977 and 1978), Mishtak (1964), Quigley (1980), and Teller (1976). This chapter presents a review of literature on the following aspects:

- Properties of stratigraphic units
- Slope stability problems in Lake Agassiz Clays
- Rockfill or stone columns as a slope stabilization technique
- Methods of slope stability analysis

2.2 PROPERTIES OF WINNIPEG SOILS

For geotechnical purposes, the stratigraphy of the Winnipeg area is divided into four layers. These layers are bedrock, glacial tills consisting of basal till and locally waterlaid till, plastic glaciolacustrine clay, and an upper complex zone of sands, silts, clays, organic soils and urban fill. Each of these layers has different geotechnical behaviour affected by its depositional and post-depositional geologic environment (Baracos et al.

1983). The next following sections will provide more details of the geotechnical properties of each layer.

2.2.1 Upper complex zone

The upper complex zone, typically 3 m thick, consists of sands, highly variable silty clay, silts, organic soils and urban fill. It varies from less than 1 m to 4.5 m. The laminated silty clays are medium-highly plastic (I_p = 20 - 40%) and heavily fissured with a nuggety structure of less than 25 mm size (Baracos et al. 1983). This complex zone represents later post-glacial and recent depositional environments. The silt is interlaid with up to 3 m thickness and varies its thickness over short distances. The irregularity and volume change potential of the interlayers cause strong swelling problems and major problems with house foundations (Baracos et al. 1983, Graham and Au 1985).

2.2.2 Glaciolacustrine clays

Lake Agassiz has been formed from many glacier-dammed lakes that occupied the Red River Valley and the lowlands to the north during late Wisconsinan and early Holocene time. It was the largest lake in North America at its maximum size. Lake Agassiz water covered about 521,000 km^2 although its maximum size at any one time was never more than 208,000 km^2. All lacustrine materials of Lake Agassiz were deposited until the ice sheet began its final retreat and drained into Hudson Bay about 13,500 years ago (Teller 1975). It has been approximately 5,000 years since layered plastic clays and silts were deposited in the Lake Agassiz basin. The thickness of the plastic clay ranges from zero to 20 m with an average thickness of 9 to 13 m. The deposit consists of typically a layer of brown clay, (blue) grey clay, and grey plastic clay from the ground surface downwards.

The thickness of each layer varies up to 4.9 m, 6.1 m, and 1 to 2 m, respectively (Freeman and Sutherland 1974).

The upper brown clay, 1.5 to 6 m thick, has been weathered and oxidized resulting in a brown to mottled grey-brown color. The brown clay consists of alternating layers of clay-rich and silt-rich layers which are typically 2 mm thick, with fissures and joints that sometimes extend to the till surface (Baracos, 1977). It is considered to be overconsolidated by fissuring and by a nuggety structure developed by drying-wetting and freeze-thaw cycles (Graham and Au 1985). Both brown and blue clays are freshwater lacustrine deposits, but the difference in colour between these clays is due to the degree of oxidation which decreases from the ground surface downwards (Baracos and Graham 1980). The blue clay is medium to highly plastic, and has few fissures containing numerous pockets of grey silt, pebbles, and occasional cobbles (Baracos et al. 1980).

The deposits of lower grey clay are coarser and more massively bedded than the upper layers (Baracos et al. 1983). The grey clay often contains ice-rafted rock fragments with range of sizes up to boulder size, and uncemented silt inclusions deposited in the clays (Baracos 1977, Baracos et al. 1983). The grey plastic clay located at the bottom several feet of the grey clay layer has very high moisture content with a low shear strength. This layer is considered not as a separate layer, but as a transitional layer from the clay to the underlying till (Freeman and Sutherland 1974). The geotechnical properties of glaciolacustrine clay are summarized in Table 2.1 (Baracos et al. 1983).

2.2.2.1 Mineralogy

Teller (1975) reported that the clay mineral content of Lake Agassiz clays had little variation. Regarding the mineral content of the clays, there are two separate components as shown in Table 2.2. In the clay component, smectite or montmorillonite and illite typically comprise more than 55 %, and kaolinite comprises more than 25% (Last 1974). Among this mineral content, the montmorillonite contributes notably high plasticity and high swelling potential in the clays (Baracos 1977).

In non-clay part, dolomite, calcite, quartz, and some feldspar are the main non-clay minerals analyzed by the diffraction tracings, and they show up very strongly in the inclusions, light coloured marbling veins (Baracos 1977). From the uniformity of clay mineralogy and Cretaceous shales widespread around the areas, it is concluded that the origin of the Lake Agassiz clays was the Cretaceous shale (Teller 1974).

2.2.2.2 Shear strength of Lake Agassiz clays

Studies of the strength properties of lacustrine clays have been conducted by a number of researchers since the 1950 flood. The first study by Mishtak (1964) was carried out to protect Winnipeg area against flooding. In the study, clay samples were taken from a depth of 9.1m near the site of the proposed trench, and were tested in both drained and consolidated-undrained conditions using triaxial equipment. The effective shear strength parameters determined at low confining pressures were $c' = 45$ kPa, $\phi' = 12°$ for consolidated-undrained tests, and $c' = 31$ kPa, $\phi' = 16.5°$ for drained tests. Crawford (1964) conducted triaxial tests with the same samples. In his consolidated-undrained

tests, the effective stress values were c' = 59 kPa, ϕ' = 9°. Crawford (1964) also performed tests for the influence of softening on shear strength. Two specimens were immersed in de-aired water for several hours before testing. This pre-treatment caused a considerable reduction in shear strength under low stresses.

Another study by Freeman and Sutherland (1973) was carried out to investigate shear strength anisotropy of Winnipeg clays. Specimens were trimmed with various orientations denoted by the angle of inclination between the axis of the specimen and the insitu vertical direction. Triaxial tests in drained and undrained conditions were conducted with pore water pressure measurement on specimens. The confining pressures were in the working stress range between 0 and 200 kPa. It was found that the effective shear strength across the layers was greater than the effective shear strength along the layers. The range of effective shear strength values across the layers for the brown clay was c' = 42 kPa, ϕ' = 19°, and c' = 11 kPa, ϕ' = 18 - 26° for the grey clay. On the other hand, the effective shear strengths along the layers for the brown clay were significantly reduced to c' = 3 kPa, ϕ' = 14°, and c' = 2 - 5 kPa, ϕ' = 14 - 26° for the grey clay. This study indicates that the shear strengths of clays are affected by their fabrics.

The influence of clay fabric on shear strengths was examined by Loh and Holt (1974) conducting unconfined compression tests with block samples obtained from a depth between 4.9 m and 12.2 m below the ground surface at the Student Union Building of the University of Manitoba. The block samples were classified as laminated brown clay and contained silt inclusions, occasional gypsum intrusions, and small pebbles. Both undisturbed and remoulded specimens were trimmed at the same angle and tested. The

test results shown in Figure 2.1 confirmed the results of Freeman and Sutherland (1974) and indicated that the undisturbed specimens had anisotropic strength behaviour while the remoulded specimens had isotropic strength behaviour. The highest and lowest shear strengths occurred from specimens with inclined angle of 82° and 45° respectively. It was also found that when failure occurred in the bedding plane, the shear stress acting on the observed failure plane was almost independent of the inclined angle.

Baracos et al. (1980) reported more solid details about both the stress-strain and strength properties of the Winnipeg grey clay taken from 6 to 12 m depth at the University of Manitoba campus. Preconsolidation pressures of the grey clay samples at different depths were determined by oedometer tests. Figure 2.2 shows preconsolidation pressures of the grey clay at different depths. A series of consolidated undrained triaxial tests with pore-water pressure measurement were also conducted to investigate the influence of overconsolidation or normal consolidation on stress-strain-porewater pressure behaviour. The test results indicated that the effective shear strength parameters were dependent on stress levels and could be divided into three linear sections as shown in Figure 2.3. In the first section, the effective shear strength values have low $c' = 6$ kPa and high $\phi' = 31.5°$ at low effective stresses. The fissured structure of the clay results in the low strength values in this section. In the second section, it has higher $c' = 33$ kPa and lower $\phi' = 13°$ than those in the first section and shows overconsolidation behaviour at intermediate effective stresses, while at high effective stresses, it shows normally consolidated behaviour with the shear strength properties of $c' = 3$ kPa and $\phi' = 22.5°$.

Any geotechnical processes such as softening and freeze-thaw cycling will disturb the mechanical properties of the clay. A study by Graham (1985) showed the influence of those processes for the behaviour and structure of Winnipeg clays. Block samples of "undisturbed" Lake Agassiz clay were taken from 8.2 to 8.5 m and 11.5 m depth at the University of Manitoba campus. The samples were medium to highly plastic (CH), had medium-stiff to stiff consistency, and contained numerous pockets of grey silt, pebbles, and cobbles. Before shearing, the samples were subjected to five freeze-thaw cycles. Freezing was at -5 or -25, and the freeze-thaw cycling lasted 1 - 4 days. The other group of samples was first allowed to swell to equilibrium in triaxial cells under low stresses. The influence of freeze-thaw cycling resulted in heavily fissured brown clay, and also pore water pressure generated due to the collapsible nature of the clay structure compared to the value for undisturbed clay. Softening significantly reduced the preconsolidation pressure of undisturbed clay. This study showed that the shear strength of the clay at shallow depths is affected by previous frost action and groundwater.

2.2.3 Glacial tills

Till units in Winnipeg area are deposits from a variety of glacial materials deposited between 12,000 and 24,000 years ago during a complex series of readvances and retreats of the continental ice in the late Wisconsinan glaciation (Teller and Fenton 1980). The till units consist of five separate till units, and their thicknesses vary from 0 to 10 m with an average of 3 - 6 m. The glacial tills consist of rockflour, silt, sand gravel and boulders, and are often found in a hard cemented condition overlying limestone bedrock at deep depths (Baracos 1978). The stiffness and composition of the till units varies from soft clayey tills to very dense cemented tills known as "hardpan" (Baracos 1960, Baracos et al. 1983, Teller and Fenton 1980).

The till units may be classified by their moisture contents which are only 4 - 6 percent in some of the lowest tills, but increase up to 15 percent in some tills overlaid by clay. The lower units are dense to very dense, well graded basal tills with various particle sizes from clay to boulder-size. A summary of the typical geotechnical properties in Winnipeg tills is presented in Table 2.3.

The dense tills have hairline fractures and irregular seams of silt and gravel that affect their permeability. The upper tills are believed to be waterlaid tills deposited during the earliest stages of Lake Agassiz and are irregularly loose or soft with both fewer cobbles and boulders (Baracos et al. 1983). The upper soft tills have unconfined compression strengths of less than 48 kPa and are mixed with the overlying few feet of grey clay in many areas (Baracos 1960).

2.3 SLOPE STABILITY PROBLEMS IN LAKE AGASSIZ CLAYS

The stability of slopes in the Winnipeg area has been studied by many researchers. The difficulty in analysing slope stability in this area has been related to the use of appropriate strength parameters and failure surfaces. In a number of cases stability analyses using shear strength parameters determined by laboratory tests have indicated that factors of safety greater than unity, yet there have been slope failures. For this reason, many studies have been carried out to resolve the discrepancies between the results of slope stability analysis using laboratory determined parameters and field performance.

In the 1950 flood, a series of riverbank failures were investigated by Baracos (1960). It was found that the average mobilized undrained shear strength, s_u in Winnipeg

riverbanks was between 19 and 29 kPa, which was only a half or one-third of undrained shear strength of Winnipeg clays measured in laboratory tests. These values were used successfully for the design of secondary flood protection dykes on restricted sites between the houses and the river. The factor of safety was as low as 1.2.

Baracos (1960) explained the reasons of using the reduced strength:

- lower strengths along old failure surfaces covered by surfacing weathering and vegetation
- low observed strengths near the toe of the bank which were not fully considered for analysis
- inadequate consideration of the role of tension cracks
- low shear strengths along the contact between lacustrine clay and till

The lower shear strength of about 14 to 24 kPa was used for old failure zones in the total analysis. It was also mentioned that many slides had large components of horizontal movement and that some included retrogressive movements.

Mishtak (1964) performed extensive geotechnical and hydrogeologic investigations for construction of the Red River Floodway. A large scale test of trench excavation along the floodway route was performed to examine the stability of clay slopes after rapid excavation and drawdown. The trench was excavated using side slopes of the trench, which were 1H:1V in the north slope and 4H:1V in the south slope. Alignment hubs and slope indicators were used to observe slope movement. Small movement of the 1H:1V slope was measured when the excavation reached a depth of 7.5 m while no opening or crack was observed. When it reached a depth of 10.4 m, the first definite movement occurred at 14.6 m. After completion of the trench excavation test, a rapid drawdown test

was simulated in the trench. During the winter the trench was filled with water, and then pumped out in the fall and showed the entire 1H:1V slope failure.

During the field tests, large block samples were obtained at intervals of 1.5 m. Laboratory triaxial testing was performed in undrained, consolidated- undrained, and drained conditions. On the basis of shear strength parameters measured by laboratory tests, total and effective stress analyses were performed for the different cross sections on the 1H:1V slope. The undrained shear strength 30 kPa was required for stability. The effective stress analysis was based on conditions that two sections existed between the first initial movement and initial active slide due to complication of measuring porewater pressure during excavation. The factors of safety ranged from 1.28 to 2.08 depending on the assumption of both failure surface and shear strength.

Freeman and Sutherland (1973) investigated the mechanism of failure for slopes in the layered Lake Agassiz clays after completing investigation of the anisotropic shear strength characteristics of the layered clays as mentioned in Section 2.2.2.2. Details of samples and test results are shown in Table 2.4. Those shear strength parameters measured along the layers and across the layers were used for stability analyses assuming circular and noncircular slip surfaces. Both total and effective stress analyses were simulated on typical riverbank slopes in Winnipeg, and the groundwater level was assumed at the ground surface in all cases.

The total stress analysis was performed using shear strength of 24 kPa, and the factors of safety ranged from 0.8 to 2.06, depending on both slope inclination and depth to the hard stratum as shown in Table 2.4. In effective stress analysis, various stability analyses were simulated varying failure slip surfaces, shear strength parameters, and

depth to a hard stratum. In case of the 6 to 1 slope, a circular failure surface and isotropic shear strength properties (see soil C,35 in Table 2.4) gave a higher safety factor of 1.86 than that in both a noncircular slip surface and shear strength properties along the layers, NC-L,35. It was found that factors of safety were reduced for noncircular failure surfaces when the lower shear strength parameters for sliding along the layered clays were used in long horizontal portion of the slip surface.

In most previous stability analyses, the peak effective stress parameters were used, and resulted in overestimation of riverbank stability. For the reason, residual shear strength was taken into account. Skempton (1964) indicated the loss of strength with time, and emphasized the importance of residual strength especially when pre-existing failure displacements had taken place. The residual shear strength is measured by direct shear reversal tests. Freeman and Sutherland (1974), Baracos (1978), and Baracos et al. (1980) showed the range of residual shear strength parameters for Winnipeg clays in Table 2.5.

At low effective stress zones such as the submerged and shallow toe of slopes, Winnipeg clays behave as cohesionless, softened materials. Baracos (1978) used residual strengths of $c_r' = 0$, $\phi' = 8 - 13°$ for stabilizing areas in Winnipeg. The typical range of residual shear strength parameters for Winnipeg clays is $c_r' = 3 - 5$ kPa, $\phi' = 8 - 13°$ from failed slopes, and $c_r' = 5$ kPa, $\phi' = 15 - 17°$ for fully softened strengths of intact clays (Graham 1986).

Mesri and Huvaj (2004) showed stability analyses using residual shear strengths mobilized in Red River slope failures outside Manitoba. Six locations were selected for

detailed stability analyses. Five locations are reactivated slides with the entire slip surface at residual condition, and the last slope that had a previous failure was stable. Residual shear strength parameters of lacustrine grey clays were determined by drained ring shear tests, and they were $c_r' \cong 0$, $\phi_r' = 7.3 - 16.7°$, which were similar to those values provided by Baracos (1978), Graham (1986). The computed factor of safety of each slide is shown in Table 2.6. Those safety factors can be varied by assumptions such as groundwater pressure.

The influence of a confined aquifer on slope stability in lacustrine clay was examined by Tutkaluk et al. (2002). Based on a series of slope geometries of the Winnipeg riverbank, piezometric levels in the confined aquifer and phreatic levels in lacustrine clay were changed. Results of their studies showed that safety factors were varied more sensitively in case of changes in piezometric level in the confined aquifer than changes in the phreatic level in the clay slope. It also found that slip surface location was dependent on piezometric elevations in the confined aquifer.

2.4 SHEAR STRESS-STRAIN CHARACTERISTICS OF ROCKFILL MATERIALS

The shear behaviour of rockfill materials is affected by such factors as mineralogical composition, particle grading, size and shape of particles, porosity of rockfill materials being influenced by compaction, and stress conditions. Laboratory testing and numerical modeling of the shear behaviour of the rockfill materials are necessary for realistic analysis and design of structures using rockfill materials.

A study by Ramamurthy et. al. (1980) showed stress-strain characteristics and volume change of rockfill materials obtained from consolidated drained triaxial shear tests. Three

particle sizes were used at a range from fine sand (38 mm diameter specimen) to fine gravel of Calcite and Quartz (100 mm diameter specimen) at various confining pressures. The volumetric strains increased with the increase in confining pressure and particle size. Axial strain at failure increased from 8 to 18 % for the tests at medium confining pressures, but at higher confining pressures beyond 20 kg/cm^2 failure was not observed up to 20% of shear strain. The deviator stresses continued to increase with the increase of axial strain. This was due to continuous degradation of the particles which is dependent on confining pressures and particle sizes.

Varadarajan et. al. (2003) conducted large-scale triaxial testing of rockfill materials and performed numerical modeling to investigate their stress-strain-volume change behaviour of the rockfill materials. The large-scale triaxial specimen has dimensions of 38.1 cm in diameter and 81.3 cm in length. Three modeled rockfill materials consist of rounded and angular particles obtained from two different dam sites (Ranjit Sagar and Purulia in India). The modeled samples were derived using the parallel gradation modeling technique (see Lowe 1964). Aggregate impact value, crushing value, and Los Angeles abrasion value were determined for two samples showing that rockfill particles from the Ranjit Sagar site were stronger than those from Purulia site. The test results obtained from consolidated drained triaxial tests confirmed the results of Ramamurthy et. al. (1980). Both materials showed an increase in axial strain and volumetric strain at failure with increasing confining pressure and particle size as shown Figures 2.4 and 2.5. The Ranjit Sagar rockfill material showed higher shear strength than that from Purulia. The values of axial strain at failure for the Ranjit Sagar rockfill material were higher than those for the Purulia rockfill material.

In Figures 2.4 and 2.5 the volume change behaviours of these two rockfill materials are significantly different from each other. During the shearing stage of the triaxial test, compression, rearrangement, and breakage of particles take place. The Ranjit Sagar rockfill material shows continuous volume compression during testing due to compression and rearrangement of the particles. The breakage of the particles also adds to the volume compression. In the Purulia rockfill material, volume compression takes place due to compression and breakage of the particles. The angular particles provide a high degree of interlocking and cause dilation during shearing. During the latter phase of shearing, dilatancy is more, leading to volume expansion. Particle breakage was observed during shearing and is expressed by the breakage factor B_g which was calculated from sieve analysis of rockfill sample. It showed the high value of the breakage factor in the Purulia material due to relatively low shear strength of the particles. The effect of the increase in interlocking is to increase the shearing resistance, while the effect of breakage of the particles is to decrease the shearing resistance.

A number of researchers have conducted tests on a wide range of rockfill materials. These include Hall and Gordon (1963), Marsal (1967), Fumagalli (1969), Ansari and Chandra (1986), Ramamurthy and Gupta (1986), and Venkatachalam (1993). They have concluded that (1) the stress-strain behaviour of the rockfill materials in nonlinear, inelastic and stress dependent, (2) an increase in confining pressure tends to increase the value of peak deviator stress, axial strain, and volumetric strain at failure, (3) an increase in the size of the particles results in an increase in volumetric strain at the same confining pressure. They have also found that the behaviour of the rockfill depends on mineral composition, grain size, shape, gradation, and relative density of the rockfill.

2.5 ROCKFILL OR STONE COLUMNS AS A SLOPE STABILIZATION TECHNIQUE

As one of several ground improvement techniques, rockfill columns (also known as stone columns and granular piles) have been widely used for many purposes such as improving slope stability, increasing bearing capacity, reducing total and partial settlements, increasing the time rate of settlement and reducing the potential liquefaction since the installation process was popularized in the later 1950s. Rockfill columns are popular in improving soft soils because replacing a portion of the soft soils with a compacted granular backfill creates a composite material of lower compressibility and higher shear strength than the unimproved native soil (FHWA 1983). In this section, the basic relationships of rockfill columns are presented. Case studies related to stabilization of slope failures using rockfill columns are also discussed.

Figure 2.6 illustrates typical layouts of rockfill columns. In most cases the equilateral triangular pattern is used because it provides the densest packing of columns in a given area. The cylinder of composite ground with effective diameter D_e is known as the unit cell as shown in Figure 2.7. For the triangular and square patterns of rockfill columns, the effective diameters of composite ground are expressed as:

[2.1] $D_e = 1.05S$ (triangular pattern) $D_e = 1.13S$ (square pattern)

where: S = the spacing of granular piles

The performance of the improved ground is highly dependent on the volume of soil replaced by rockfill columns. The area replacement ratio is defined as the ratio of the granular pile area to the total area within the unit cell area and followed as:

[2.2] $$a_s = \frac{A_s}{A_s + A_c}$$

where: A_S = the horizontal area of a granular pile

A_C = the horizontal area of clayey ground surrounding the pile

The area replacement ratio can be expressed in terms of the diameter and spacing of the pile as follows:

[2.3] $$a_s = C_1\left(\frac{D}{S}\right)^2$$

where : D = diameter of the compacted rockfill column

S = center to center spacing of the rockfill columns

$C_1 = \pi/4$ for a square pattern, $\pi/(2\sqrt{3})$ for a triangular pattern

When load is applied in the reinforced composite, concentration of stress occurs in the rockfill column because the column is stiffer than the surrounding soil (FHWA 1983). The distribution of vertical stress within the unit cell can be expressed by a stress concentration factor as follows:

[2.4] $$n = \frac{\sigma_s}{\sigma_c}$$

where : σ_s = the vertical stress in the granular pile

σ_c = the vertical stress in the surrounding soil

The average vertical stress, σ, over the unit cell area at a given depth is expressed in terms of area replacement ratio, a_s:

[2.5] $$\sigma = \sigma_s a_s + \sigma_c (1 - a_s)$$

[2.6] $$\sigma_s = \frac{n\sigma}{1+(n-1)a_s} = \mu_s \sigma \qquad \sigma_c = \frac{\sigma}{1+(n-1)a_s} = \mu_c \sigma$$

where μ_s and μ_c are the ratio of stresses in the rockfill column and clay to the average stress over the tributary area. The stress in the rockfill column and clay can be determined using equation [2.5] (FHWA 1983, Bergado et al. 1994). The average resistance of the composite soil is calculated by the shear resistance of the rockfill columns and the shear resistance provided by the clay soil at the slide surface as follows (Goughnour et al. (1991) :

[2.7] $$\tau_{av} = \tau_{rockfill}\left(\frac{A_{rockfill}}{A_{total}}\right) + \tau_{clay}\left(\frac{A_{total} - A_{rockfill}}{A_{total}}\right)$$

[2.8] $$\tau_{av} = \tau_{rockfill} \times a_r + \tau_{clay} \times (1 - a_r)$$

A study by Goughnour et al. (1991) used stone columns for stabilization of three natural slopes. It was found that during penetration of the probe, negative excess pore water pressures were developed. The reason could be due to a combination of soil remolding, reduction in lateral pressure and pore water being forced away by air pressure of the probe. Once compaction started, the pore water pressure increased rapidly. After

compaction, the excess pore water pressures were dissipated in a short time between 5 hours and 2 days. The rate of lateral movement increased during construction of the bottom two rows. After completion of the bottom two rows, the displacement rate decreased and only small movement occurred during the construction of the remaining columns. Vane shear testing was also carried out on samples taken within 2 weeks of the completion of column installation. It indicated a significant increase of vane shear strength especially in the upper 3 m of soil due to reconsolidation over their initial stress condition by lateral stress imparted by the column installation. All three slopes have had no slope movement. This study proved that the stone column method was an effective solution for the slope stability problem.

In Winnipeg, stabilization of slope failures along riverbanks was conducted using rockfill columns by Yarechewski and Tallin (2003). Two riverbanks were stabilized by two different methods, rockfill columns and a combination of ribs and shear key. During installation, both methods led to riverbank movements due to the temporary decrease in stability, however the displacement rate decreased after completion of construction by both methods shown in Table 2.7 and 2.8. The results indicated that in terms of reducing the immediate post-construction movements the combination of shear key and ribs would provide better performance than rockfill columns that could cause much disturbance of clay between columns. However, installation of shear keys and ribs is restricted to shallow depths while installation of rockfill columns has no depth restrictions.

Another case history of using rockfill columns for embankment slope stabilization, this time in Alberta, was reported by Tweedie et al. (2004). The foundation of the embankment consisted of high plastic clay which was also partially frozen. It was also found that the rate of movement following installation of rockfill columns increased

initially and was decreasing with time, similar to what was observed by Yarechewski and Tallin (2003).

2.6 METHODS OF SLOPE STABILITY ANAYSIS

Many numerical methods for analyzing slope stability have been developed. For geotechnical engineers the two-dimensional limit equilibrium methods (LEM) or methods of slices for slope stability analyses are still most often used because of their simplicity and their ability to accommodate complex geometries and variable soil and water pressure conditions (Terzaghi and Peck 1967). However, these methods have several disadvantages and neglect some important factors. For those reasons, Finite Element Method (FEM) and Finite Difference Method (FDM) are now becoming popular among practicing engineers for carrying out slope stability analyses (Griffiths and Lane 1999, Cala and Flisiak 2001). The following section will explain firstly brief comparison of six methods of slices and then describe the application of finite element and finite difference method using shear strength reduction technique for estimating the stability of slopes.

2.6.1 Limit equilibrium method (LEM) or methods of slices

Methods of slices are divided into six common methods as follows:

- Ordinary or Fellenius method
- Simplified Bishop method
- Spencer's method
- Janbu's simplified method
- Janbu's rigorous method
- Morgenstern-Price method

The Ordinary Method is the simplest method and assumes that interslice forces can be neglected because they are parallel to the base of each slice. This assumption can result in significant errors in factor of safety by the fact that interslice forces are not parallel due to change in direction (Fredlund 1977).

The Simplified Bishop Method also neglects interslice shear forces on both sides of each slice assuming that a normal or horizontal force can be defined the interslice forces. The factor of safety is determined from the summation of moments, which is the same as that obtained by the Ordinary method.

Spencer's method assumes that there is a constant relationship between the interslice shear and normal forces with an angle of the resultant interslice force from the horizontal. Two factors of safety are obtained. One is from the summation of moments, and the other one is from the summation of forces for each angle of side forces. Both moment and force equilibrium are satisfied when they are equal at some angle of the interslice forces.

Janbu's simplified method uses a correction factor for the effect of the interslice shear forces while neglecting the interslice forces. The correction factor is related to cohesion, angle of internal friction, and the shape of the failure surface. Janbu's rigorous method assumes that the point at which the interslice forces act can be defined by a 'line of thrust' on the base of each slice. The interslice shear and normal forces are considered to determine a factor of safety.

Morgenstern-Price method assumes a function of the direction of the interslice forces. The interslice forces are determined in a manner similar to Janbu's rigorous method. Two factors of safety are determined by both moment and force equilibrium while interslice forces are determined using Janbu's rigorous method. Experience and judgement are required to estimate the function of interslice force direction because the forces vary across the slide mass. The characteristics of commonly used methods of slices are summarized in Table 2.9.

The factor of safety indicates the degree of slope stability. At failure, it will be equal or less than unity. The safety factor is defined in LEM as the ratio of total resisting forces or moments to total driving forces or moments over the critical slip surface:

$$FS = \frac{\text{resisting forces or moments}}{\text{driving forces or moments}}$$

It is also determined as the ratio of the magnitude of shear strength to shear stress applied along a potential failure slip surface:

$$FS = \frac{\text{shear strength of soil}}{\text{shear stress required for equilibrium}}$$

2.6.2 Finite element method (FEM) and finite difference method (FDM)

Finite element method and finite difference method have been used for slope stability analysis because these methods lead to more accurate and reliable results than those

from any conventional methods. The advantages of both FEM and FDM to slope stability analysis over the transitional limit equilibrium methods are (Griffiths and Lane 1999):

- No assumption is required for the shape or location of the failure surface because failure occurs naturally through the zones of soil mass until the soil mass can not resist the applied shear stresses.
- No assumption is needed for slice side forces since the failure mass is not divided into slices in the FEM and FDM.
- The FE and FD solutions can also provide values of deformations for stable slopes.
- Both progressive failure and overall shear failure can be monitored.

2.6.2.1 Shear strength reduction (SSR) technique

This shear strength reduction (SSR) technique is used with the finite element or finite difference method to solve sophisticated problems such as analyzing stability of slopes with reinforcements. To perform slope stability analysis, iterations are run for a series of trial factors of safety F^{trial} with soil's strength parameters, c' and ϕ' reduced by the following equations of [2.9] and [2.10]. This process will be repeated until non-convergence occurs and then the factor of safety will be determined.

$$[2.9] \qquad c^{trial} = \frac{1}{F^{trial}} c$$

$$[2.10] \qquad \phi^{trial} = \arctan\left(\frac{1}{F^{trial}} \tan\phi\right)$$

Definitions of failure should also be clarified in the SSR technique with the FEM and FDM. Zienkiewica and Taylor (1989) defined the meaning of 'failure' was non-convergence of the solution. Under the condition where both the Mohr-Coulomb failure and global equilibrium criteria are satisfied but the algorithm is not converging within a maximum number of iterations specified by users, failure is thought to occur. Slope failure and numerical non-convergence occur at the same time, and are caused by a dramatic increase in the nodal displacement in the mesh (Griffiths and Lane 1999).

Matsui and San (1992) conducted slope stability analyses using shear strength reduction (SSR) technique with finite element method (FEM). Stability analyses of both embankment and excavation slope were performed to verify the SSR technique. It was found that the location and shape of failure slip surfaces by the SSR technique were very similar to those estimated by Bishop's and Fellenius's methods.

Griffiths and Lane (1999) used the shear strength reduction technique with finite element analysis in conjunction with an elasto-plastic stress-strain method. Results of their study showed that the FEM was a reliable and effective method in assessing the safety factor for slopes. Swan and Seo (1999) also compared results of the FEM using the SSR technique and those of the LEM. They found that the SSR technique seemed to be well suited for assessing the stability of slopes particularly where unconfined active seepage occurred.

The accuracy of the shear strength reduction (SSR) technique for slope stability using finite difference method (FDM) has been demonstrated by a number of researchers. Dawson and Roth (1999), and Cala and Flisiak (2001) demonstrated its accuracy in comparison of results from LEM. Cala and Flisiak (2001) simulated slope stability

analyses using two dimensional FLAC (Fast Lagrangian Analysis of Continua) code. For a simple, homogeneous slope, the factor of safety by the SSR technique was the same as the factor of safety from LEM. However, for a simple geometry consisting of two geological units, the factor of safety by the SSR technique was 20% less than that obtained from LEM. This was also observed by Griffiths and Lane (1999) in their finite element analysis, and explained that slip surfaces obtained from the SSR technique were localized deeper than slip surfaces from the LEM.

It can be concluded that SSR technique with FEM or FDM has been able to provide reasonable and reliable results for slope stability. For this reason, SSR technique with FDM was used in this study to analyze the stability of the Winnipeg riverbank with or without rockfill columns.

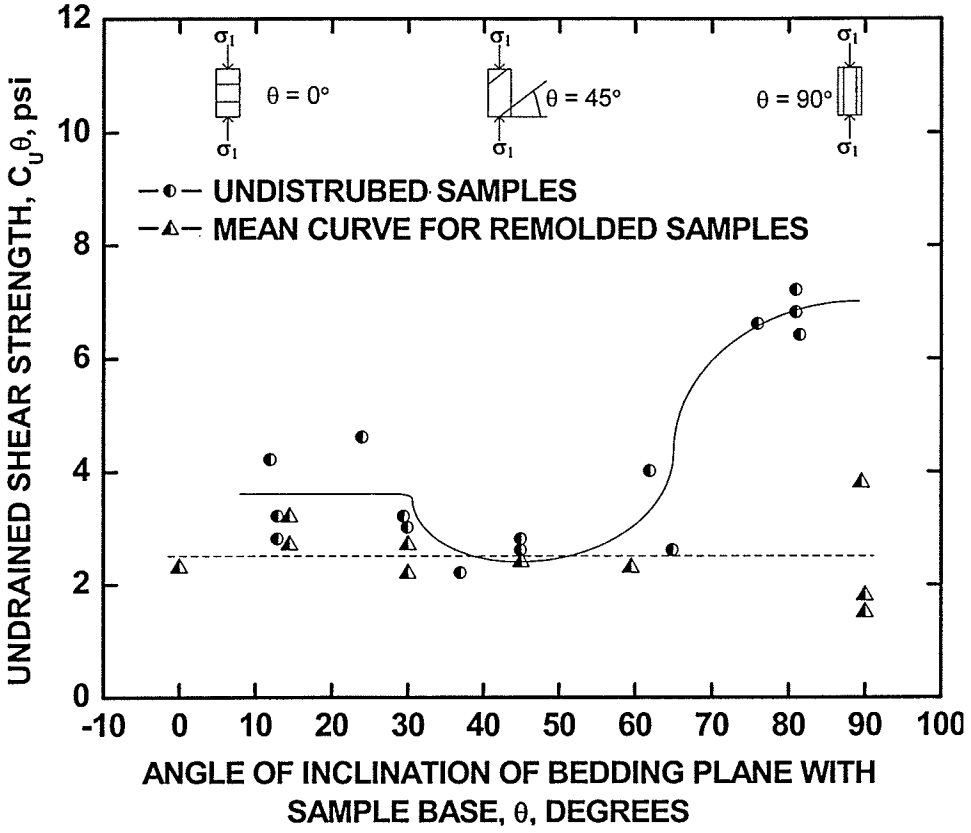

Figure 2.1 Unconfined compression test results of Winnipeg brown clay (after Loh and Holt 1974)

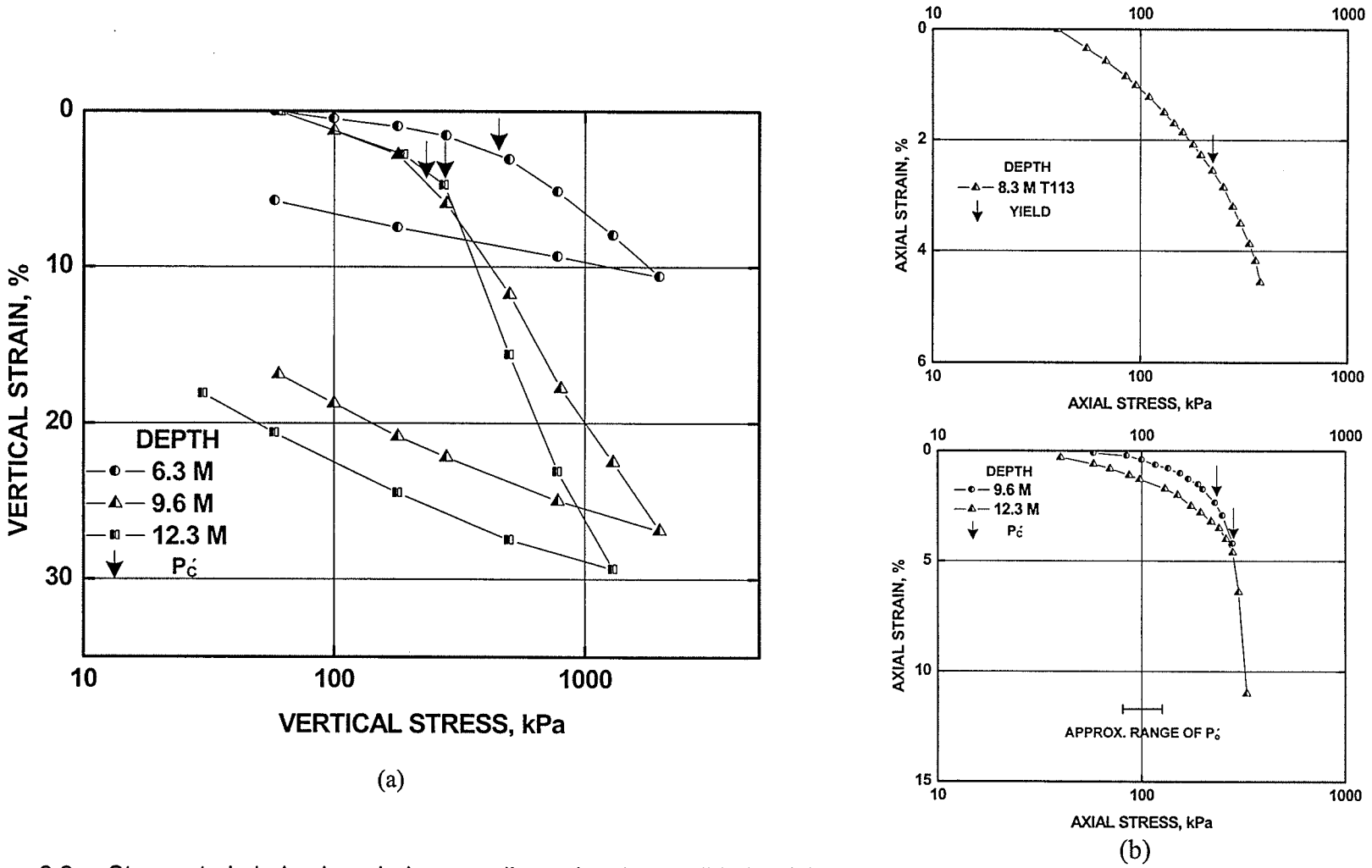

Figure 2.2 Stress-strain behaviour during one-dimensional consolidation (a) oedometer tests; (b) triaxial tests (after Baracos et al. 1980)

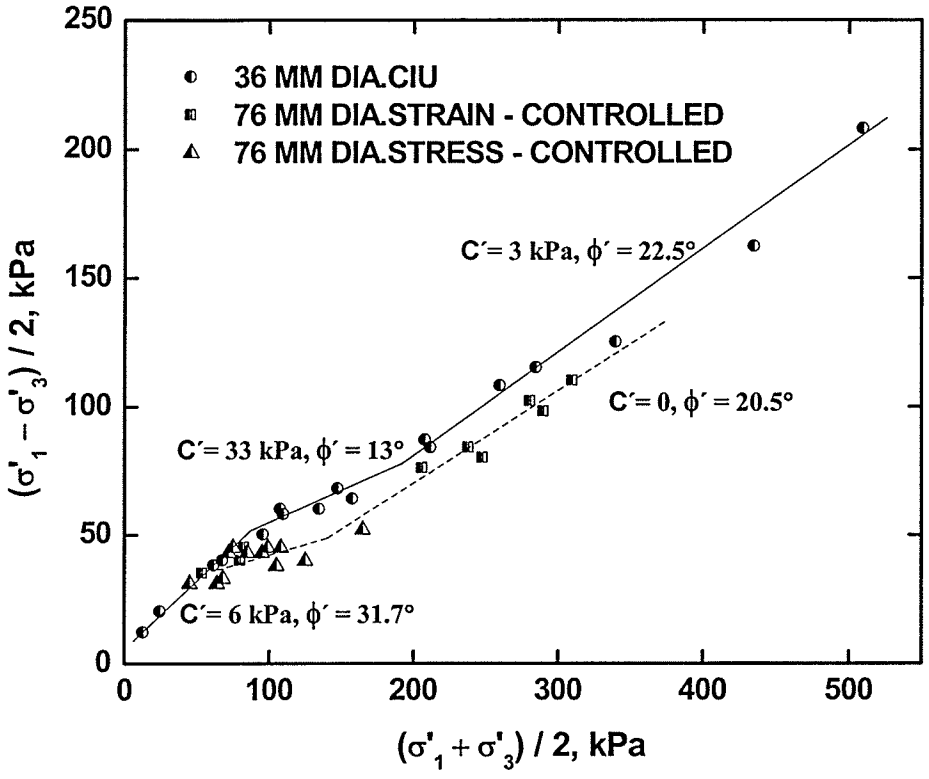

Figure 2.3 Triaxial test results for Winnipeg grey clay (after Baracos et al. 1980)

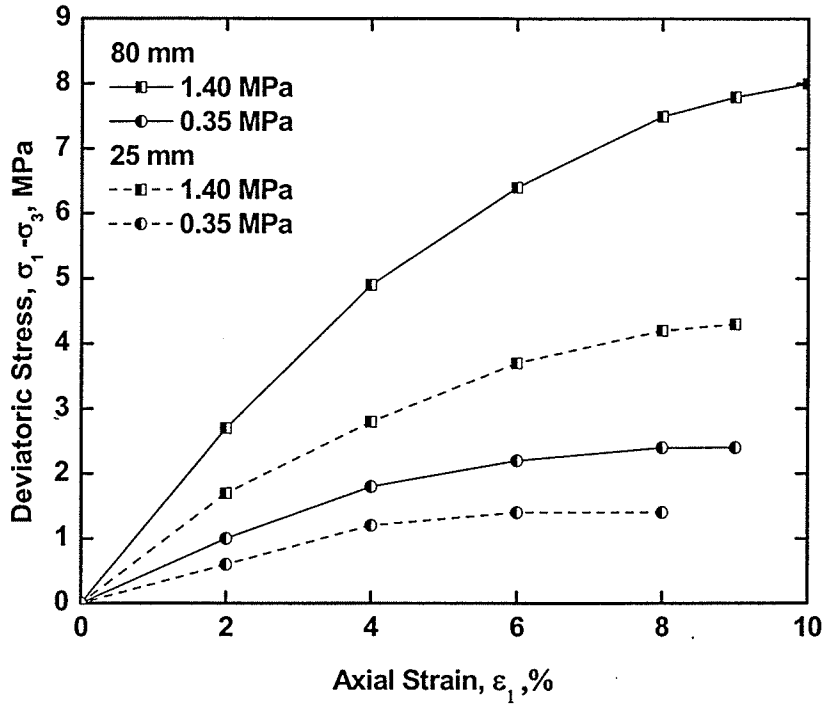

(a) Stress-strain behaviour

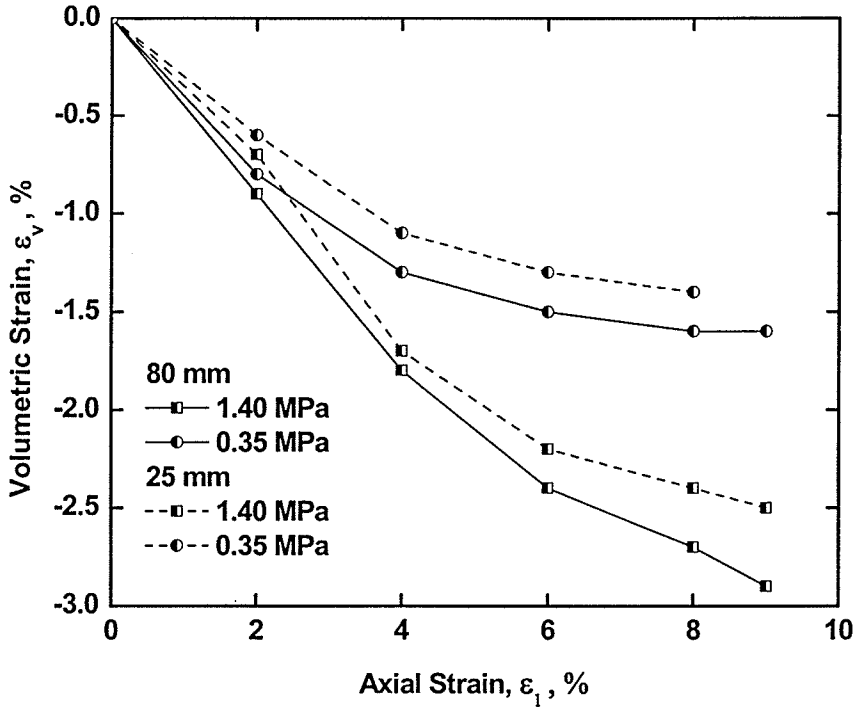

(b) Volume change behaviour

Figure 2.4 Stress-strain-volume change relationship for Ranjit Sagar rockfill material (after Varadarajan et.al. 2003)

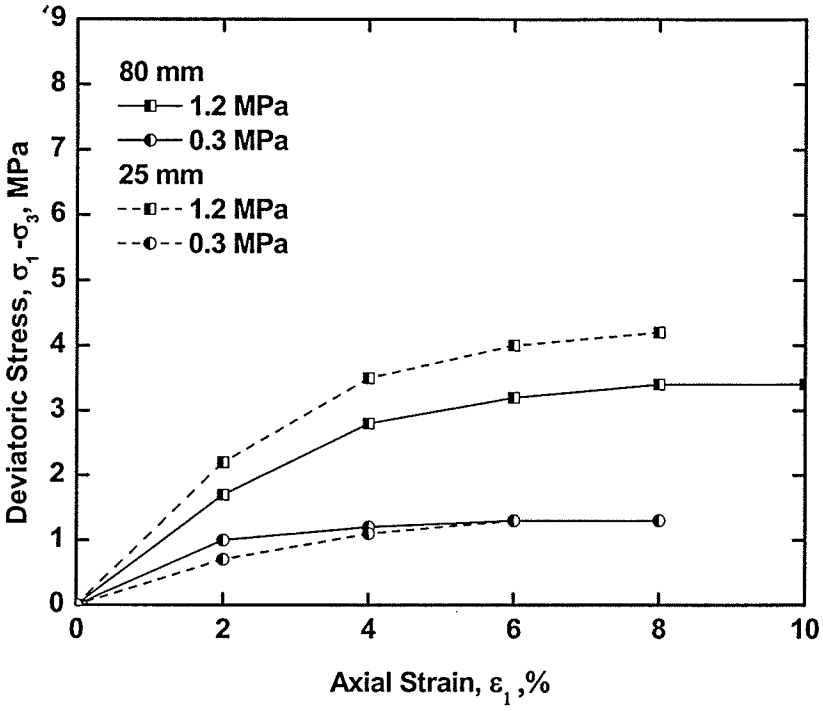

(a) Stress-strain behaviour

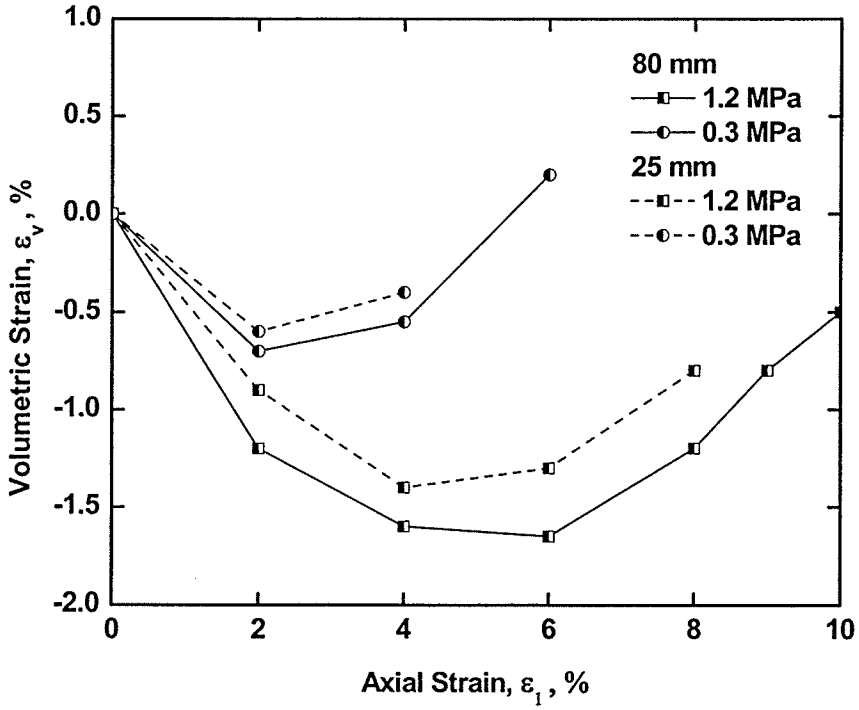

(b) Volume change behaviour

Figure 2.5 Stress-strain-volume change relationship for Purulia rockfill material (after Varadarajan et.al. 2003)

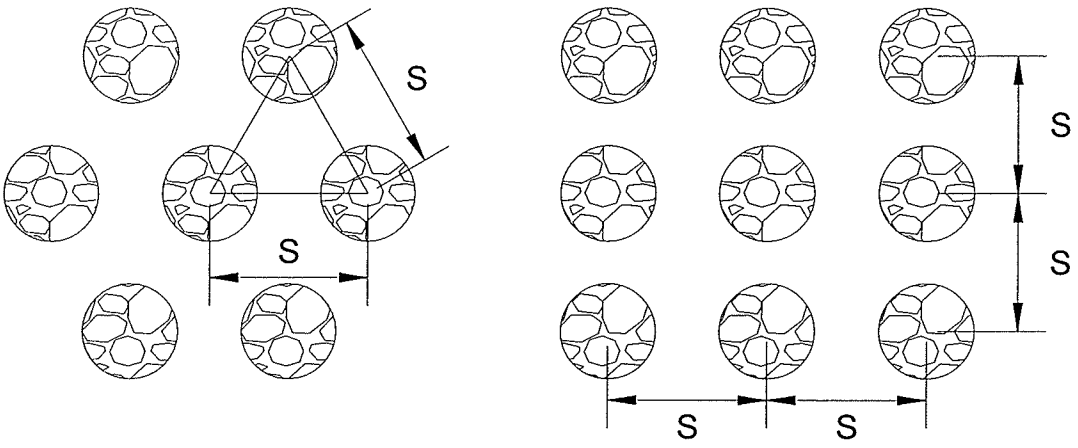

Figure 2.6 Layouts of rockfill columns

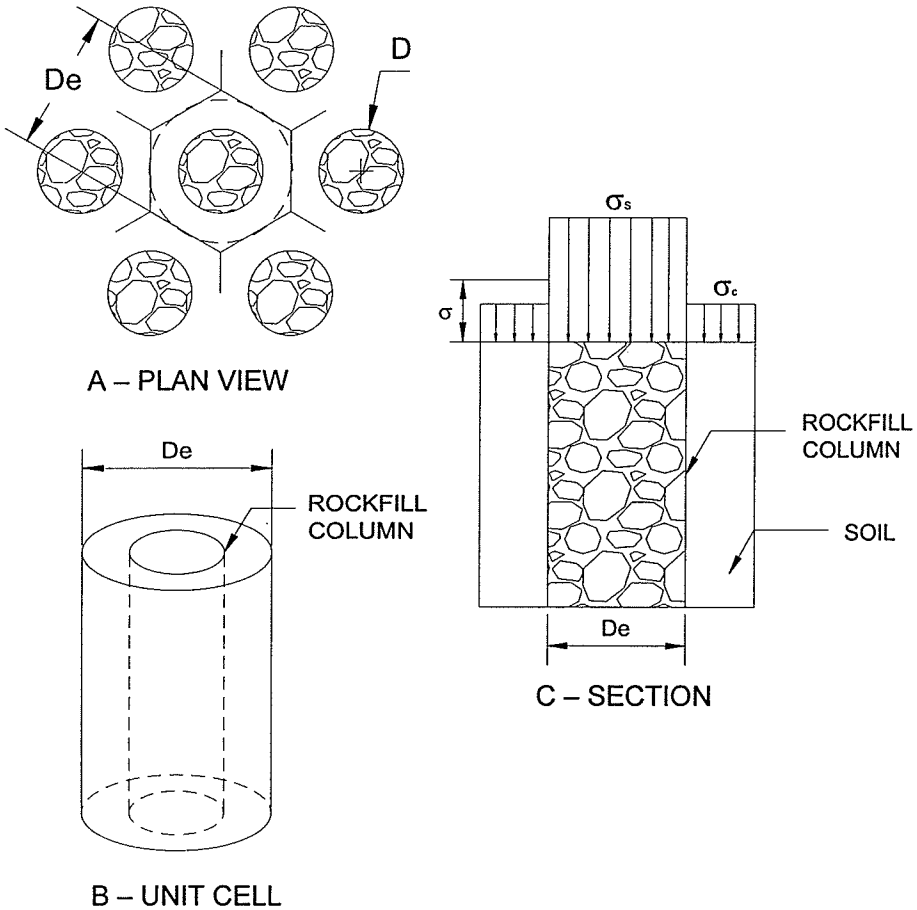

Figure 2.7 Unit cell idealization (after Barsdale and Bachus 1983)

Table 2.1 Geotechnical properties of glaciolacustrine clay (after Baracos et al.1983)

Geotechnical property	Typical Lower	Range Upper
Unit weight (moist), kN/m^3	15.7	18.1
Unit weight (dry), kN/m^3	10.2	13.3
Liquid limit, %	65	110
Plasticity Index, %	40	75
Clay size fraction, %	70	85
Sensitivity	2	4
Compression Index	0.5	1.0
Overconsolidated ratio	1	5
Swelling pressure[1], kPa	0	74.2
Unconfined compression strength, kPa	47.9	119.8
N. cons. Angle of shearing resistance, peak, degrees	17	23
N. cons. Angle of shearing resistance, residual, degrees	8	12
Deformation modulus[2], kPa	24	143.7
Modulus/undrained strength[3], E/s_u	230	360

Note: [1]*Higher values may be experienced upon desiccation and rewetting.*

[2]*Based primarily on pressuremeter tests.*

[3]*Results from University of Manitoba campus*

Table 2.2 Results of X-ray diffraction tests (after Baracos 1977)

Sample	Main minerals present (in order of decreasing showing)	
	Non-clay	Clay
Tan silt	Mostly dolomite Quarts Some calcite Some feldspar Trace gypsum	Mostly illite Mixed layer (predominantly smectite) Some chlorite and/or kaolinite
Tan silt light coloured layer	Mostly dolomite Quartz	Some illite
Brown clay	Some quartz Dolomite (equally) Calcite (equally) Some felspar	Mostly mixed layer (predominantly smectite) Illite (equally) Kaolinite (equally)
Inclusion in brown clay	Mostly calcite Dolomite (equally) Quartz (equally) Some felspar	Some illite Some mixed layer
Grey clay	Mostly quartz Dolomite (equally) Calcite (equally) Some felspar	Illite Mixed layer (predominantly smectite) Some chlorite and/or kaolinite Some mixed layer
Inclusions in grey clay	Dolomite (equally) Quartz (equally) Calcite (equally)	Some mixed layer
Grey plastic clay	Quartz Dolomite Calcite	Illite Kaolinite Mixed layer (predominantly smectite)
Inclusion in grey plastic clay	Dolomite (equally) Felspar (equally) Calcite (equally) Quartz (equally)	Some illite and mixed layer

Table 2.3 Geotechnical properties of tills (after Baracos et al. 1983)

Geotechnical property	Typical Range	
	Lower	Upper
Unit weight (moist), kN/m^3	-	23.6
Unit weight (dry), kN/m^3	-	22.0
Liquid limit, %	13	20
Plasticity limit, %	11	13
Clay size, %	10	20
Silt size, %	30	40
Sand size, %	25	35
Pressuremeter Modulus, MPa	-	172.4-241.3

Table 2.4 Results of stability analysis of representative slopes (after Freeman and Sutherland1973)

	Factors of safety				
	Preliminary analyses		Detailed analyses		
Soil case	Shear strength, 24 kPa	Residual strength	A	B	C
2 to 1 slope					
C, 35	1.06	0.19	0.63	0.89	0.71
NC,35	-	-	0.68	0.84	0.80
NC-L,35	-	-	0.58	0.77	0.62
C,70	0.80	0.19	0.60	0.71	0.71
3 to 1 slope					
C, 35	1.31	0.27	0.90	1.18	1.01
NC,35	-	-	0.89	1.16	1.06
NC-L,35	-	-	0.79	0.94	0.83
C,70	0.82	0.27	0.80	0.90	0.97
4 to 1 slope					
C, 35	1.55	0.37	1.14	1.47	1.27
NC,35	-	-	1.12	1.13	1.34
NC-L,35	-	-	0.98	1.20	1.04
C,70	0.88	0.37	0.94	1.06	1.17
6 to 1 slope					
C, 35	2.06	0.58	1.68	2.05	1.86
NC,35	-	-	1.55	1.77	1.87
NC-L,35	-	-	1.35	1.55	1.44
C,70	1.05	0.51	1.26	1.35	1.55

Note: C – circular failure surface, NC – noncircular surface, NC-L – noncircular surfaces and shear strength properties along the layer

Table 2.5 Ranges in residual shear strength of Winnipeg clays (after Freeman and Sutherland 1974, Baracos 1978, Baracos et al. 1980, and Graham 1986)

	Range of residual shear strength	
Soil type	c', kPa	ϕ', degrees
Brown clay	0 – 0.67	8 – 13
Grey clay	0 – 10.3	7 – 11.5

Table 2.6 Red River slopes in Grand Forks (after Mesri and Huvaj 2004)

Slope	Inclinometer	Strength condition	Factor of safety
27th Avenue	No	Entire at residual	1.02
Alpha Avenue	No	Entire at residual	1.02
Riverside Drive	At crest, midslope, and toe	Entire at residual	0.82
Water Tank	At crest, midslope, and toe	Entire at residual	0.92
Reeves Drive	At midslope	Sherack and alluvial at fully softened, rest at residual	0.93
Northridge Hills	At midslope	Entire at residual	1.20

Table 2.7 Displacement rates for rock columns (Yarechewski and Tallin 2003)

Location of riverbank	Casing displacement ratio relative to construction timing (mm/year)			
	Before	During	1 Year after	2 years after
Mid bank SI-1	42	460	58	14
Mid bank aqueduct SI-2	30	2500	-	3
Between columns SI-3	-	-	40	5

Table 2.8 Displacement rates for shear key and ribs (Yarechewski and Tallin 2003)

Location of riverbank	Casing displacement ratio relative to construction timing (mm/year)				
	Before	During	1 Year after	2 to 4 Years after	4 to10 Years after
Mid bank SI-1	38	1200	11	6	2
Mid bank aqueduct SI-2	13	500	-	-	-

Table 2.9 The characteristics of commonly used methods of slices (Budhu 2001)

Method	Force equilibrium		Moment equilibrium	Application
	X	Y		
Ordinary	No	No	Yes	Circular slip surface
Bishop's simplified	Yes	No	Yes	-
Janbu's simplified	Yes	Yes	No	Any shape of slip surface
Spencer's	Yes	Yes	Yes	Any shape of slip surface
Bishop rigorous	Yes	Yes	Yes	Circular slip surface
Janbu's rigorous	Yes	Yes	No	Any shape of slip surface
Morgenstern-Price	Yes	Yes	Yes	Any shape of slip surface

CHAPTER 3

LABORATORY TESTING PROGRAM

3.1 INTRODUCTION

Laboratory simulation provides accurate solutions in many research studies. In geotechnical engineering, for instance, laboratory simulation has been used to solve geotechnical problems such as interaction between different strengths of soils, interaction between substructure and soil, or soil with water flow. Moreover, results from laboratory model tests have been used to develop numerical models to simulate field conditions. Therefore, in this research study laboratory model tests have been carried out and numerical models have been developed to simulate laboratory model tests and subsequently field conditions.

Studies about the performance of Winnipeg riverbanks stabilized with rockfill columns have been performed based on the material properties that were characterized in-isolation. The current study involved characterizing individually the clay and the rockfill materials. It will also characterize the clay and rockfill materials together so that behaviour of rockfill-clay composite during shearing can be properly understood. This chapter describes the laboratory testing program using large-scale direct shear test equipment.

3.2 TESTING EQUIPMENT AND INSTRUMENTATIONS

A direct shear test is conducted at a strain rate controlled by a user on a single shear plane predetermined by the configuration of the device. The shear box is divided vertically by a horizontal plane into two halves of equal or different thickness which are fitted together with alignment screws. Because of its configuration, direct shear test device can closely simulate a particular shear failure mechanism of riverbanks stabilized with rockfill columns. As slope displacement occurs, the upper portion of the rockfill columns tends to move with the slope soil and the lower portion of the rockfill columns tends to stay in the original location as shown in Figure 3.1.

Shear failure mechanisms of rockfill materials, lacustrine clay soils and rockfill-clay composites were simulated by large-scale direct shear test equipment shown in Figure 3.2. The equipment is capable of performing tests with both circular and square cross-sections whose dimensions are 600 mm diameter or 600 x 600 mm, respectively. The soil thickness is 140 mm above and 270 mm below the predetermined shear plane. A schematic diagram of the testing apparatus including some of the instrumentation is shown in Figure 3.3. On top of the equipment, three linear variable displacement transducers (LVDT's) are installed to measure vertical displacements. A fourth LVDT is connected to the upper box to measure shear displacements.

A rubber diaphragm sheet is used to apply a uniformly distributed vertical pressure (or normal stress) through a compressed air applied on top of the specimen. The direct shear force is measured by means of a load cell attached to the front of the upper box. The upper box can then be pulled or pushed relative to the lower box as shown in Figure 3.3. More detailed description of the equipment can be found in Alfaro et al. (1995).

The horizontal displacements (Δx), vertical displacements (Δz), shear load (P_X), and applied normal stress (σ_N) are monitored at desired time intervals and are connected to a personal computer through an electronic data acquisition system.

3.3 SHEAR STRENGTH PARAMETERS FROM DIRECT SHEAR TESTING

Generally, three or more specimens are tested at different levels of normal load or stress to determine the stress-strain characteristics within a given range of normal stress and to estimate the strength properties using the Mohr-Coulomb strength criterion. The average shear stress is determined from the shear load divided by the corrected cross–sectional area (A_c) of the test sample. That is,

$$[3.1] \qquad \tau_p = \frac{P_x}{A_c}$$

The cross-section area (A_c) is the nominal area of the specimen corrected by the change of shear displacement of the sample:

$$[3.2] \qquad A_c = \frac{D^2}{2}(\theta - \frac{\Delta x}{D}\sin\theta) \times s$$

where:

D = the cylindrical box of internal diameter (mm)

Δx = shear displacement (mm)

$\theta = \cos^{-1}(\Delta x / D)$

The shear response of the rockfill materials generally exhibits dilatant behaviour particularly for those that are densely compacted. The shear strength envelope can be described using a simple model following Coulomb's law. The net effect of dilation angle, ψ, makes the failure envelope curved with increase of normal stresses. Using Coulomb's frictional law, the general form of the shear strength, τ_f, of soils is given in the following form:

[3.4] $$\tau_f = \sigma'_{nf} \tan(\phi'_{cs} \pm \psi)$$

where:

σ'_{nf} = effective normal stress at failure

ϕ'_{cs} = friction angle at critical state

where the positive sign refers to soils in which the net movement of the particles during shearing is upward known as dilation and the negative sign refers to when the net particle movement is downward known as contraction. Once dilation or contraction has taken place the material will tend towards a large strain frictional behaviour at a constant volume known as critical state. The friction angle at the critical state, ϕ'_{cs}, is a fundamental soil parameter while the friction angle at peak shear stress, ϕ'_p, for dilating soil is not a fundamental soil parameter but depends on the capacity of the soil to dilate (Budhu 2001). The general equation for the dilation angle, ψ, is given as:

[3.5] $$\psi = \tan^{-1}\left(\frac{\Delta z}{\Delta x}\right)$$

where:

Δz = vertical (normal) displacement

Δx = horizontal displacement

3.4 TESTING OF UNDISTURBED LACUSTRINE CLAY

Large 'undisturbed' cylindrical clay samples were obtained from 12 - 15 m below ground surface in northern Winnipeg. This range of depth is where the weak layer of clay is usually located, which is near the proximity of the interface between clay and till. Therefore, this is the location where the potential failure slip surfaces can usually occur.

As indicated earlier, the testing program included conducting rockfill-clay composite samples to understand how the composite material responds to shear loading in the field. Therefore, it was preferable to get large undisturbed samples of the actual materials down to 15 m. The samples that have been taken at this depth have diameters of about 700 mm. Nobody had ever been able to get such a large sample at that depth. The contractor who provided both logistic and financial support for this research, Subterranean (Manitoba) Ltd., found a very innovative way to collect large samples.

Figure 3.4 illustrates the process of sampling large 'undisturbed' lacustrine clay. A steel sleeve casing was inserted into the ground to the required depth by applying a hydrostatic pressure on top of the casing as shown in Figure 3.4-A. After reaching the required depth, the casing was pulled up from the ground while being twisted to reduce the adhesion between the casing and the surround soil as shown in Figure 3.4-B. The samples were cut out by a wire saw with sample heights of 700 mm as shown in Figures 3.4-C and 3.4-D. Each sample was placed on a circular metal plate and wrapped with

plastic sheets (Figure 3.4-E). The samples were waxed to preserve the moisture content and stored in a moisture room at the University of Manitoba.

Prior to direct shear testing, classification tests were performed, such as Atterberg limits tests (ASTM D 4318), water content determination (ASTM D 2216-90), hydrometer analysis (ASTM D 422) and specific gravity (ASTM D 854). The results of the testing for basic geotechnical properties are summarized in Table 3.1. These properties are very similar to those examined by Baracos et al. (1983) mentioned in Section 2.2.2. Based on these properties, the clay can be classified as "CH", high plastic clay, according to the Unified Soil Classification System.

3.5 TESTING OF ROCKFILL MATERIAL

Rockfill has been used as a construction material for many years. Common uses of these materials included as stabilizing material for slope, protection against erosion on riverbanks, and construction of hydraulic dams. Rockfill columns have been successful to stabilize riverbanks in Winnipeg for over ten years. A recent study by Yarechewski and Tallin (2003) used crushed limestone as rockfill columns for increasing the stability of riverbanks.

In this research, crushed limestone materials obtained from quarries in northwest Winnipeg were used for rockfill columns in laboratory tests. Sieve analysis was first carried out in general accordance with ASTM standards (ASTM D421-85 and D422-63, 1998). The quantity of materials required for the test depends on the maximum particle size. The British standard (BS 1377, 1990) specifies the minimum quantity of materials based on the maximum size of the particles. In case of the maximum particle sizes up to

100 mm, the minimum quantity can be taken as 150 kg. Therefore, a sample of 250 kg of rockfill material was used in this study following the recommended procedure of using a quarter of a 1000 kg representative sample. Sieve analysis was performed on two sets of samples. One sample was made of an original size of rockfill materials used for rockfill columns in the construction site. The other was a scaled-down mixture of rockfill materials for laboratory testing. The grain size of the rockfill materials was reduced from its original size to conduct laboratory testing of rockfill-clay composite soil sample in the 600 mm diameter shear box.

Four techniques are mainly used to reduce the size of the rockfill materials: the scalping technique (Zeller and Wullimann 1957), parallel gradation technique (Lowe 1964), generation of quadratic grain-size distribution curve (Fumagalli 1969) and replacement technique (Frost 1973). The parallel gradation method is considered most appropriate in many geotechnical applications (Ramamurthy and Gupta 1986). Experimental and theoretical evidence (Marsal 1973, Gupta et al. 1995, Sitharam 2000) also indicates that as long as the grain size distributions of the reduced scale material are parallel for larger granular mixtures (of similar material), the stress-strain characteristics may be relatively similar. Hence, the reduced-scale sample was reproduced by using the parallel gradation method.

Direct shear tests on both original and scaled-down samples were conducted to confirm their similar stress-strain behaviour. The grain size distributions for the two samples are shown in Figure 3.5. Figure 3.6 shows the fractions of rockfill materials prepared for mixing. The maximum diameters for original and reduced-scale materials were approximately 60 and 27 mm, respectively. This proportioning ensured that the maximum grain size of the modeled rockfill material would be less than $1/10^{th}$ of the

modeled rockfill column size in the direct shear test setup. The long-term durability of the rockfill materials was assessed based on Los Angeles abrasion testing (small size coarse aggregate ASTM C-535). It was found that for crushed limestone used in this study, the weight loss was about 28.2%. This value satisfied the specification 3110-R5 of the City of Winnipeg that crushed limestone should have a weight loss of not more than 35% for base course material. It is assumed that this specification holds true for the rockfill column applications, although this assumption needs to be verified by further studies.

3.6 TEST CONDITIONS AND PROCEDURES

3.6.1 Introduction

The purpose of the experimental portion of this study is to assess the displacement required to mobilize shear resistance in rockfill columns used in the stabilization of Winnipeg riverbanks. The mobilization of shear resistance of the rockfill-clay composite is also assessed. Large-scale direct shear tests have been conducted in the following six different conditions:

(1) Rockfill material only

(2) Undisturbed clay only

(3) Rockfill-undisturbed clay composite (1, 2 and 5% of cemented rockfill columns)

(4) Remolded clay only

(5) Rockfill-remolded clay composite

(6) Rockfill columns in groups, shear key and rib layouts

3.6.2 Rockfill material samples

The grain size distributions of the original and reduced-scale samples were first determined using the parallel gradation method. Relative densities were then determined on both samples. The relative densities represent the different degrees of densification of materials at the construction site.

The frictional strength and mobilization of shear resistance of the rockfill materials depend highly on the relative density, D_r, of the material. Relative density is defined as:

$$[3.6] \qquad D_r = \frac{e_{max} - e}{e_{max} - e_{min}}$$

where:

e_{max} = maximum void ratio (from the loosest condition)

e_{min} = minimum void ratio (from the densest condition)

e = current void ratio

The determination of maximum and minimum dry densities (minimum and maximum void ratios) was carried out in general accordance with ASTM standards (ASTM D 4253-93 and D 4254-91, 1996). One deviation from the standard test was a change in the size of the mold used in the test. The mold had an inner diameter of 600 mm and 500 mm in height. Three relative densities were specified to represent a wide variation to cover the range of density that might be expected using various placement methods in the field. The rockfill materials were densified using a vibrator probe in three equal layers. The three relative densities examined in the testing program are as follows:

(1) Loose condition ($D_r < 15\%$)

(2) Medium-dense condition ($D_r \approx 67\%$)

(3) Dense condition (D_r > 90 %)

The dry unit weights of both the original and reduced-scale samples at different relative densities are summarized in Table 3.2.

A total of nine tests were conducted on the rockfill materials at different densities and three levels of normal stresses, 50, 75 and 100 kPa. These normal stresses represent a reasonable range of in-situ effective stresses for rockfill columns that would be installed up to approximately 12 - 15 m depth from the ground with the length of any rockfill column being dependent on the thickness of clay deposits.

Each specimen in the direct shear test was sheared until the shear displacement reached approximately 30 mm, which was about 5% of shear strain. The displacement rate of 2.4 mm/min was a slight modification of the ASTM standard wherein the maximum rate of shearing is 10 mm/min. During all tests, horizontal, vertical displacements, and shear forces were monitored.

3.6.3 Large undisturbed clay samples

The main purpose of testing undisturbed clay samples was to measure the mobilization of shear resistance of the undisturbed lacustrine soft clay under the same boundary conditions and scale effects with rockfill-clay composite tests. Clay sample diameter was 700 mm and the height was approximately 700 mm as mentioned in Section 3.4. It was necessary to trim the samples to fit into the circular shear box with 600 mm diameter. A special edged trimmer was manufactured by Subterranean (Manitoba) Ltd. as shown in Figures 3.7-A, B, C. The trimmer was attached to a piston and pushed down by

hydraulic pressure. Extra care was taken in trimming the undisturbed clay specimens to prevent the natural soil structure from any disturbance. Once trimming was completed, a special metal frame consisting of two circular metal plates (10 mm thickness) connected by four screw rods was used to facilitate the handling of the large clay specimen and fit the clay specimen for fitting the circular shear box (see Figures 3.7-D and E). All components of the frame were removed, except the bottom plate, before shearing the clay. The extra height of a clay sample was trimmed out as shown in Figure 3.7-F. A rubber diaphragm sheet was placed on the top of the circular shear box to apply a uniformly distributed vertical pressure (Figures 3.7-G and H).

3.6.4 Rockfill-clay composite soil samples

Either the replacement or displacement method is used to install rockfill columns into the ground. In Winnipeg, the replacement method has been used by local contractors. Figure 3.8 shows the process of rockfill column installation using replacement method. Rockfill columns are formed by drilling a hole about 2 m diameter into the ground, then backfilling the void space with rockfill materials up to the ground surface. Each lift is compacted by inserting a vibratory probe to achieve a desired density.

The laboratory testing for rockfill-clay composites was simulated as close as possible to the field installation method described above. Once the clay sample was set up in the direct shear box (Figures 3.9-A and B), a hole was drilled by a manual auger shown in Figure 3.9-C. Rockfill materials were then filled and densified in three equal layers by a hand vibrator (Figures 3.9-D, E, and F). Additionally, to investigate the influence of different area replacement ratios, three column diameters, 220, 270, and 320 mm were used equivalent to area replacement ratios of 14, 22 and 30%, respectively.

3.6.5 Cemented rockfill-clay composite samples

It was of interest to examine the influence of adding small amounts of cement to the rockfill materials on the shear mobilization of rockfill columns. Type 50 Portland cement was added at ratios of 0.5, 2 and 5% cement by weight. Pozzutec 20+ admixture was added to accelerate setting time and to increase the early strength of the mixture. It was recommended by the manufacturer to use 16% of Pozzutec 20+ of the total cement weight.

A similar procedure was followed in installing model cemented rockfill column material in clay as for untreated rockfill columns. The only difference is the addition of cement in the rockfill materials. Dry cement was first added, followed by adding water and Pozzutec 20+ admixture. Mixing was manually done. The dry density of 18.45 kN/m^3 was achieved through the same procedure of densification as in the untreated rockfill column.

3.6.6 Rockfill columns in group

The purpose of conducting tests on rockfill columns in a group was to investigate the effects of different spacing on the shear mobilization of column groups. Two groups were tested with a total of five columns in each group and were installed in a square cross-section of shear box, 600 x 600 mm in dimensions. The column diameter was 170 mm and the columns were laid in a triangular pattern. It is noted that rockfill columns are usually constructed in the field either in a triangular or square pattern. The triangular pattern is usually preferred because it provides the densest packing of columns in a given area (FHWA 1983).

The test on the first group is called an 'open-spacing' test. Three columns were placed in the first row and the remaining two columns were placed in the next row as shown in Figure 3.10 In the second group, the test was called a 'close-spacing' test and the layout of the columns is shown in Figure 3.11.

In the column group testing, remolded clay was used due to the limited amount of undisturbed samples. The water content of the remolded clay was the same as that of undisturbed clay. To achieve the desired density, the remolded clay was compacted manually by tamping in layers. A PVC pipe was then pushed to extract the clay in the holes where the rockfill columns were to be installed.

3.6.7 Shear key and ribbed-type layouts

Rockfill materials for stabilizing riverbanks have been used in other layouts. Shear key and rib layouts are used for stabilization of riverbanks in Winnipeg (see Yarechewski and Tallin 2003). These have been investigated in the large-scale direct shear testing program to better understand the shear mobilization of rockfill-clay composites corresponding to the different layouts for stabilization measures.

Figure 3.12 shows the shear key layout in the shear box. In installing the modeled shear key, wooden plates attached to each other were placed to support the placement of the remolded (compacted) clay. The clay was first compacted and as soon as this was done, the wooden plates were removed leaving the compacted clay unsupported. The rockfill materials were subsequently placed and densified in the gap between the compacted clay. Similar procedures were used for the case of the rib layout as shown in Figure 3.13.

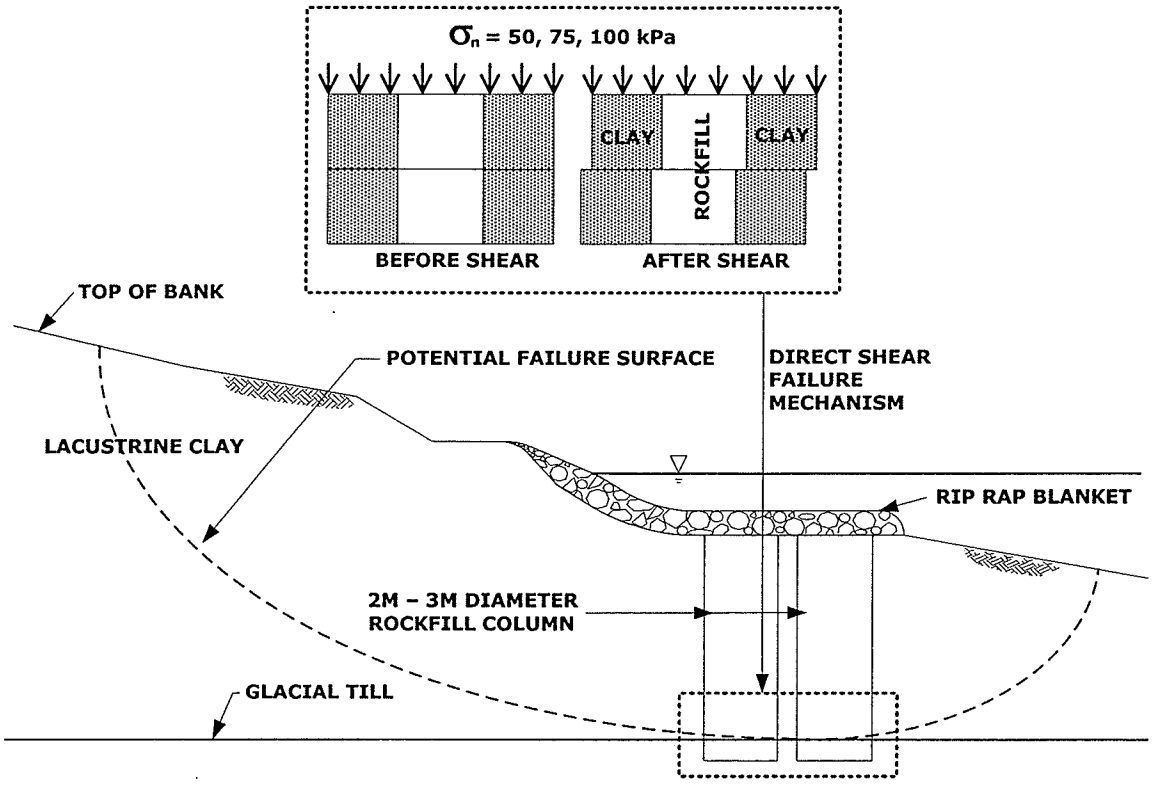

Figure 3.1 Typical failure mechanism of stabilized riverbank in Winnipeg (after City of Winnipeg 2000)

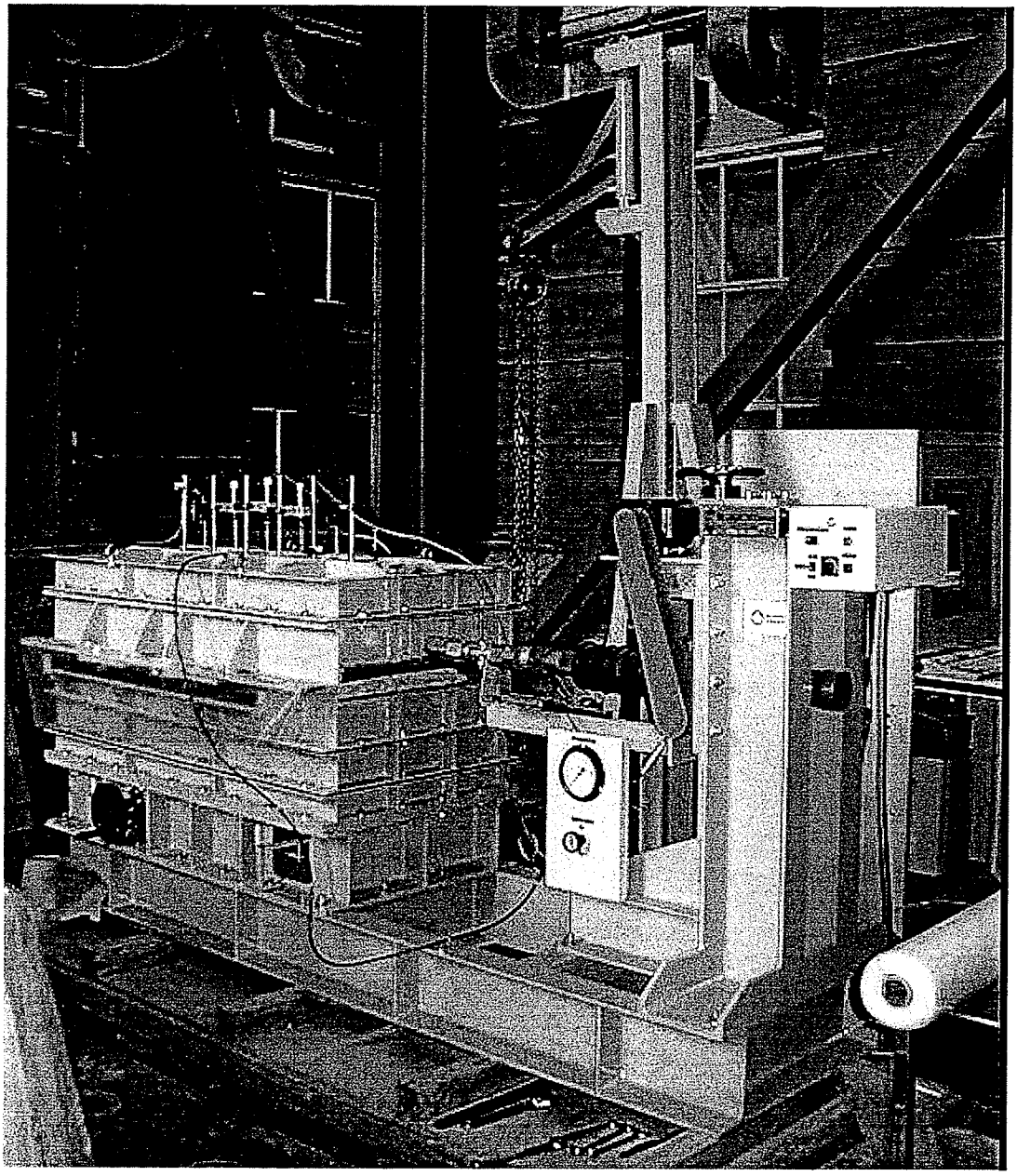

Figure 3.2 Large direct shear test apparatus

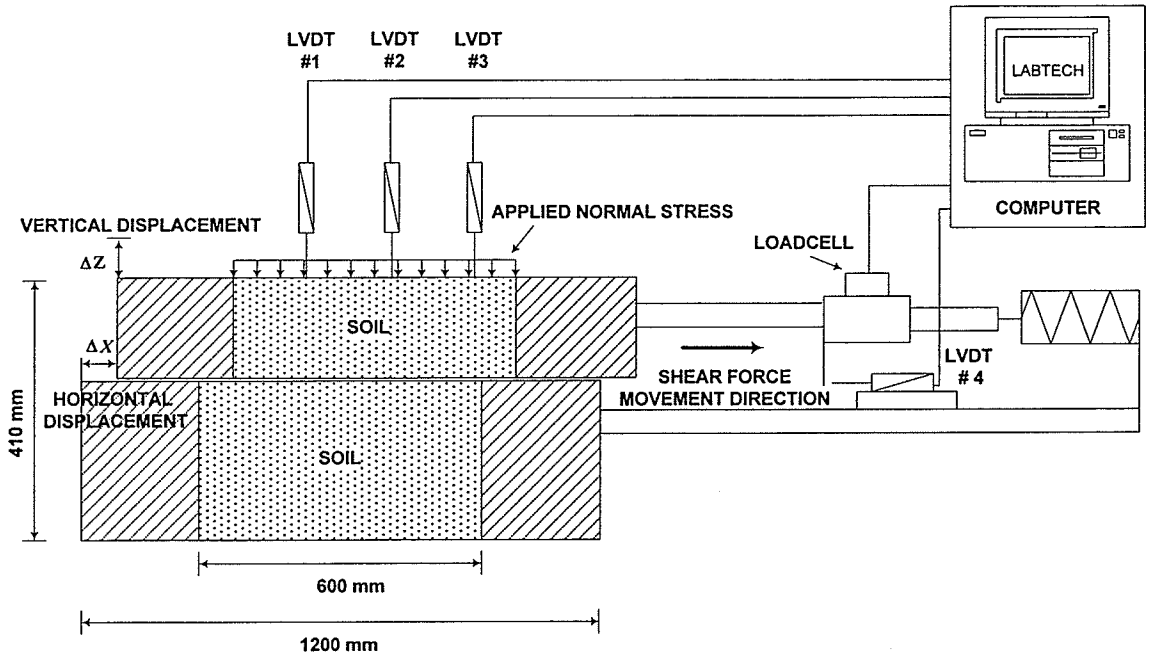

Figure 3.3 Schematic of direct shear test apparatus

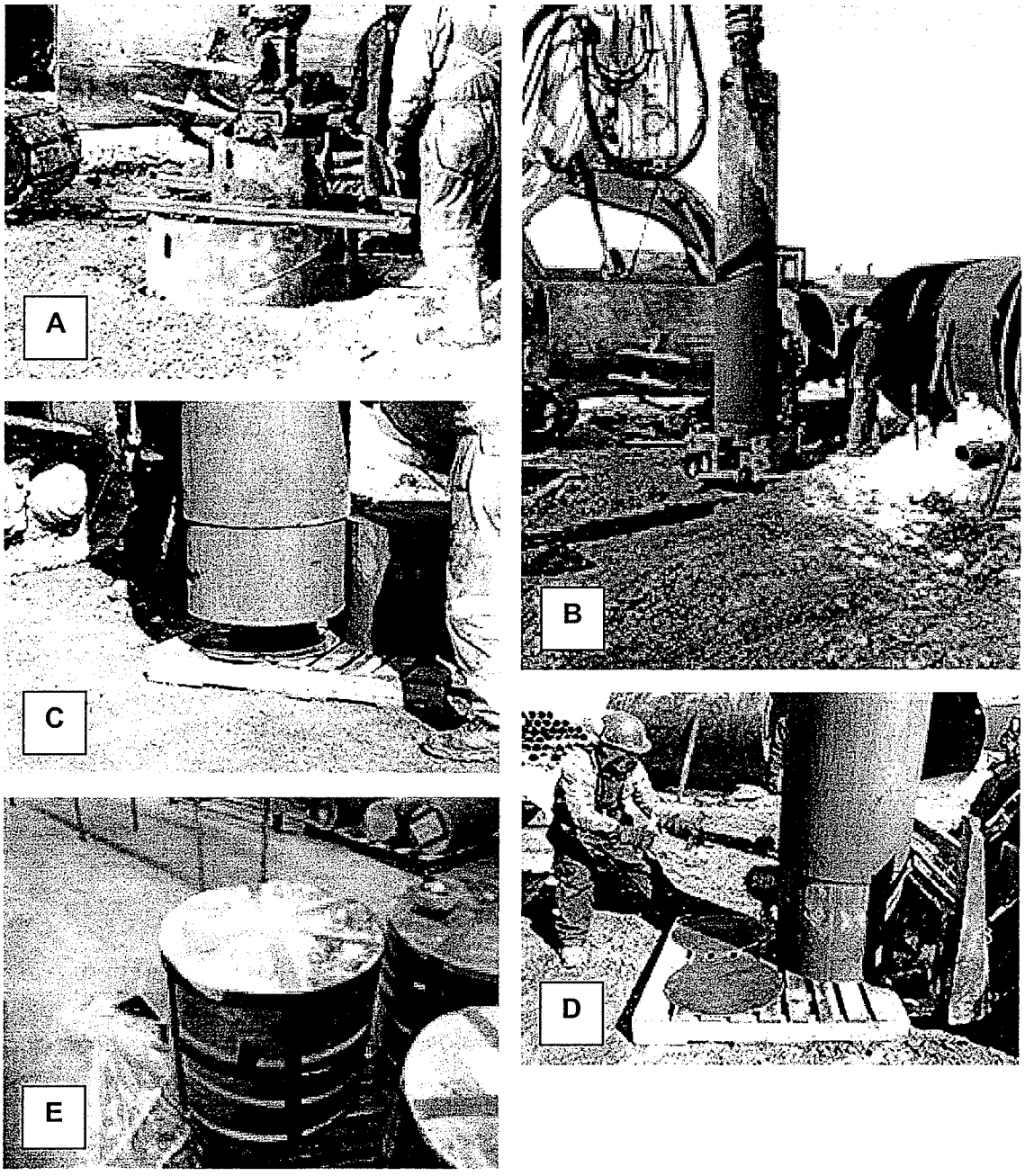

Figure 3.4 Sampling of large 'undisturbed' lacustrine clay

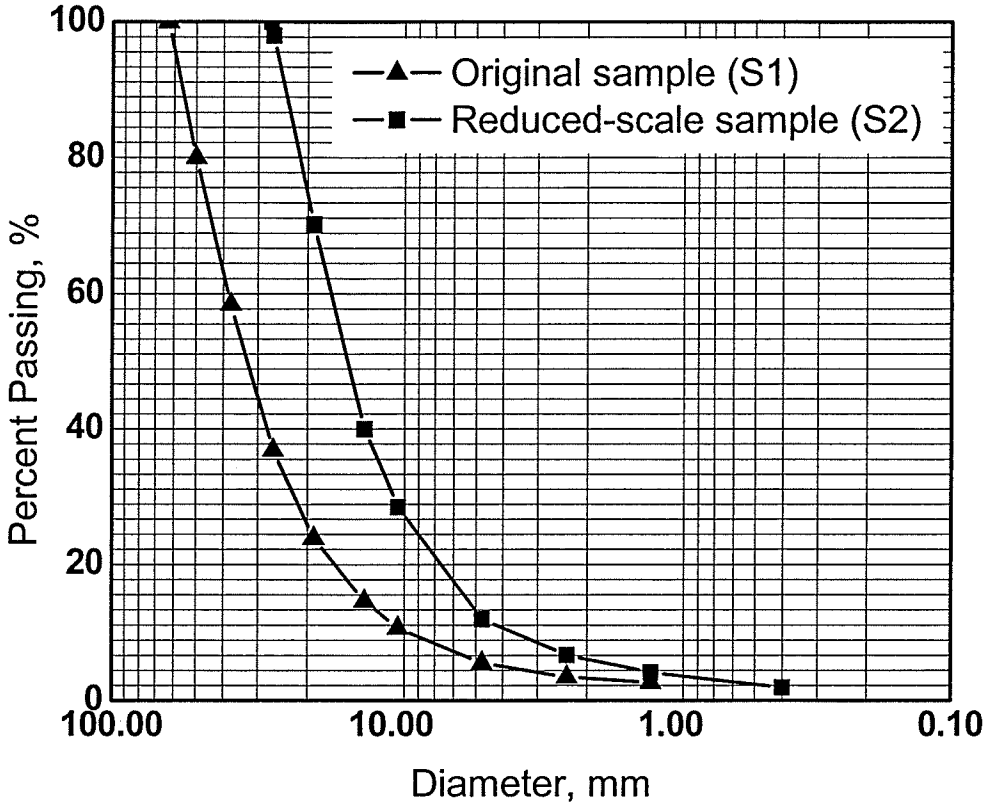

Figure 3.5 Grain size distribution of the original sample (S1) and reduced-scale sample (S2) of rockfill materials

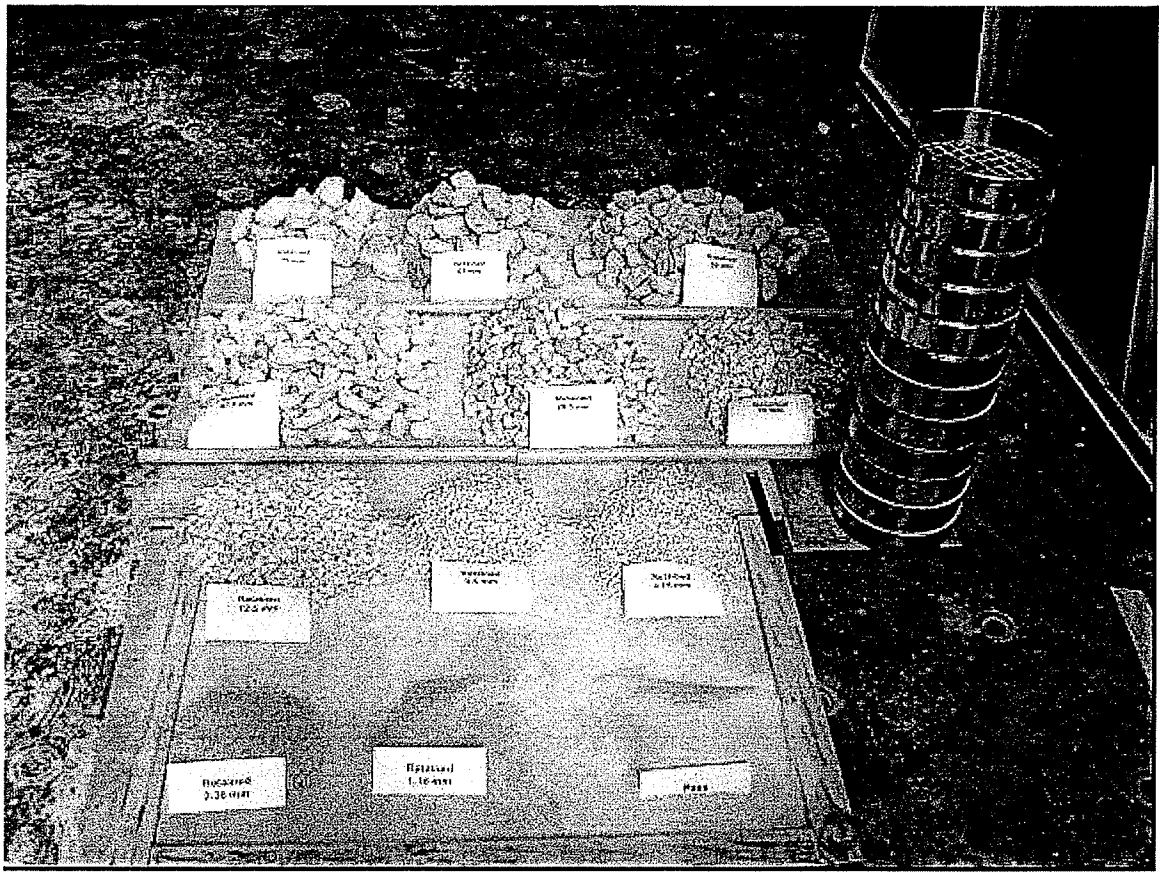

Figure 3.6 Fractions of rockfill material prepared for mixing

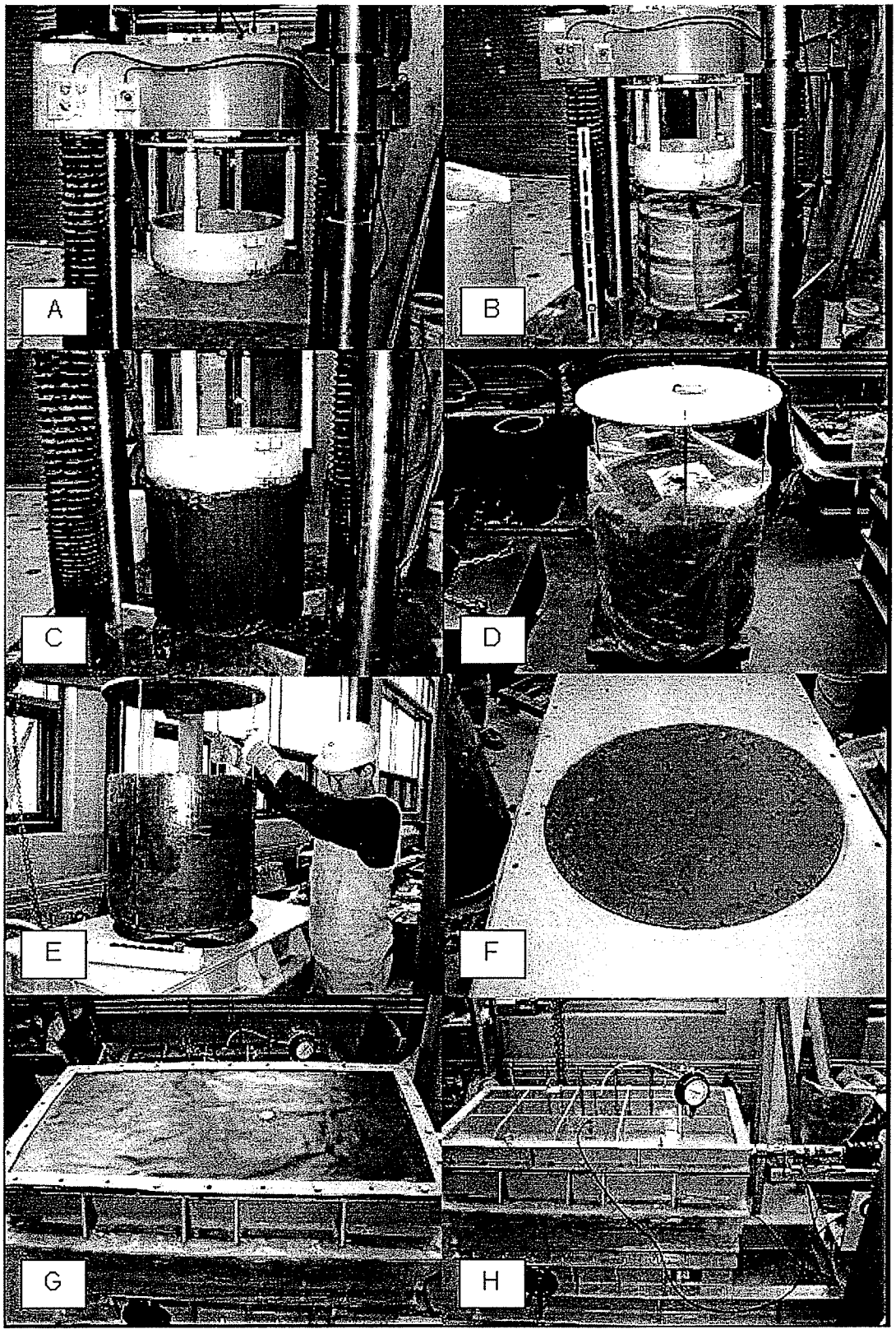

Figure 3.7 Procedure of direct shear testing for undisturbed clay specimen

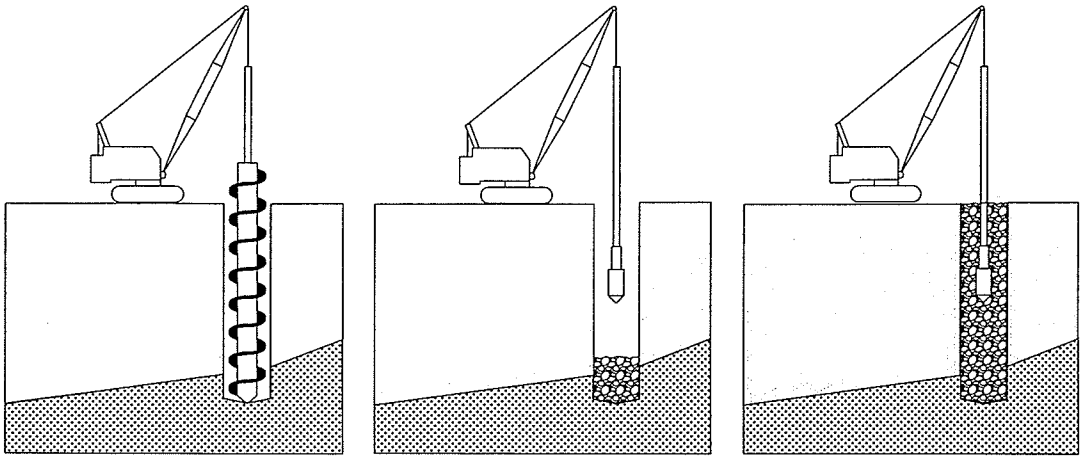

Figure 3.8 Replacement method for installation of rockfill columns (after Baumann and Bauer 1974)

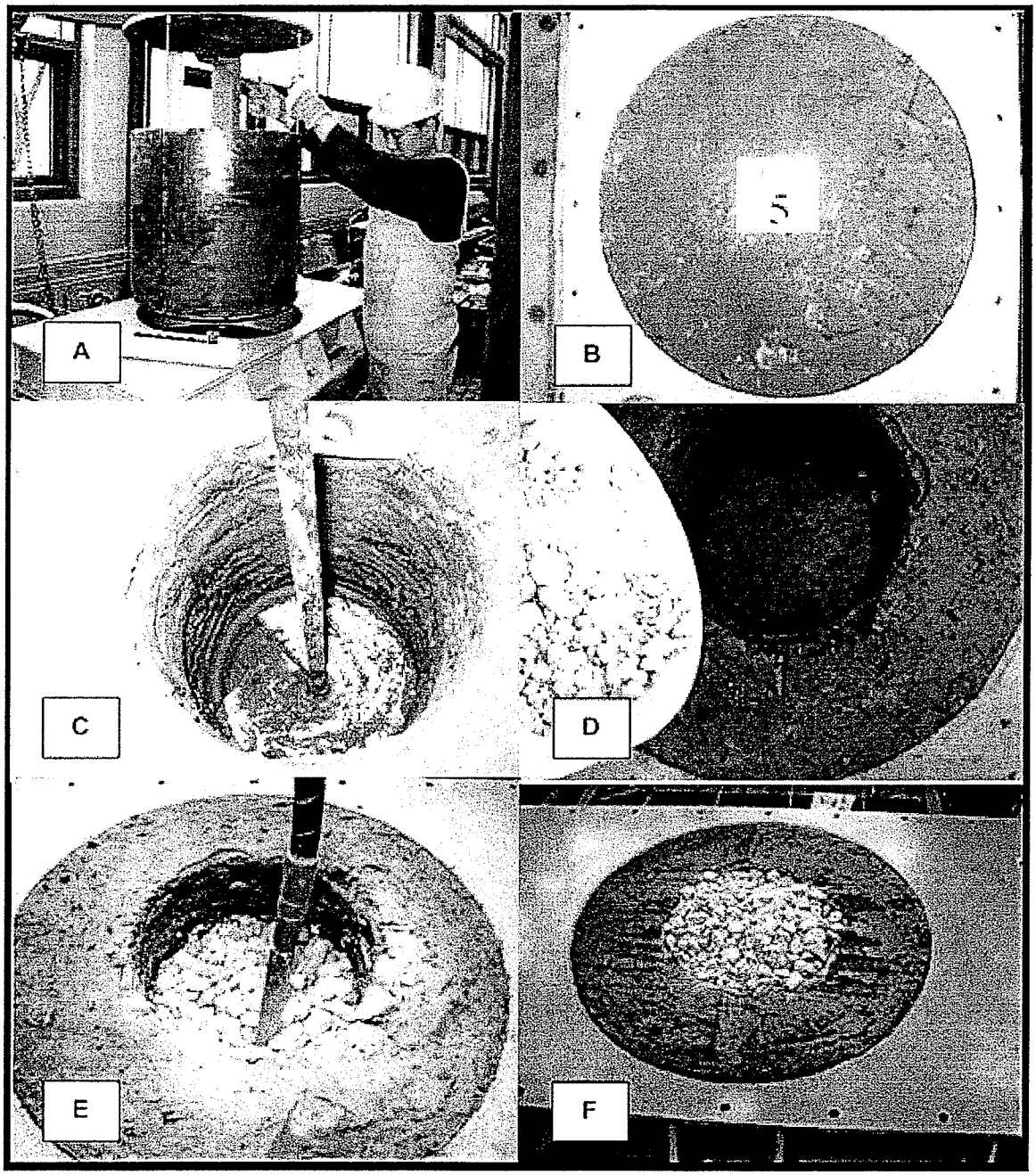

Figure 3.9 Procedure of direct shear testing for rockfill-clay composite

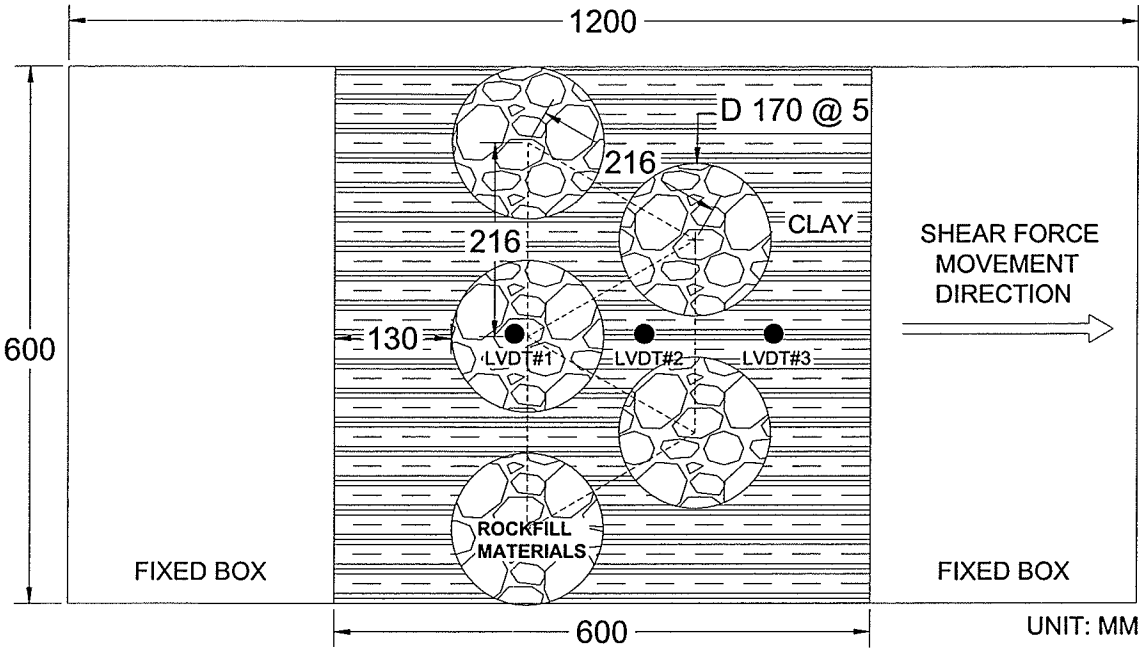

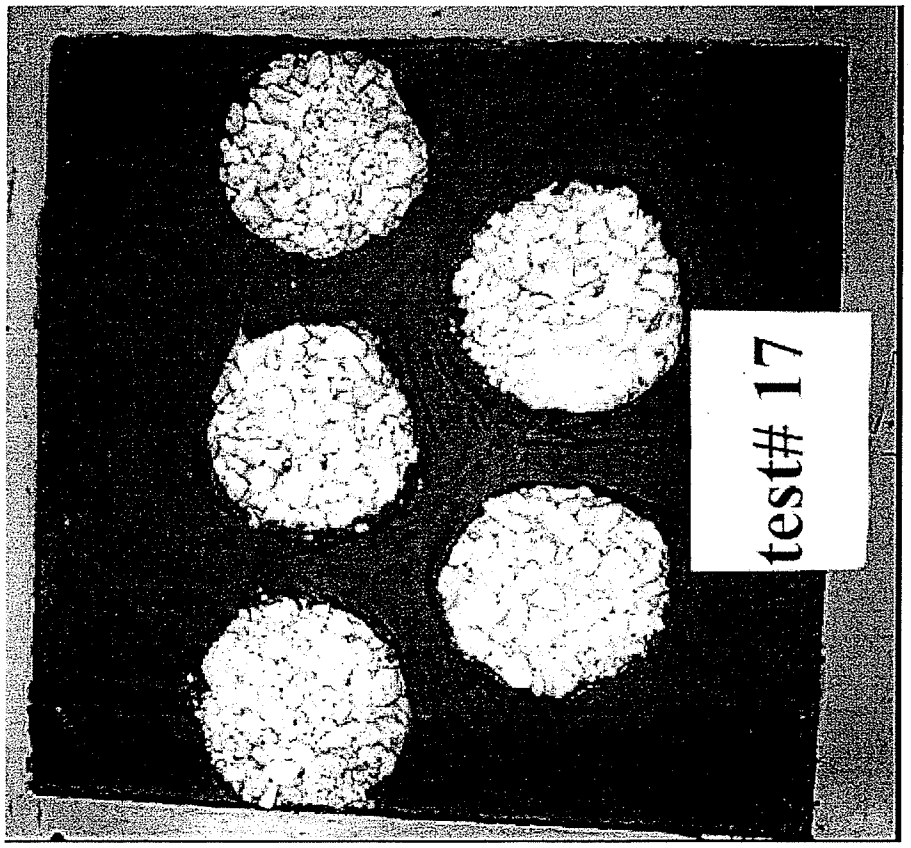

Figure 3.10 Layout of open-spacing rockfill columns in group

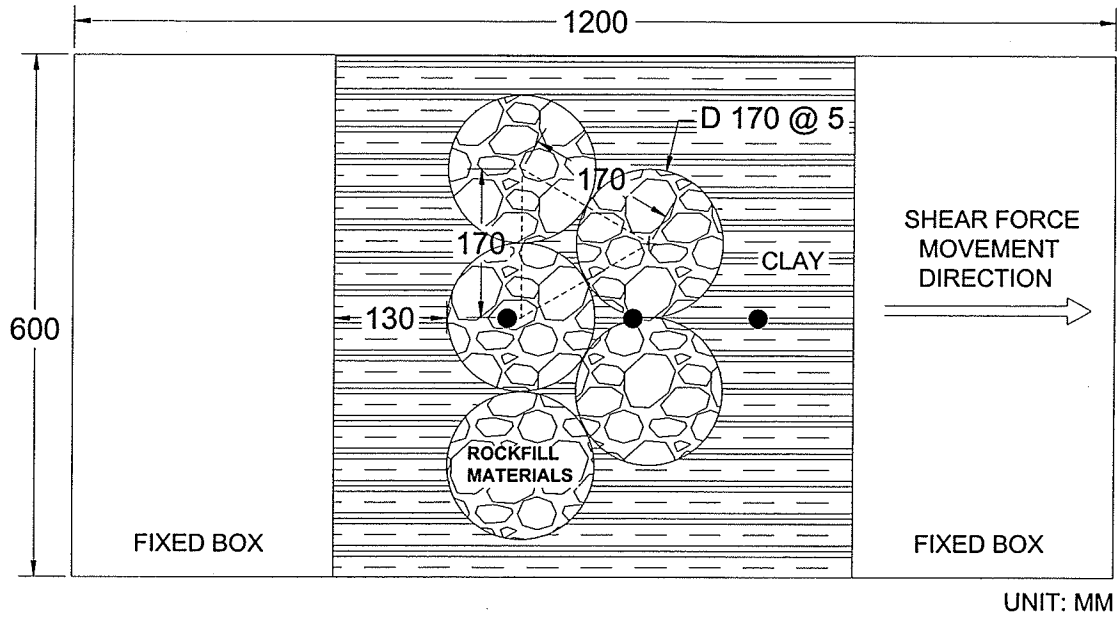

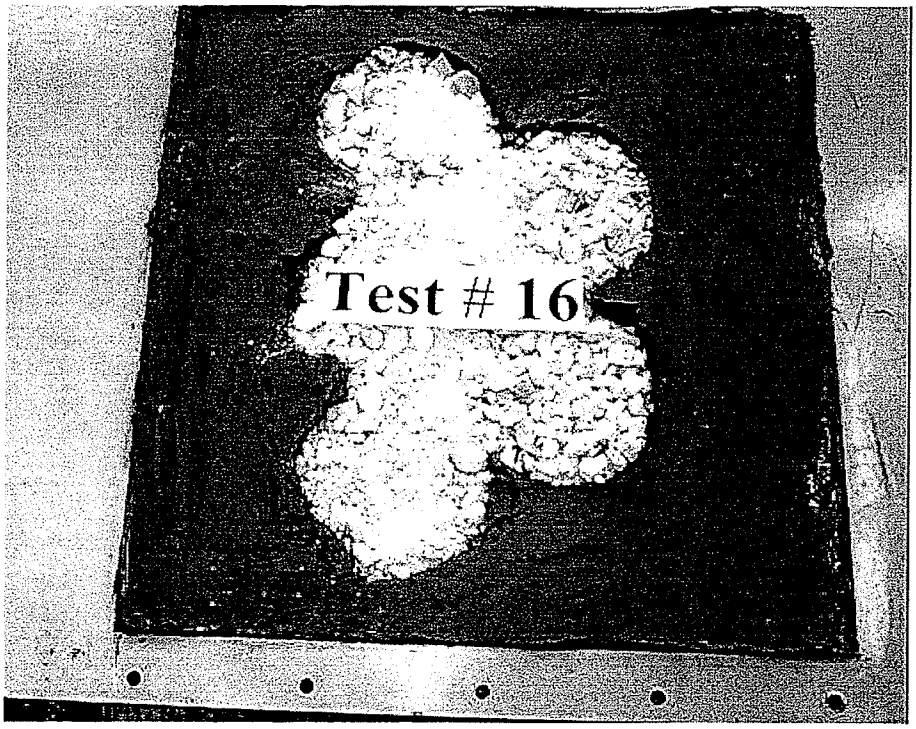

Figure 3.11 Layout of close-spacing rockfill columns in group

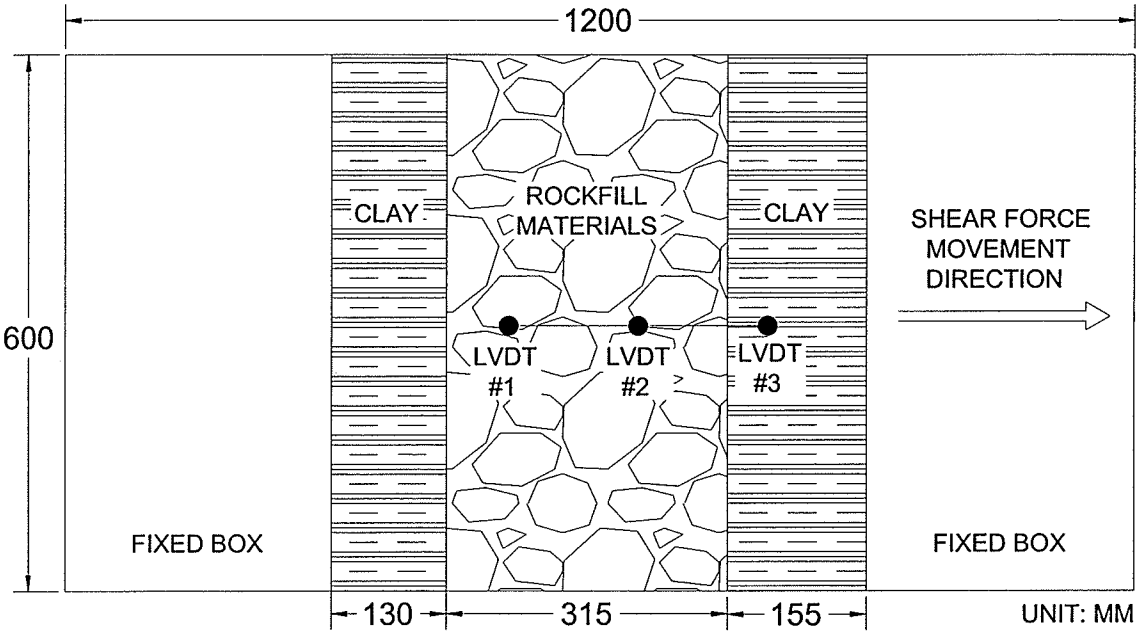

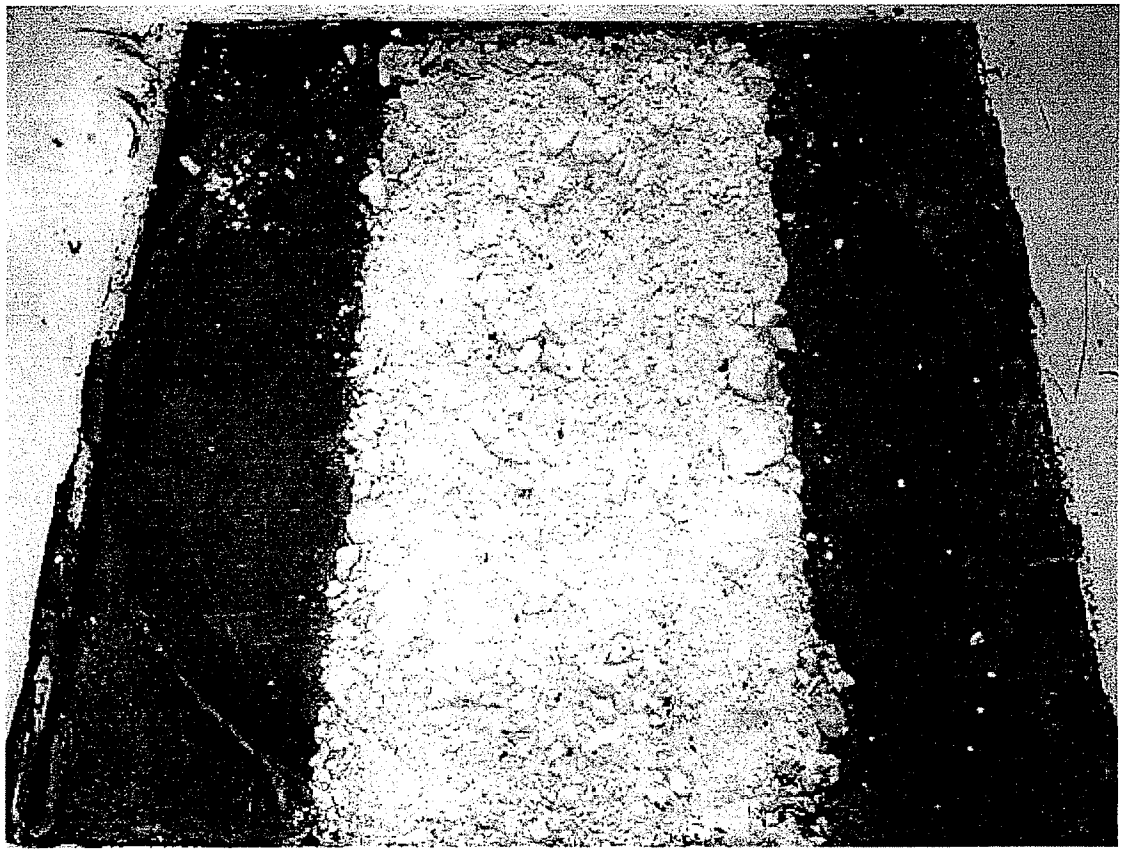

Figure 3.12 Shear key layout

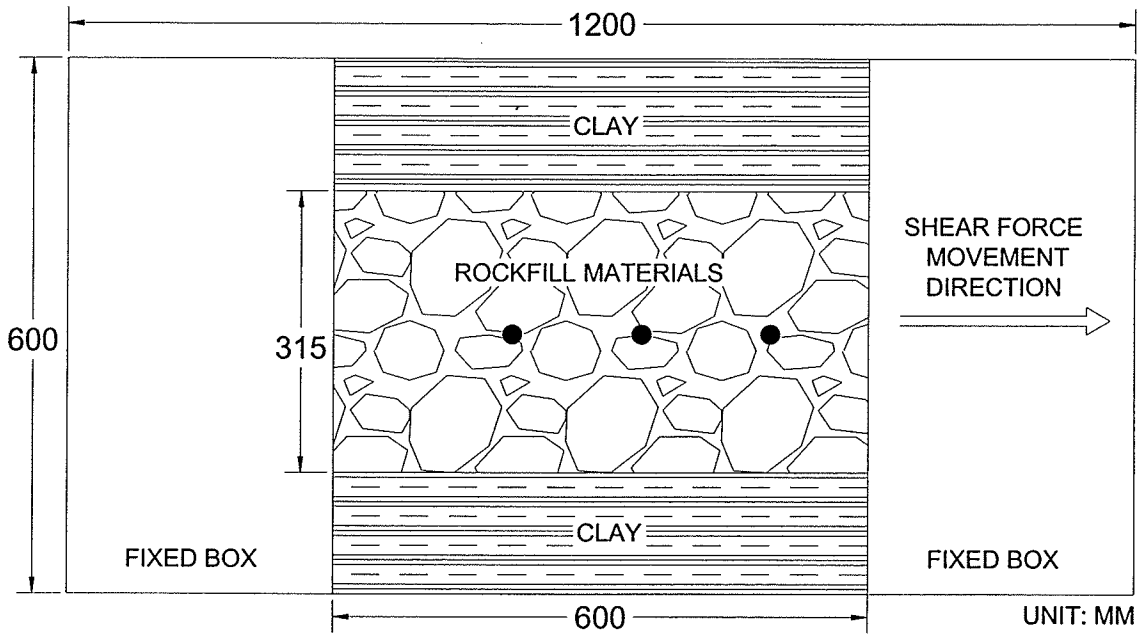

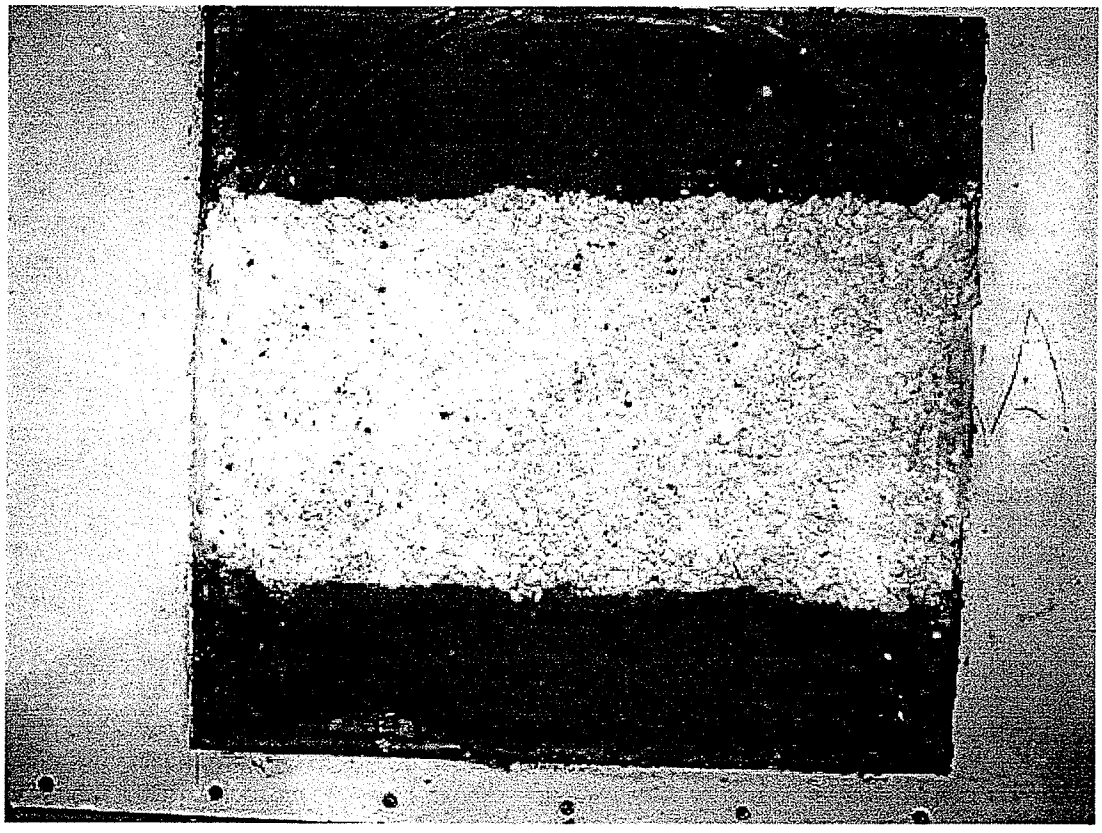

Figure 3.13 Ribbed-type layout

Table 3.1 Geotechnical properties of lacustrine clay samples

Test	Range of values
Natural water content	57-67 %
Liquid limit	76-80 %
Plastic limit	27-29 %
Plasticity index	50 %
Total unit weight	15.7 - 17.0 kN/m^3
Specific gravity	2.68

Table 3.2 Unit weight of the original and reduced size samples

	Relative density	Original sample kN/m^3	Reduced-scale sample kN/m^3
1	Loose	14.7	15.0
2	Medium-dense	17.0	17.3
3	Dense	18.6	19.1

CHAPTER 4

RESULTS AND DISCUSSIONS

4.1 INTRODUCTION

The mobilization of shear resistance of rockfill materials, native clay and rockfill-clay composite soil samples were investigated using large-scale direct shear test equipment. The effects of various normal stresses and different densities on stress-strain behaviour of rockfill materials and native clay specimens are presented in the Section 4.2 and 4.3. Section 4.4 discusses the mobilization of shear resistance of rockfill-clay composite materials. The succeeding sections evaluate the effects of different area replacement ratios, cementation in rockfill column materials, and the influence of rockfill columns in groups and shear key and rib layouts.

4.2 STRESS-STRAIN CHARATERISTICS OF ROCKFILL MATERIALS

The stress-strain relationships of rockfill materials are shown in Figures 4.1 and 4.2 corresponding to dense and loose conditions, respectively. They were tested under the applied normal stresses of 50, 75 and 100 kPa. Plots of shear load normalized with normal load (T/N) versus shear displacement normalized with diameter of sample ($\delta l/D$) are also shown in these figures. Higher shear resistance was mobilized at higher applied normal stress as would be expected. The mobilized shear stresses in the densely compacted rockfill material were almost twice higher than those in the loosely compacted rockfill material under the same applied normal stresses. The shear stiffness

for the dense material was up to four times higher than the loose material, depending on the shear strain level and applied normal stress. This indicates that the density achieved with the placement of rockfill materials during column installations has a significant impact on the movements required to mobilize shearing resistance. In addition, the mobilization of shear resistance is associated with volume change during shear, which is also dependent on the density of rockfill materials, as presented in the following section.

4.2.1 Volume change during shear

The term dilatancy has been applied to the relationship between shear stress and volume change in particulate materials. When the densely compacted rockfill material is subjected to shear stress as shown in Figure 4.3(a), the particles above the contact surface must roll up and over each other. As a result of the shear deformation, the increase in the volume of rockfill materials will occur. By contrast, in case of the loosely compacted rockfill material, particles are compressed when subjected to shear stress as shown in Figure 4.3(b).

Vertical displacements were measured by LVDT #1, #2 and #3 mounted on the top cover of the equipment while LVDT #4 was used to measure horizontal (shear) displacements. LVDT #1, #2, and #3 are equally spaced and arranged from the farthest to the closest from the direction of movement (see Figure 3.3). Figure 4.4 shows progressive mobilization of shear resistance from the back of the direct shear apparatus to the front. The vertical displacement of #1 at a given shear displacement is higher than that of LVDT #2 and LVDT #3 in that order. This means that there is a progressive mobilization of shear displacement along the length of sheared surface (i.e. from the back of the shear box to the front). The implication of this observation is that the shear

mobilization of rockfill material is higher at a higher point on the slope and the lower point on the slope has lesser shear mobilization than the point above. This can be valuable information that will determine the best arrangement of rockfill columns at the riverbank. This behaviour was similar for all relative density conditions; dense and loose. It can be seen in Figure 4.4 that LVDT #2 (middle LVDT) is a reasonable average of all the three readings and therefore can be interpreted as the representative of the vertical displacement during shearing along the entire sample diameter.

Figures 4.5 and 4.6 show plots of vertical displacements against the horizontal displacement for the dense and loose materials, respectively. The densely compacted rockfill material underwent small volume compression at the beginning of shearing due to compression of the particles and rearrangement of the particles by the sliding of the rounded particles. Volume expansion or dilatancy occurred during the latter phase of shearing as shown in Figure 4.4. For the loosely compacted rockfill material, more volume compression took place but later exhibited dilatancy at larger shear displacements. This observation deviated from the common understanding that granular materials in a smaller density (loose) would contract during shearing until they reached the critical state where there is constant shear stress and constant volume during shearing. Dilation at large shear displacements even for loose rockfill materials may be attributed to progressive mobilization of shear for this particular test setup as discussed in the previous paragraph. The progressive mobilization of shear would somehow result in rearrangement of particles. This rearrangement would lead to a transition from contraction to dilation. The transition period represents minimal volume change during shearing and this can be considered as the period of no volume change (i.e. corresponding to critical state). The measurements of vertical displacements during

shearing are therefore important in evaluating the mobilized shear strength of rockfill material.

Varadarajan et. al. (2003) provided the possible reason to show dilation in rockfill materials was due to the breakage of particles. The angular particles provide a high degree of interlocking and cause dilation during shearing. During the latter phase of shearing, dilatancy is more, leading to volume expansion.

4.2.2 Shear strength of rockfill materials

Typical stress-strain relationships for dense granular materials would generally show three points (B, C, and D) in the stress-strain plot as shown in Figure 4.7 (Atkinson 1992). The first point is termed 'transition' shear resistance (Point B) at which the rate of volume change is zero ($\psi = 0$). Further shearing leads to 'peak' shearing resistance (Point C) and then 'critical state' shear resistance (Point D). The conditions of critical state (Point D) could not be reached in the test equipment used in this research due to the offload capacity limitation of the large-scale direct shear equipment. However, the 'transition' shear resistance (Point B) occurs at a relatively smaller shear strain and was found to be generally equivalent in value to the critical state shear resistance (Atkinson 1992). Therefore, the 'transition' friction angle, $\phi'_{transition}$ is also equivalent to the 'critical state' friction angle, $\phi'_{critical}$ for densely compacted rockfill material that engineers used in the stability analysis of riverbanks. The transition shear resistance lies on a straight line of gradient tan $\phi'_{transition}$ in the τ - σ_N space as shown in Figure 4.8. As such the critical friction angle, $\phi'_{critical}$ can be determined to be about 37°. For the loosely compacted rockfill material, the shear stress at critical state was determined by the shear stress

corresponding to shear displacement at the transition period from contraction to dilation. It was found that the $\phi'_{transition}$ value for the densely compacted rockfill material was comparable with the $\phi'_{critical}$ value for the loosely compacted rockfill material.

Figures 4.9 and 4.10 show the peak friction angles, ϕ'_{peak} decreased as applied normal stresses increased. It should be noted that the peak shear resistance (Point C) is considered transient and sustainable only while the soil is dilating although there has been an on-going debate on the use of ϕ'_{peak} or $\phi'_{critical}$ in designing geotechnical structures (Bolton 1991, Powrie 1997). The envelope generated by the peak strength tended to be curved until it reached to the critical state value. The results confirm the general observation for the shear strength of densely compacted rockfill materials as illustrated by Budhu (2001) in Figure 4.11.

It was found that for a particular rockfill material, the peak strength was dependent on the initial void ratio and the normal stress applied at the planes of shearing. Lower applied normal stress led to greater dilation angle and more mobilized peak friction angle. As shown in Figure 4.9 the peak friction angle was 65° at 50 kPa normal stress and it dropped to 57° and 56° at 75 and 100 kPa normal stresses, respectively.

As mentioned in Section 3.5, the stress-strain characteristics of the granular materials will be similar as long as their gradations are parallel. Reduced-scale rockfill materials for rockfill-clay composite soil samples were tested to compare the stress-strain behaviour with the original rockfill material. The maximum grain diameter of the original and reduced-scale rockfill materials was 60 and 27 mm, respectively. Figure 4.12 shows the comparison between two different grain sizes. Their stress-strain behaviour was very

similar and therefore justified the use of reduced-scale rockfill materials for tests on rockfill-clay composite materials.

4.3 STRESS-STRAIN CHARACTERISTICS OF LACUSTRINE WINNIPEG CLAY

Large-scale and conventional direct shear tests were conducted on undisturbed lacustrine clay to determine the mobilization of shear resistance under the same boundary condition and scale effects with rockfill-clay composite test setup. Figure 4.13 shows the resulting stress-strain curves from large-scale undrained direct shear tests at 50 and 100 kPa normal stresses. As anticipated, the results for two normal stresses were similar under undrained conditions where there was no change of effective normal stress with increase in applied normal stress.

In order to determine the effective shear strength parameters, conventional direct shear tests were performed at 50, 100 and 200 kPa normal stresses under drained conditions. The peak strength parameters were estimated to be c' = 6 kPa and ϕ'_{peak} = 16° while the post peak strength parameters were c' = 4 kPa and ϕ'_{cs} = 15° as shown in Figure 4.14. The residual shear strength parameters of lacustrine clay were c' ≈ 3 kPa and ϕ'_{cs} = 8°. As discussed in Section 2.4, using peak strength parameters led to inaccurate and overestimated factors of safety for slope stability. Therefore the post peak strength parameters (critical state parameters) are used in a series of numerical simulations performed in this study. The residual shear strength parameters are usually used in cases when the riverbank being stabilized has undergone previous failures.

4.4 STRESS-STRAIN CHARACTERISTICS OF ROCKFILL- CLAY COMPOSITES

The maximum sizes of reduced-scale rockfill material were 22, 27 and 32 mm corresponding to diameters of 220, 270, and 320 mm of rockfill column that are installed in the shear box. In the case where one rockfill column was installed in the undisturbed clay, only a 270 mm column diameter was used at 50 and 100 kPa applied normal stresses. Figure 4.15 shows a comparison of shear mobilization of rockfill-clay composite and native clay. It indicates that in terms of the mobilization of shear resistances of both soil samples, the shear resistance of rockfill column did not mobilize its full component of strength until the clay reached at about 2% shear strain. This means that the shear resistance in the rockfill column will mobilize only at shear strain greater than the strain corresponding to the peak strength of the clay. In this case, there could already be significant movements in the riverbanks before the stabilizing forces of rockfill columns will be in effect, depending on where the columns are located in the slope. These movements should be evaluated in the design as to whether or not they are acceptable for the structures at the proximity of the riverbank, even though the installation of rockfill columns raises the factor of safety against instability to acceptable levels.

4.4.1 Cementation effects in rockfill material and in rockfill-clay composite

Direct shear testing of cemented rockfill materials was first conducted. In Figure 4.16 the shear strength using 0.5% cement content increased significantly at small shear strain compared to the untreated rockfill material. However, the rate of shear resistance with the increase in shear strain started to decrease, which then converged to that of the untreated rockfill material at large shear strain. The results indicated that using a small

amount of cementation had little effect on the mobilization of shear resistance especially at large shear strain although the shear stiffness of the cemented rockfill material at relatively small shear strain was almost twice greater than that of the untreated rockfill material.

Figure 4.17 shows the stress-strain characteristics of cemented rockfill-clay composite samples for cases where 2% and 5% of cement by dry weight were added to the rockfill material. It was found that the addition of different percentages of cementation in the rockfill material had little effect on both the shear stiffness and the ultimate shear strength of the composite soil. The most likely reason for the insignificant effect of cementation was the change in the mode of failure between the composite material with and without cementation. In the rockfill material without cementation, the mode of failure was direct shearing through the clay and rockfill materials in sequence. With cementation, the dominating mode of failure was a passive-type of failure governed by the shear strength of clay which is much less than the shear strength of the rockfill as shown in Figure 4.18. This was verified by visual inspection of the failure mode where the clay moved around the intact cemented rockfill column during the tests. This finding suggests that the cemented rockfill columns should be arranged close enough and in staggered manner so that they act as a group and not to allow the clay to move in between them during slope movements.

4.4.2 Effects of various area replacement ratios

The effects of different column sizes (D) relative to the spacing (s) were investigated on rockfill-clay composite soil samples using the area replacement ratio (a_s) discussed in the Section 2.5. Remolded clay was used for these series of tests due to the limited

amount of large undisturbed clay samples. Figure 4.19 shows the results of various area replacement ratios of 14%, 22% and 30% corresponding to column diameters of 220 mm, 270 mm and 320 mm, respectively. As would be expected, the mobilized shear resistance increased as area replacement ratios increased. However, increasing area replacement ratios did not increase the shear stiffness of the composite particularly at smaller shear strain as at this strain level the resistance of the composite material is governed by the resistance of the clay.

4.5 STRESS-STRAIN CHARACTERISTICS OF ROCKFILL COLUMNS IN GROUPS COMPARED WITH SHEAR KEY AND RIBBED-TYPE LAYOUTS

The behaviour of rockfill columns in group was investigated and then compared with shear key and rib layouts that have also been commonly used to stabilize riverbanks in Winnipeg. The effects of column spacing were first examined. Five rockfill columns were installed by using casing and each column diameter was 170 mm with a close column spacing of 216 mm. The stress-strain behaviour of rockfill columns in a group compared with the shear key layout is shown in Figure 4.20. The closed spacing pattern led to higher shear strength while the shear strength in the opened spacing pattern was almost the same as that in the shear key layout. The result indicated that variation of spacing within groups of rockfill columns had little improvement on both the mobilized shear resistance and shear stiffness of the composite soil.

In testing for columns in groups, casing was first pushed into the clay and then drilled holes for rockfill columns. The casing was used to prevent the surrounding clay from collapsing during installation of the neighbouring rockfill columns. In the field, casing is only required if there is potential for hole instability. The effect of using casing in the

installation of rockfill columns on the shear mobilization has been investigated. The result indicated that there was no difference on the stress-strain behaviour of both tests as shown in Figure 4.21. In spite of the result, casing is generally recommended for in-situ soil conditions where borehole stability is questionable and the ground water table is very high (FHWA 1983).

A comparison between the ribbed-type and shear key layouts is shown in Figure 4.22. Higher mobilization of shear strength mobilized is observed in the ribbed-type layout compared to the shear key. This is attributed to the simultaneous mobilization of shear resistance by both rockfill materials and clay in the rockfill-clay composite. The practical implication is that rockfill columns can be installed perpendicular to the riverbank (rib layout) to mobilized shear strength than the columns laid along the length of the riverbank (shear key layout).

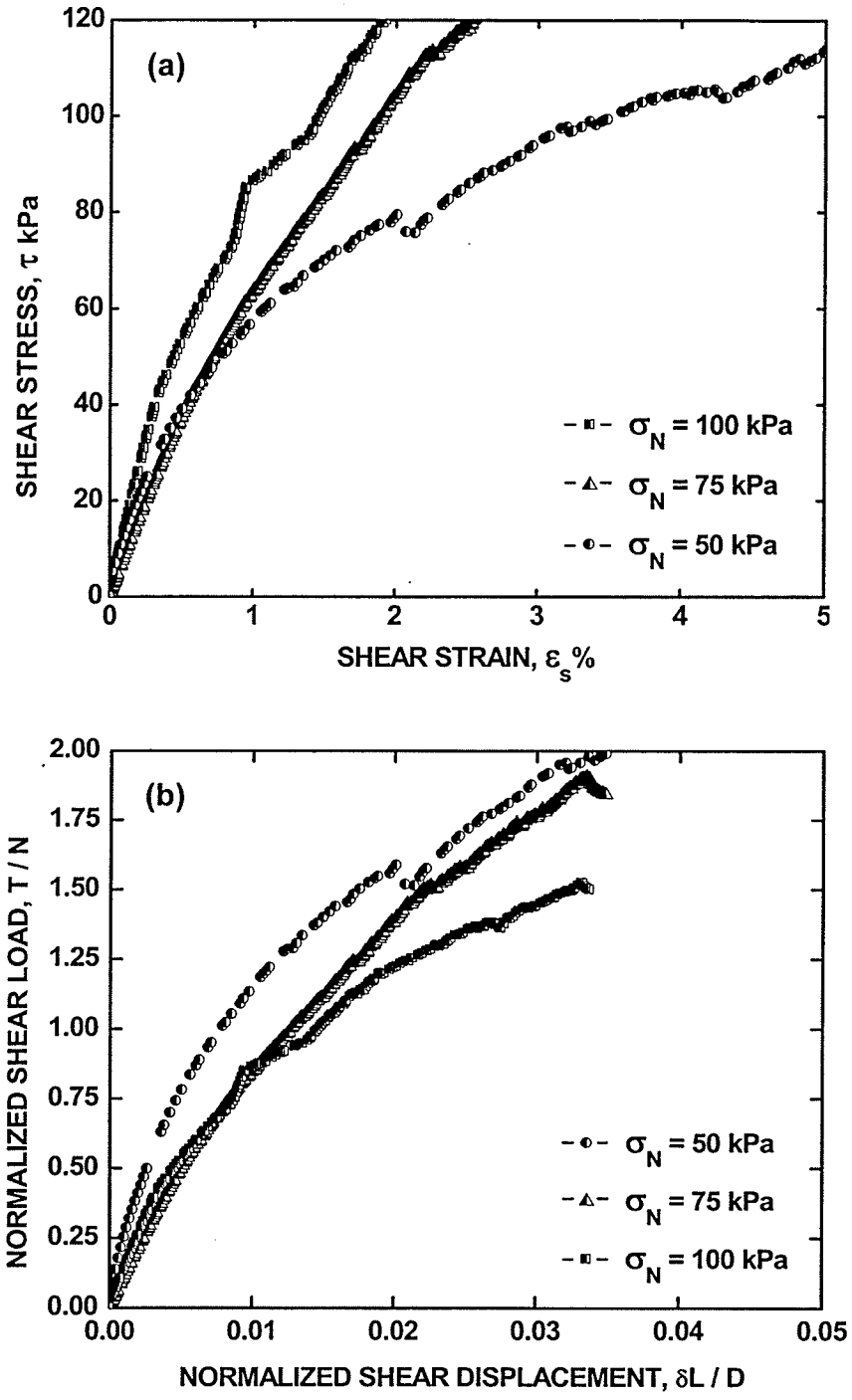

Figure 4.1 Shear mobilization on the densely compacted rockfill material
(a) shear stress vs. shear strain
(b) normalized shear load vs. normalized shear displacement

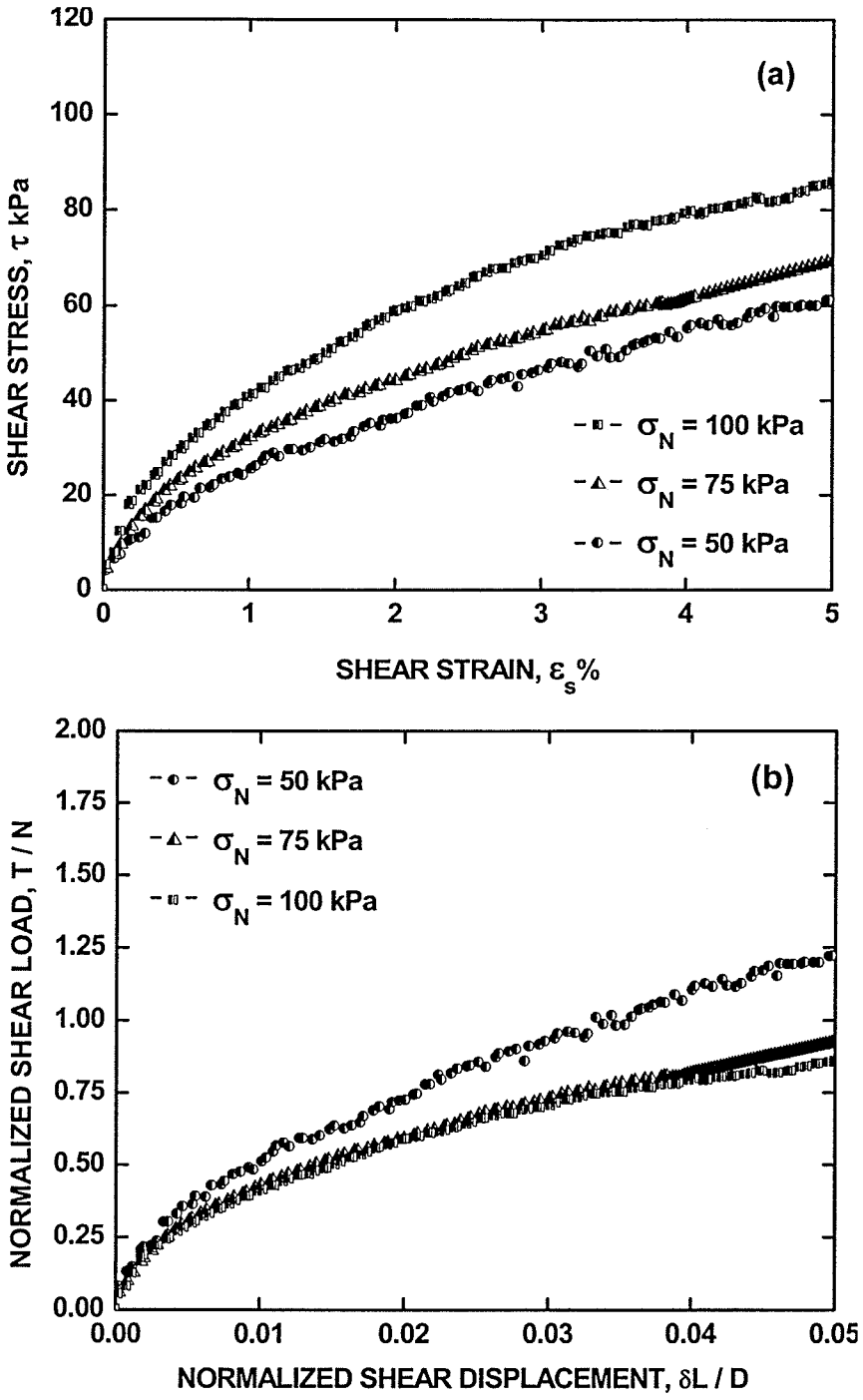

Figure 4.2 Shear mobilization on the loosely compacted rockfill material

(a) shear stress vs. shear strain

(b) normalized shear load vs. normalized shear displacement

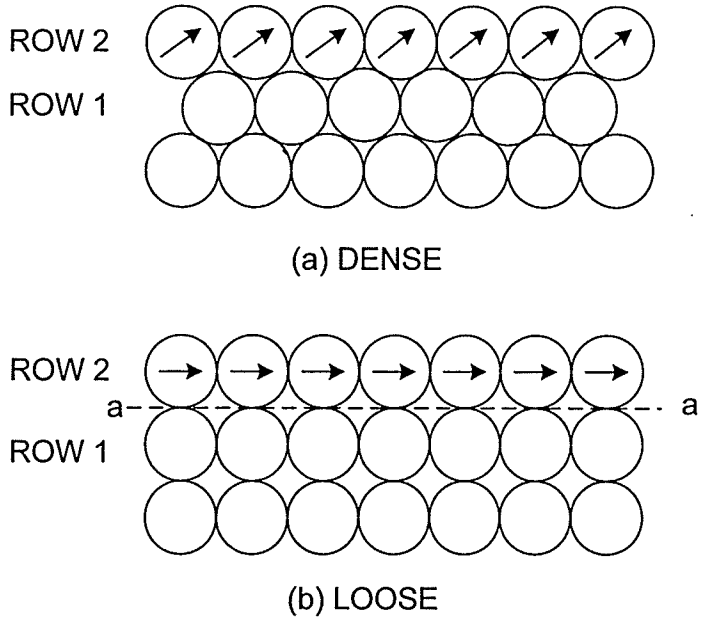

Figure 4.3 Packing of disks representing loose and dense granular materials (after Budhu 2001)

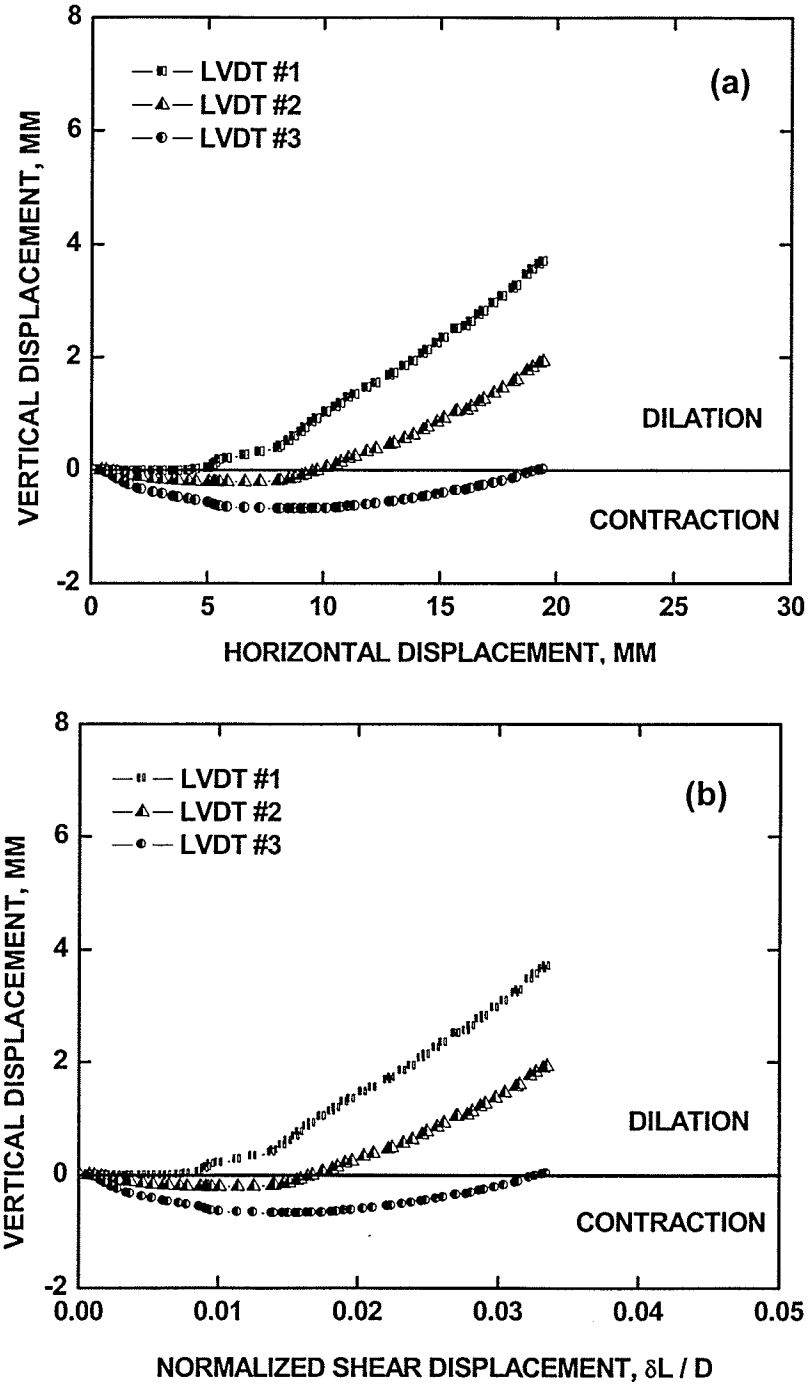

Figure 4.4 Vertical displacements of LVDTs during shearing on the densely compacted rockfill material (σ_N = 100 kPa)

(a) vertical displacement vs. horizontal (shear) displacement

(b) vertical displacement vs. normalized shear displacement

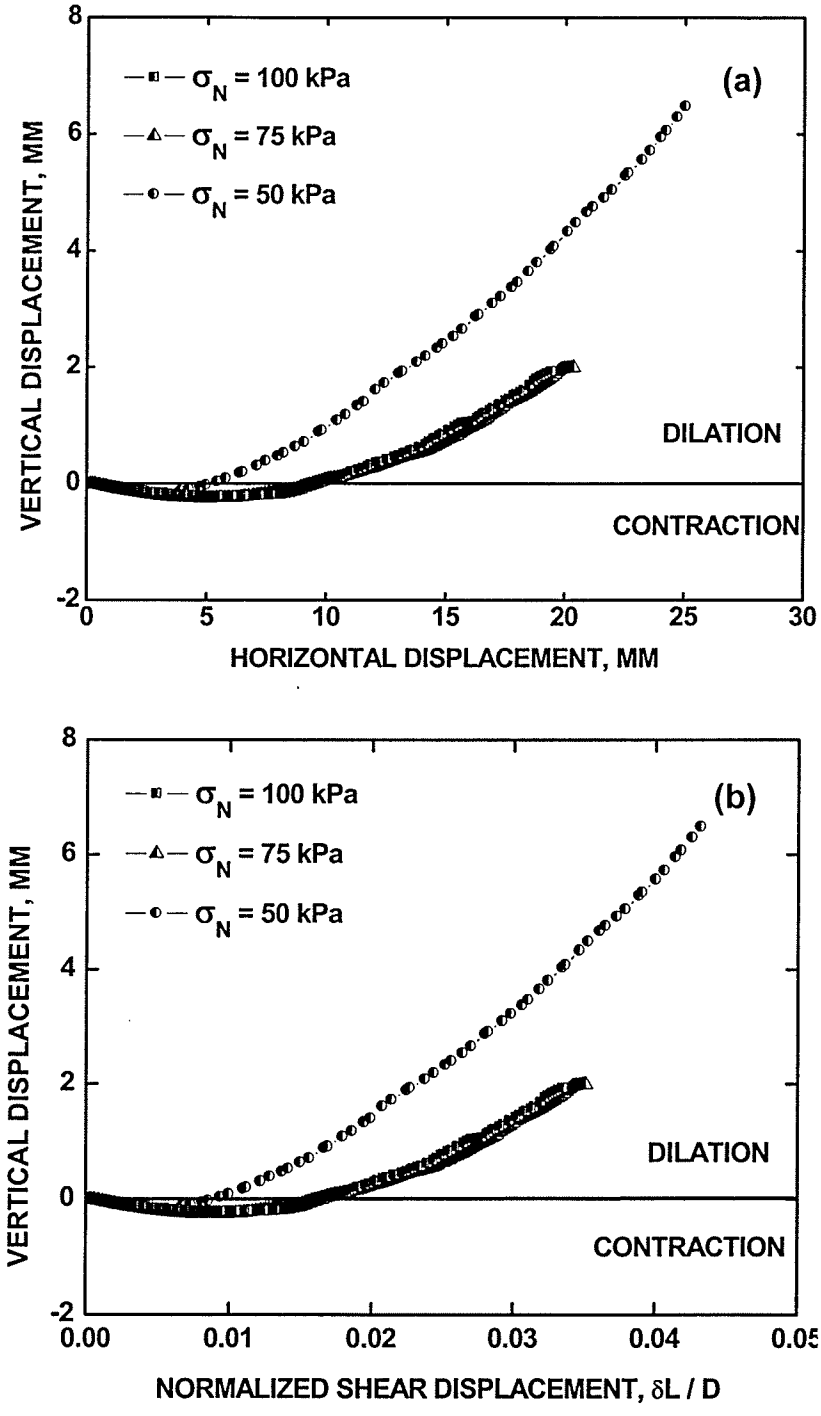

Figure 4.5 Volume change during shearing on the densely compacted rockfill material
(a) vertical displacement vs. horizontal displacement
(b) vertical displacement vs. normalized shear displacement

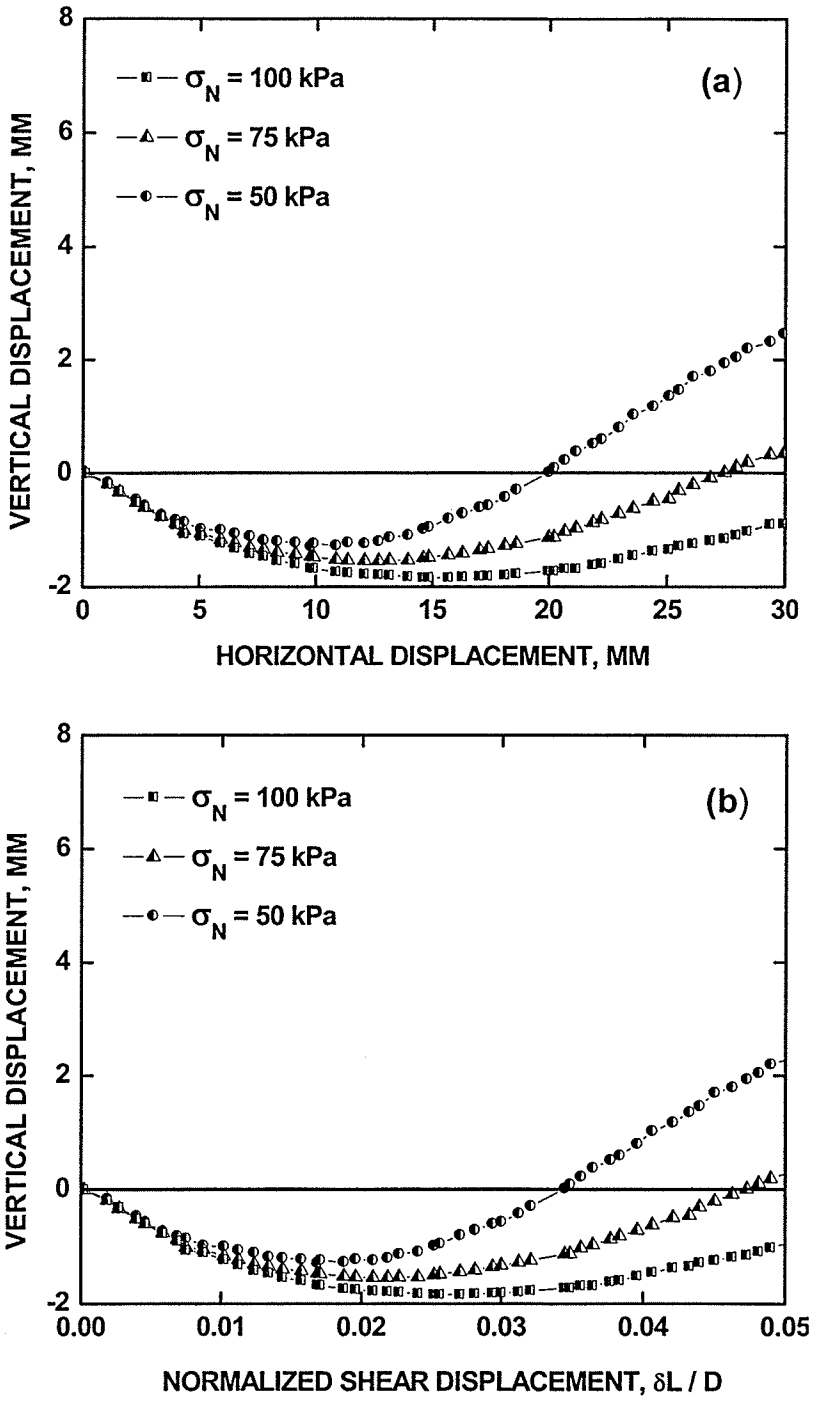

Figure 4.6 Volume change during shearing on the loosely compacted rockfill material

(a) vertical displacement vs. horizontal displacement

(b) vertical displacement vs. normalized shear displacement

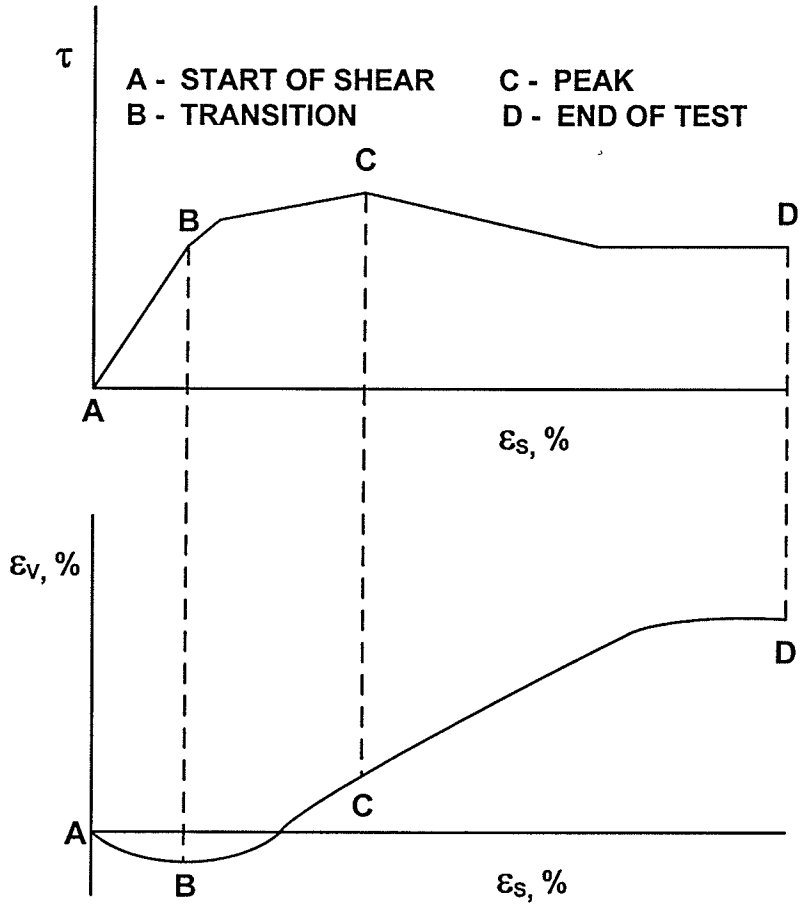

Figure 4.7 Shearing and dilation in shear test (after Atkinson 1992)

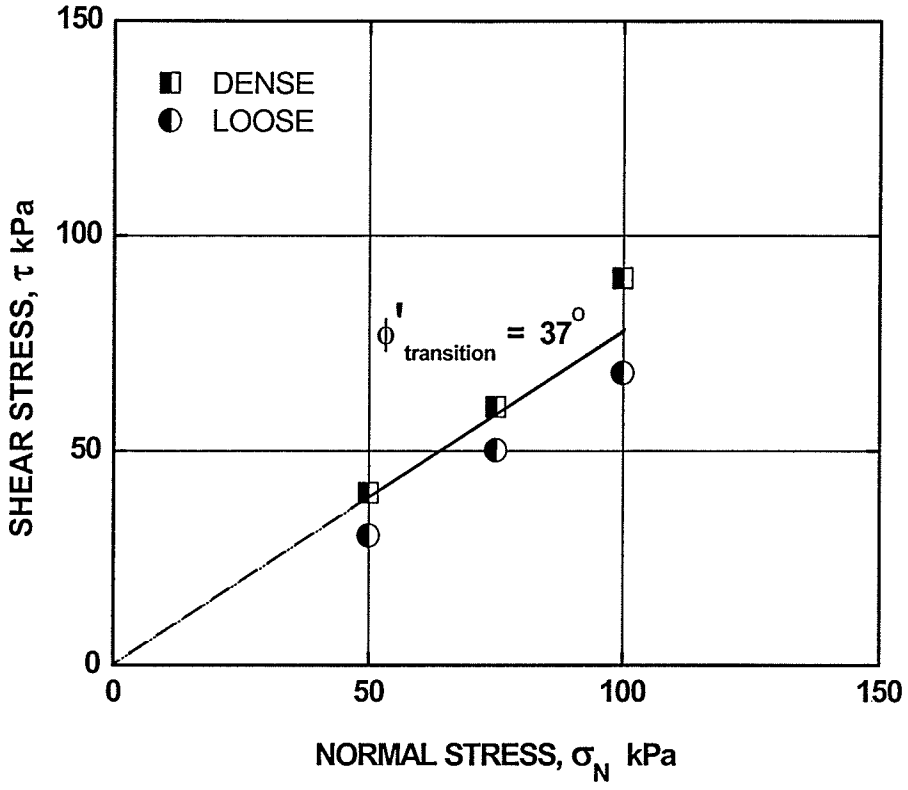

Figure 4.8 Transition friction angle of rockfill materials

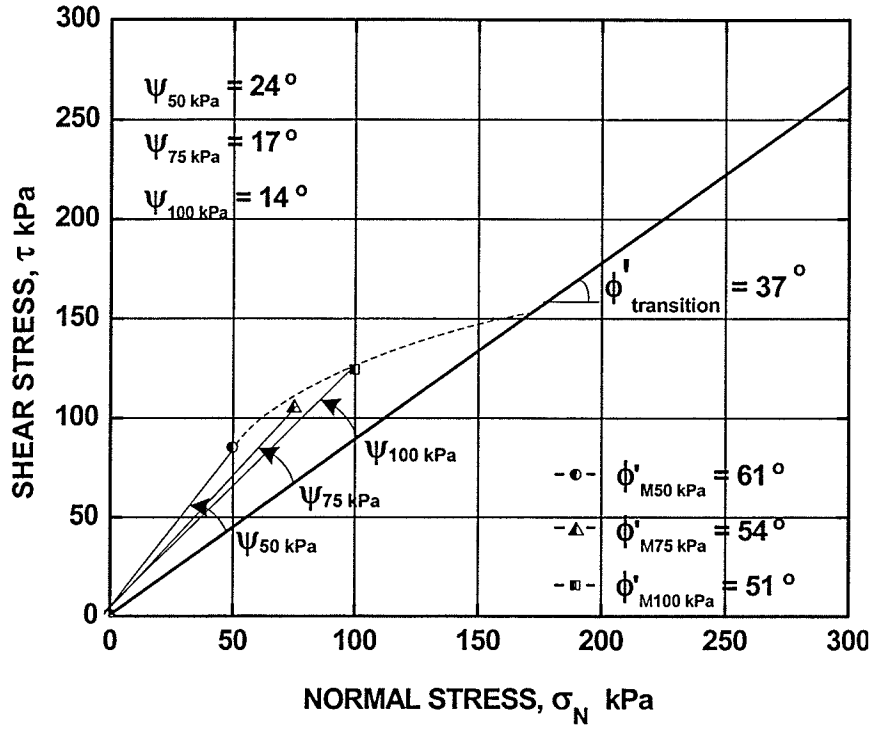

Figure 4.9 Mobilized friction angles of the densely compacted rockfill material

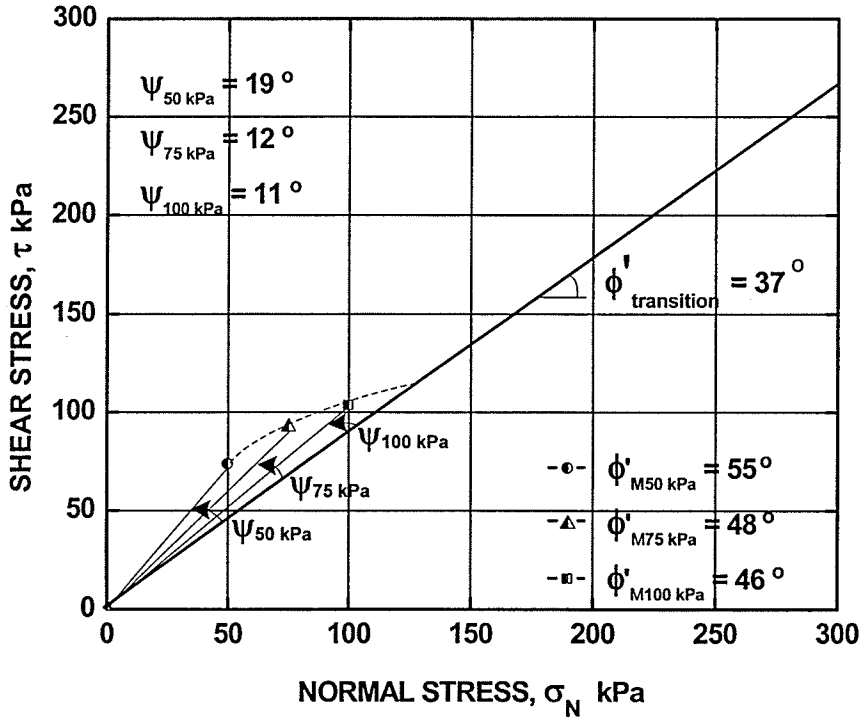

Figure 4.10 Mobilized friction angles of the loosely compacted rockfill material

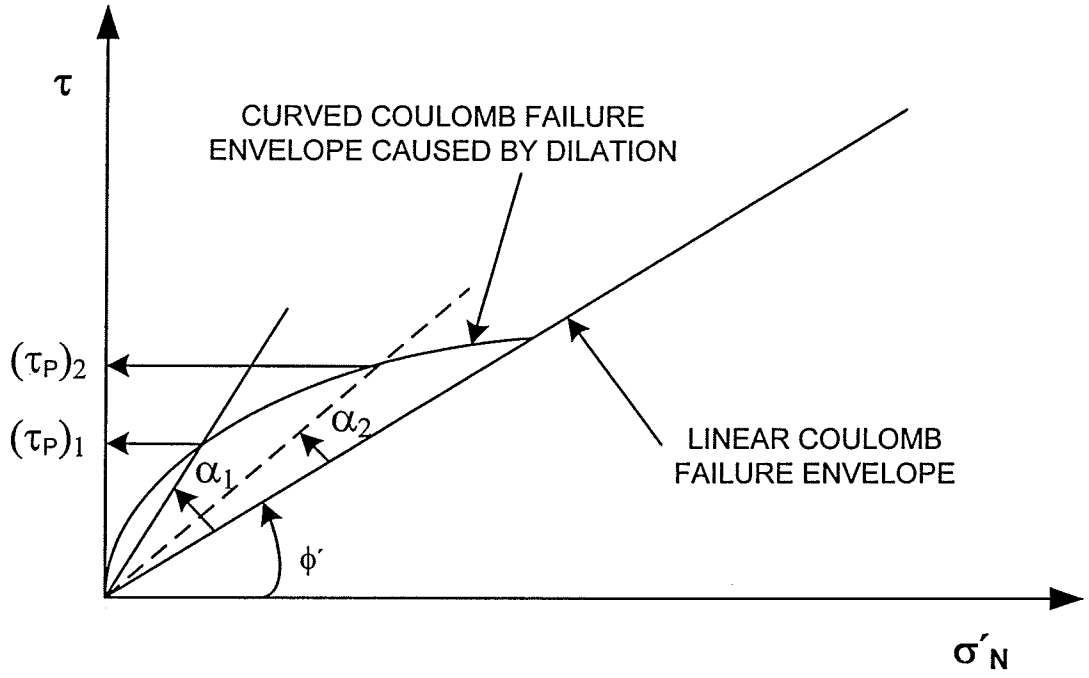

Figure 4.11 Dilation friction angles of granular materials (after Budhu 2001)

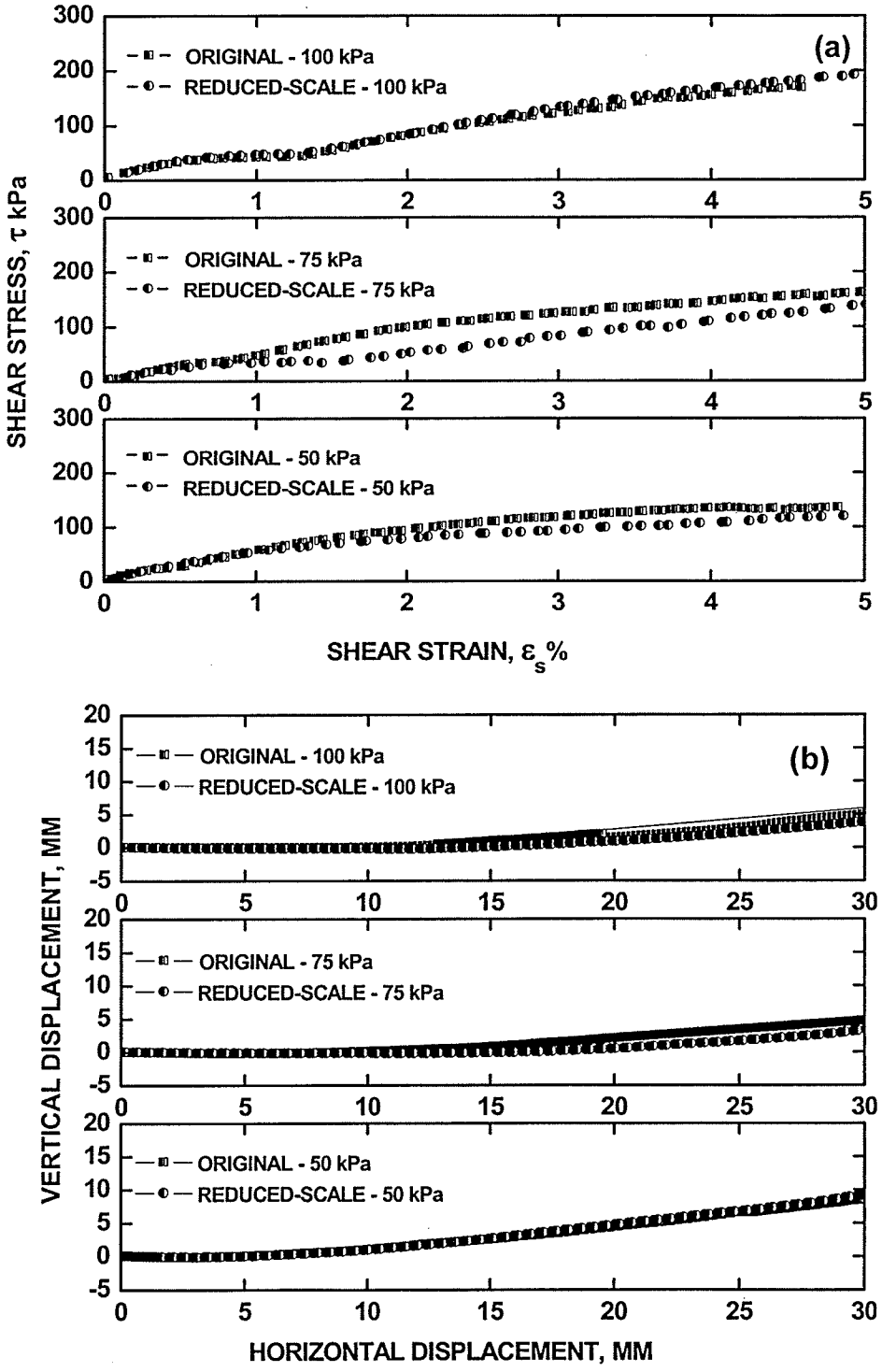

Figure 4.12 Comparisons between original and reduced-scale sizes

(a) shear stress vs. shear strain

(b) vertical displacement vs. horizontal displacement

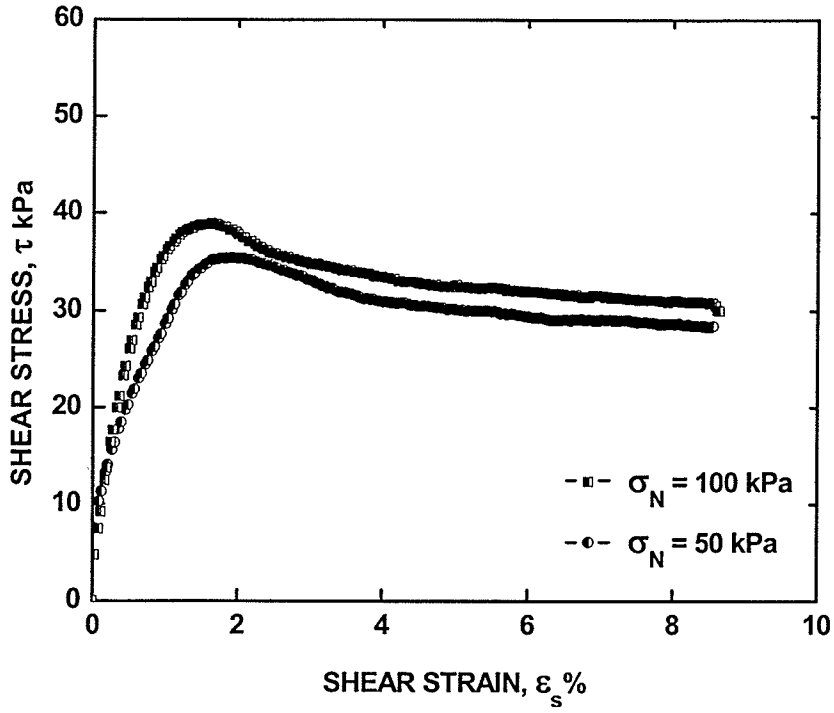

Figure 4.13 Shear stress-strain behaviour of undisturbed lacustrine clay (undrained)

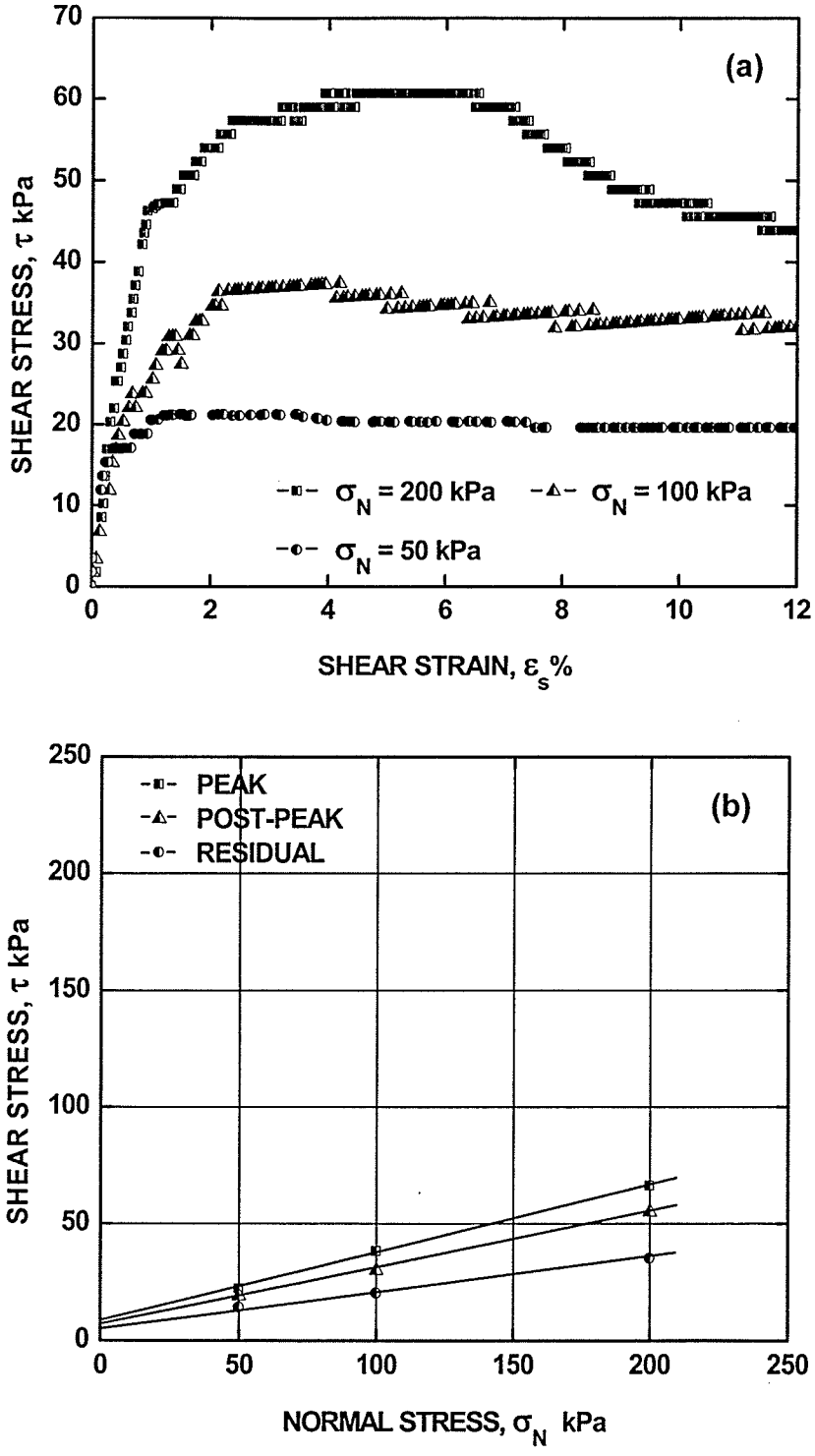

Figure 4.14 Conventional drained direct shear test for undisturbed plain clay

(a) shear stress vs. shear strain

(b) shear stress vs. normal stress

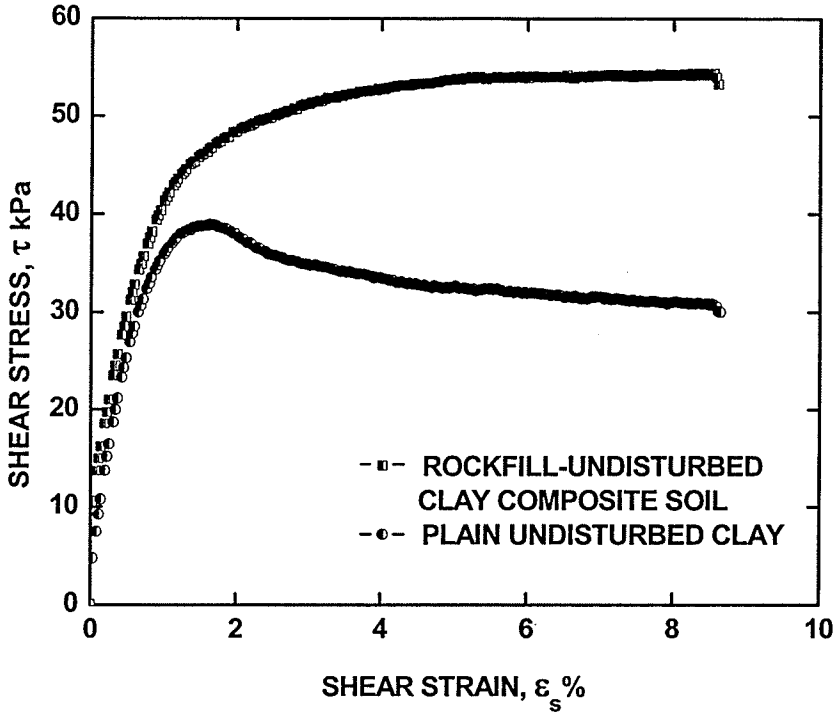

Figure 4.15 Shear mobilization between rockfill-undisturbed clay composite soil and undisturbed clay (σ_N = 100 kPa)

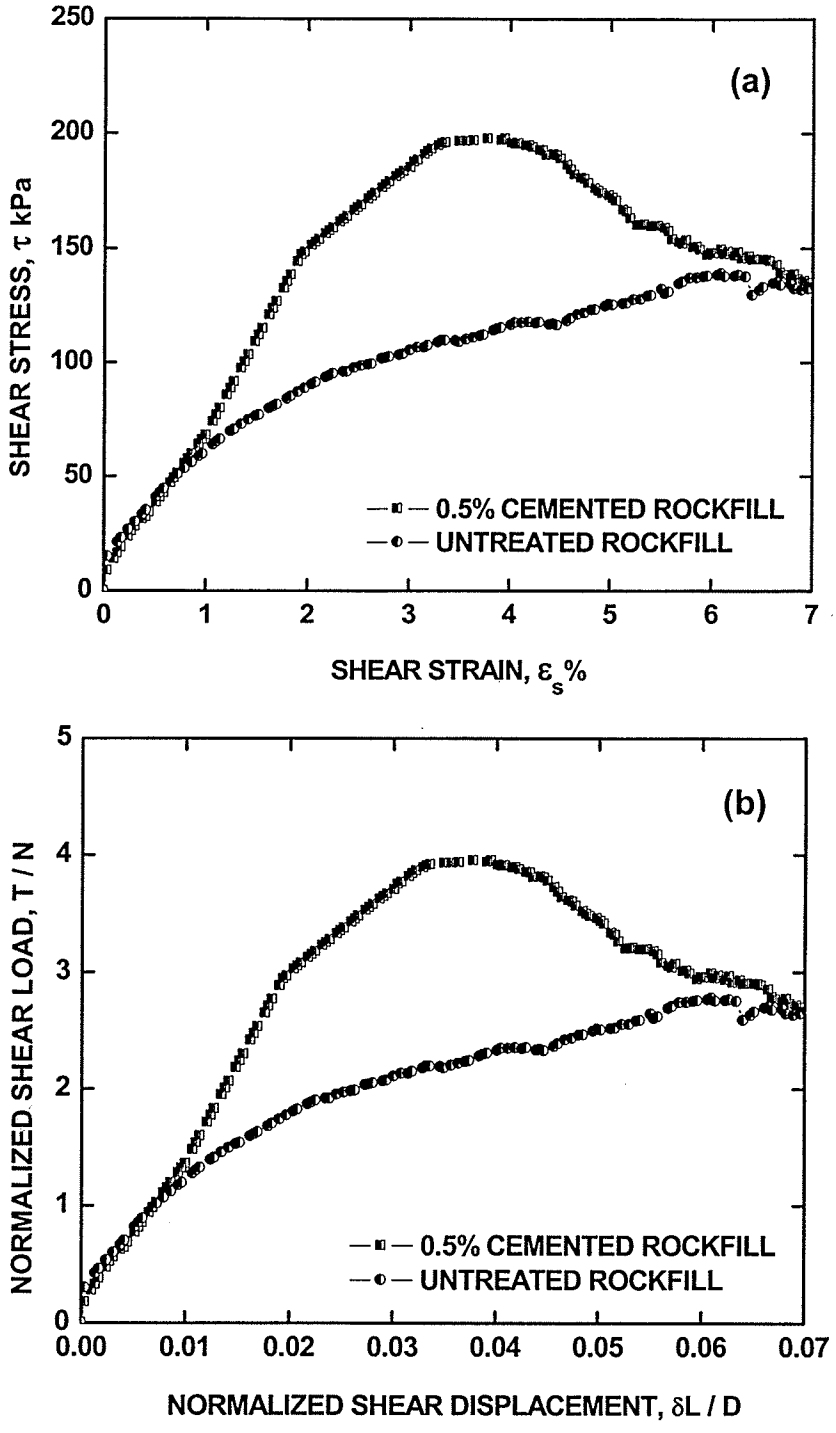

Figure 4.16 Shear mobilization of cemented rockfill materials (σ_N = 50 kPa)

(a) shear stress vs. shear strain

(b) normalized shear load vs. normalized shear displacement

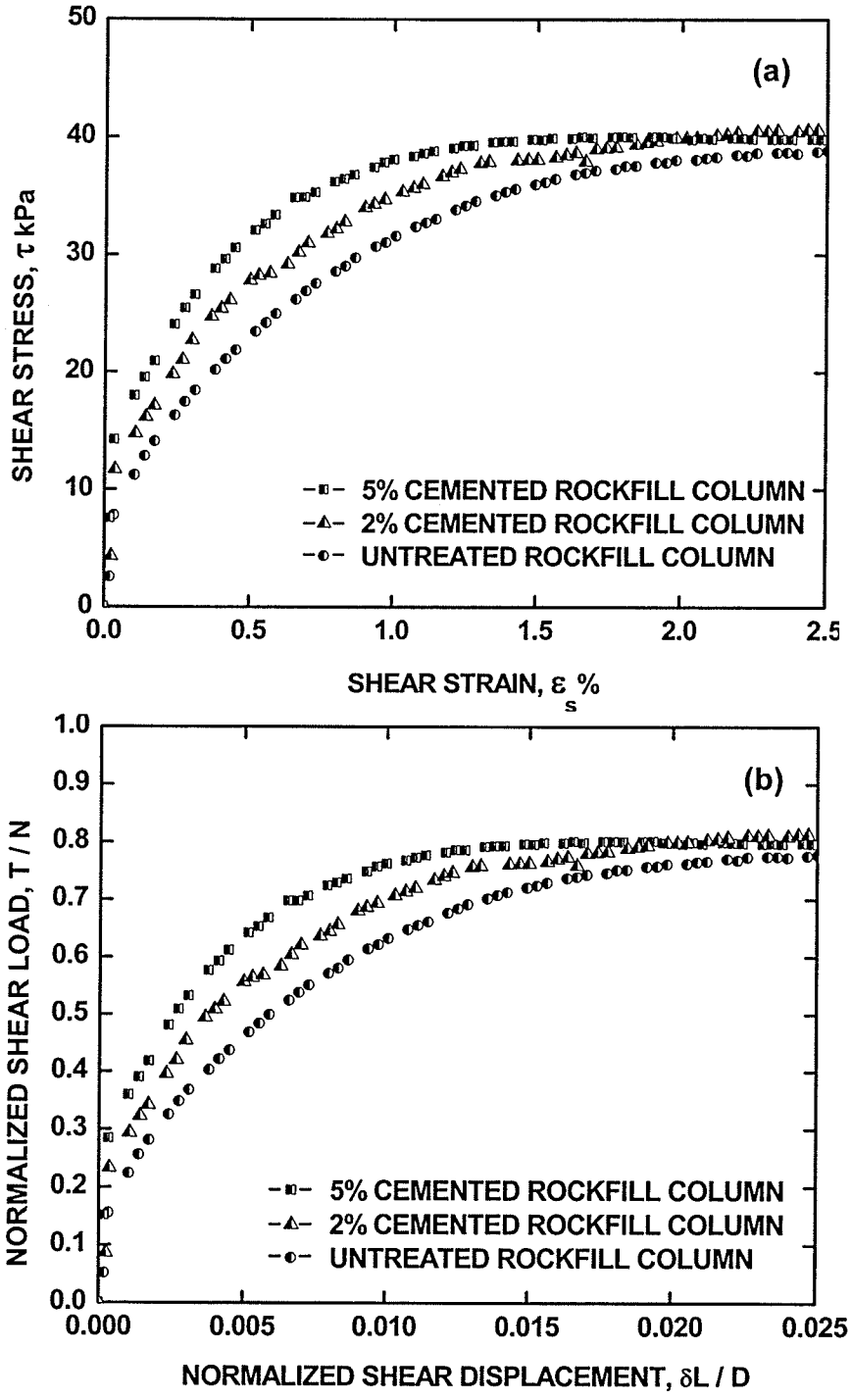

Figure 4.17 Shear mobilization of composite soil using cemented rockfill columns (σ_N = 50 kPa)

(a) shear stress vs. shear strain

(b) normalized shear load vs. normalized shear displacement

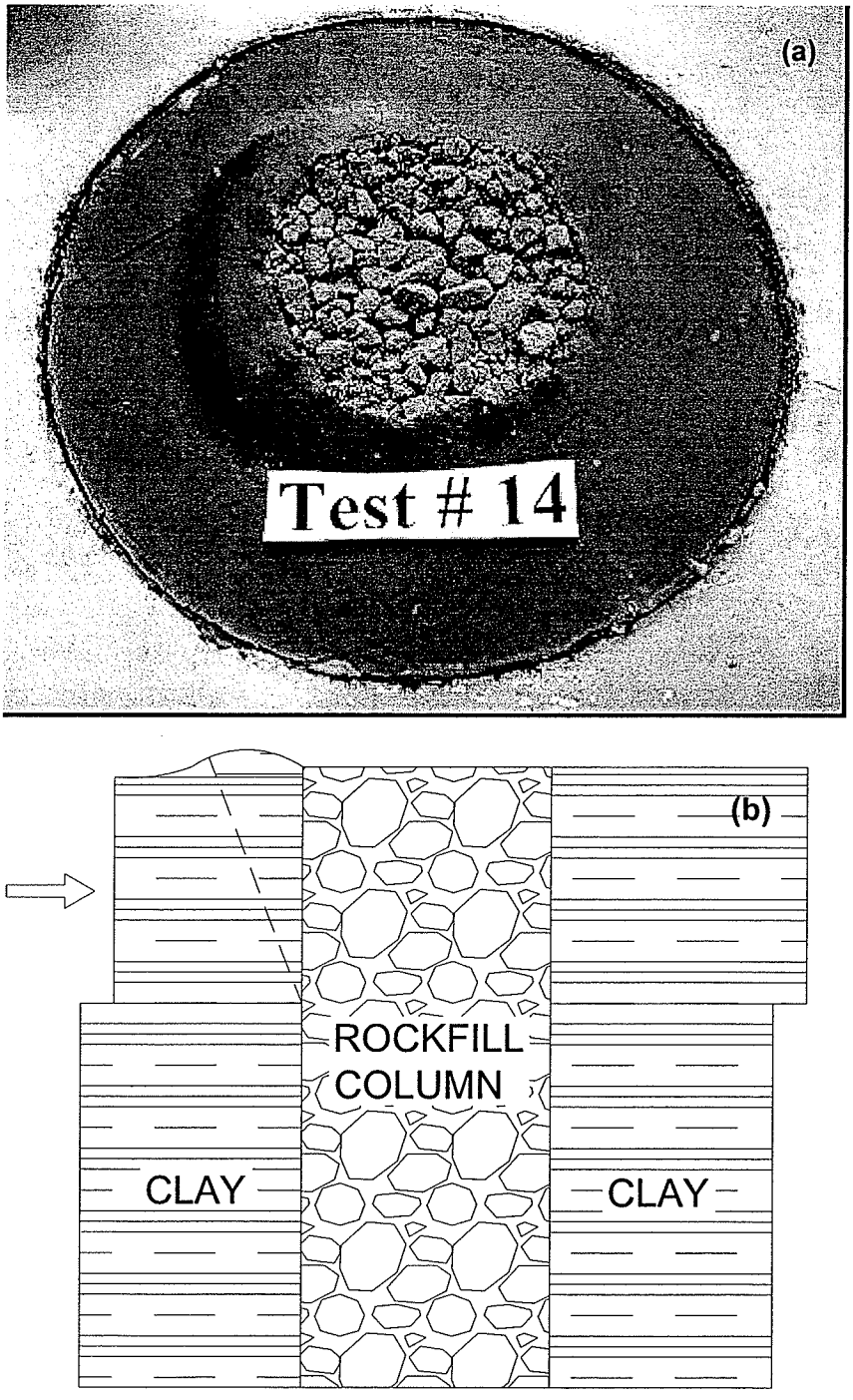

Figure 4.18 Conceptualized shear mobilization of cemented rockfill-undisturbed clay composite by a passive failure mode

(a) failure mode shown at the end of the test

(b) conceptualized failure mode

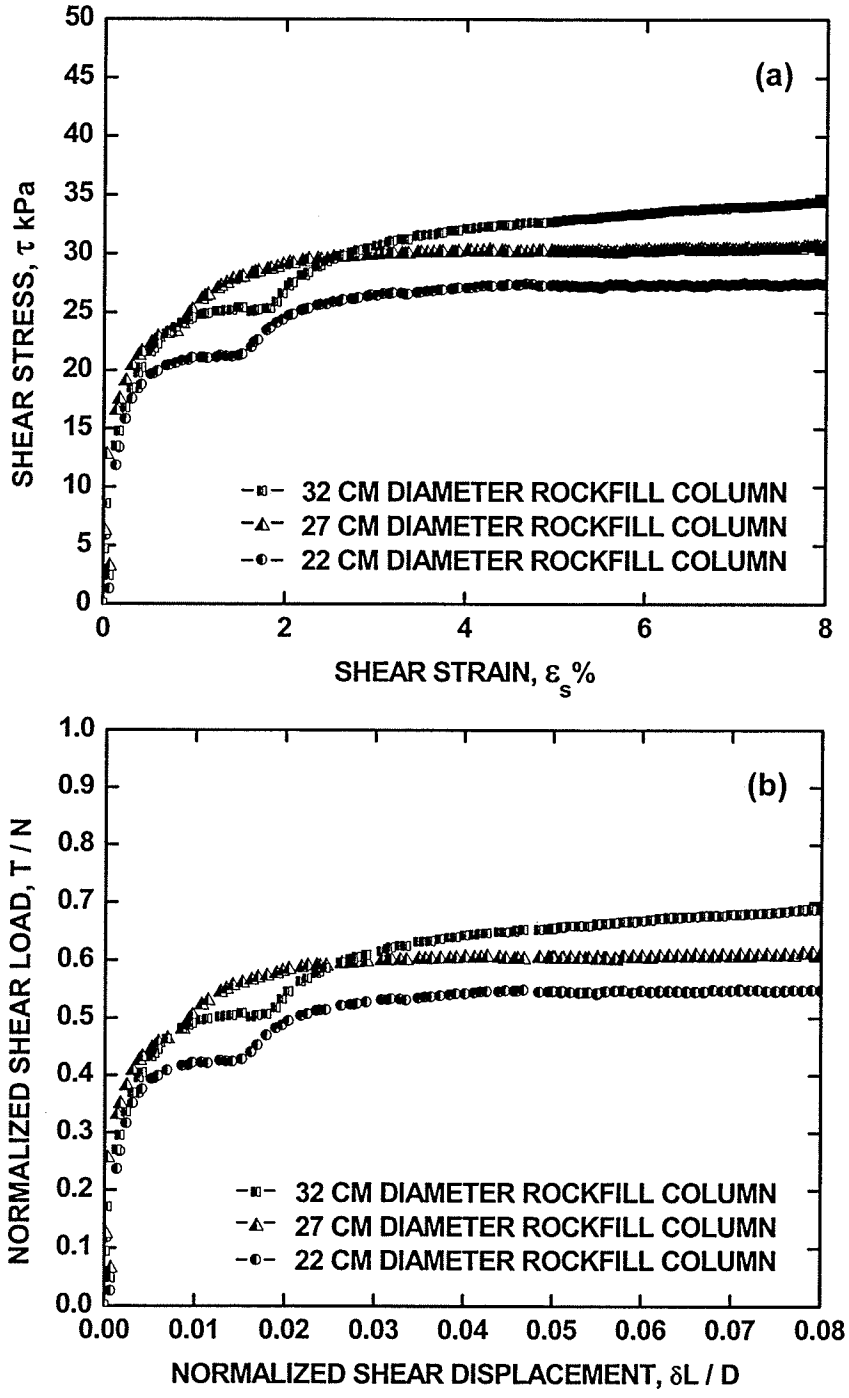

Figure 4.19 Shear mobilization of rockfill-remolded clay composite by various area replacement ratios (σ_N = 50 kPa)

(a) shear stress vs. shear strain

(b) normalized shear load vs. normalized shear displacement

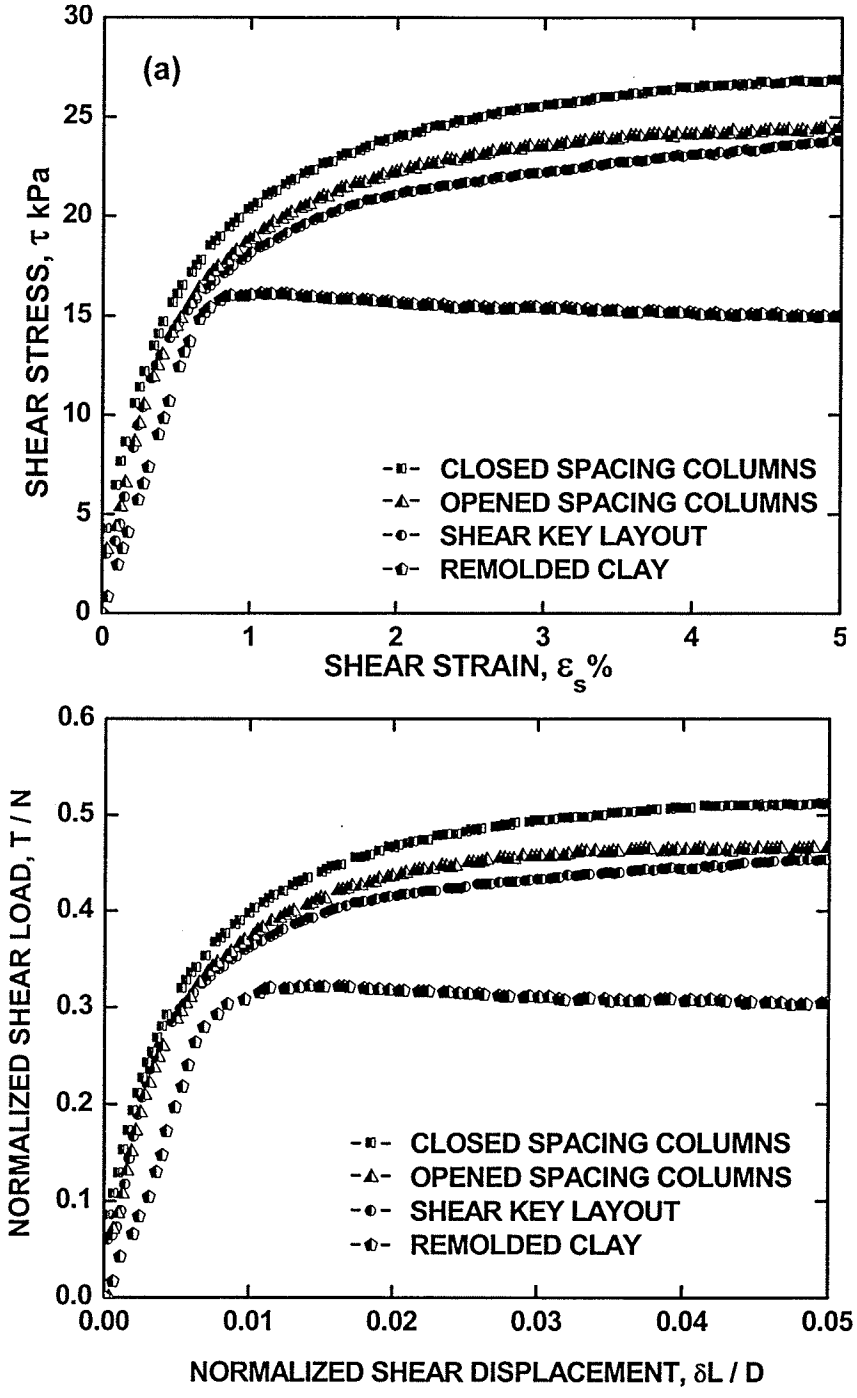

Figure 4.20 Shear mobilization of group columns in both opened and closed spacing compared with shear key layout (σ_N = 50 kPa)

(a) shear stress vs. shear strain

(b) normalized shear load vs. normalized shear displacement

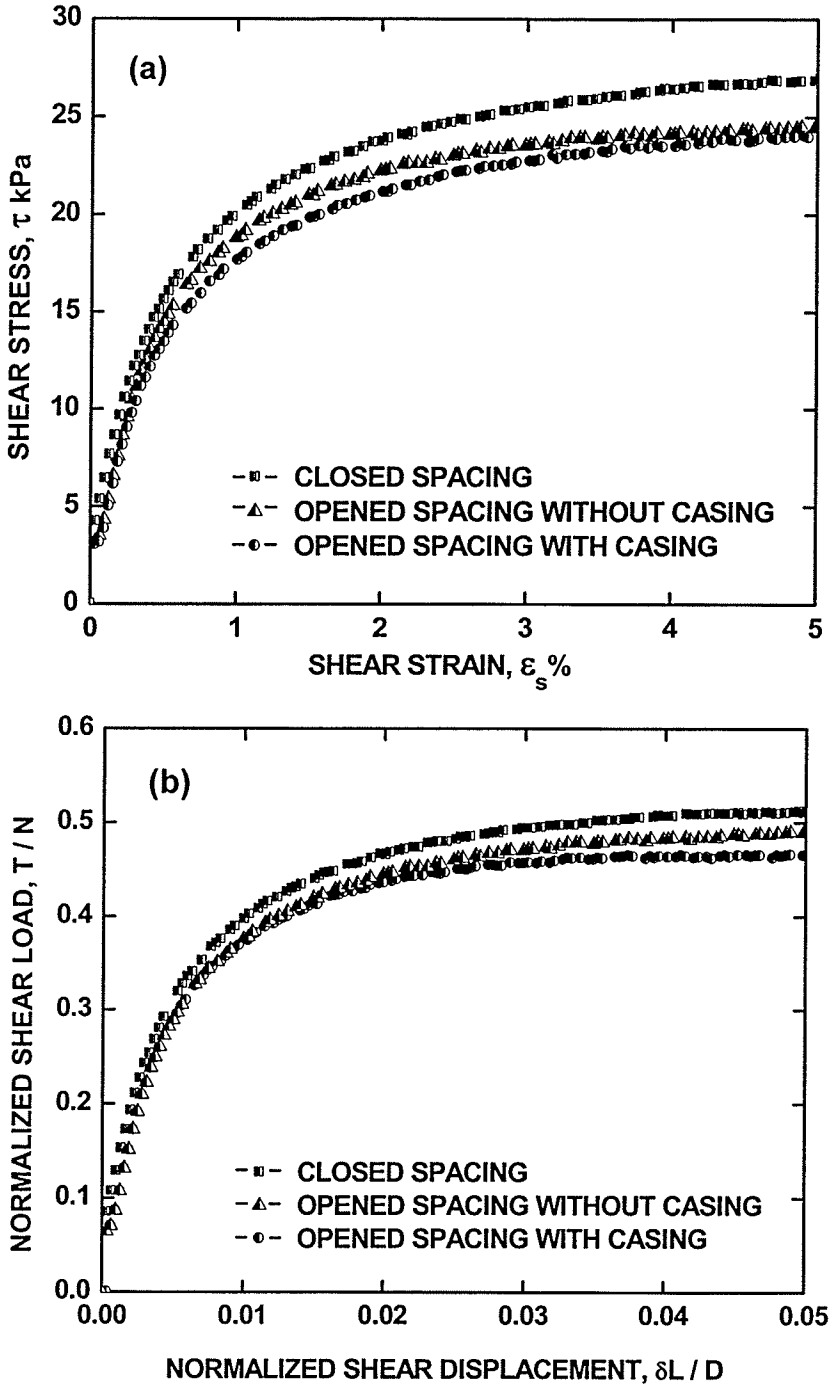

Figure 4.21 Shear mobilization of group columns with using casing and without using casing during installation of columns (σ_N = 50 kPa)

(a) shear stress vs. shear strain

(b) normalized shear load vs. normalized shear displacement

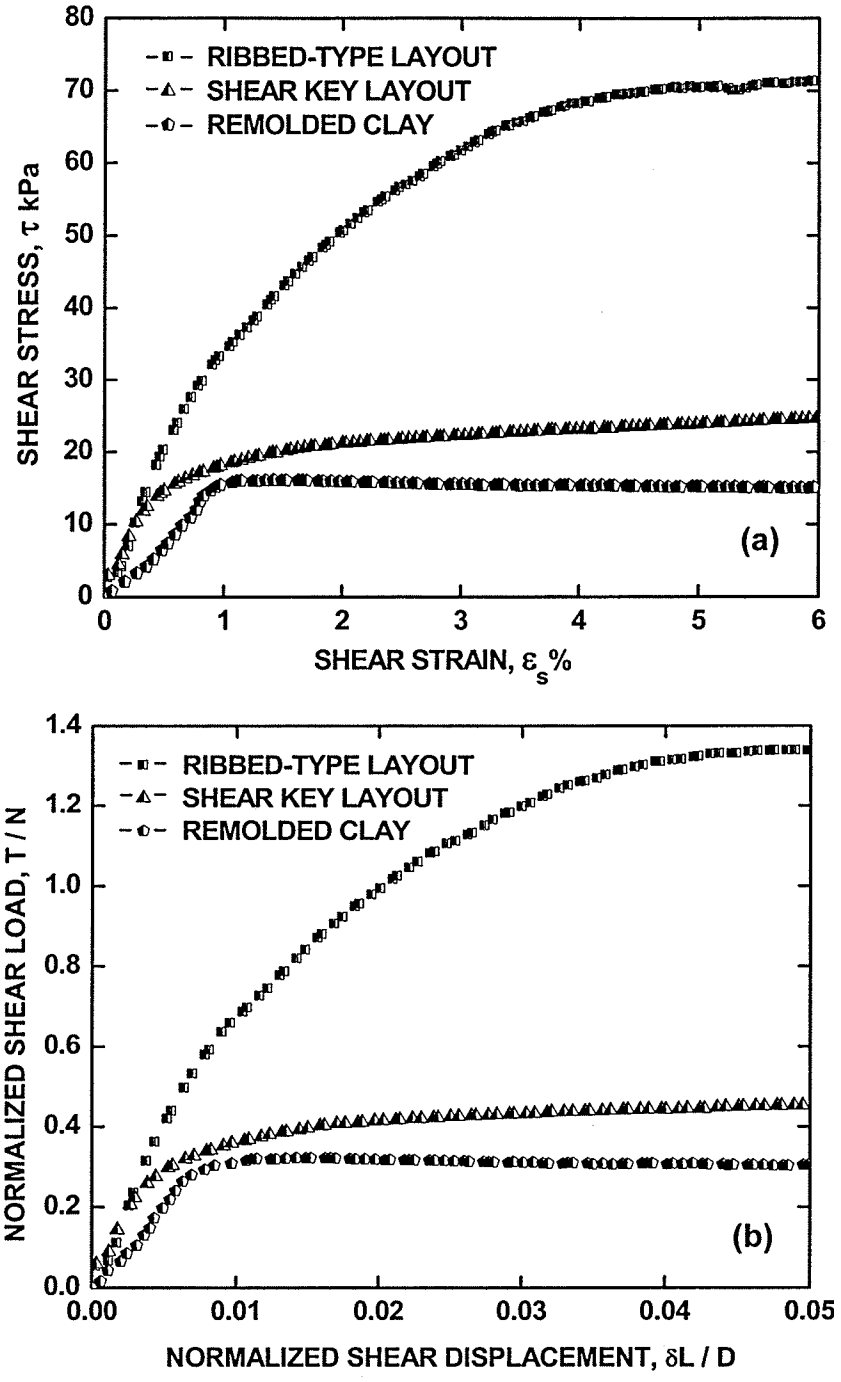

Figure 4.22 Shear mobilization of both shear key and ribbed-type layouts (σ_N = 50 kPa)

(a) shear stress vs. shear strain

(b) normalized shear load vs. normalized shear displacement

CHAPTER 5

NUMERICAL MODELLING OF DIRECT SHEAR TESTING

5.1 INTRODUCTION

A numerical model was developed to simulate the experimental results from large-scale direct shear tests. The model was then used to evaluate the performance of a typical riverbank stabilized with rockfill columns. The computer program FLAC, Fast Lagrangian Analysis of Continua (Itasca, 2005) was chosen as the modeling platform.

5.2 INTRODUCTION OF FLAC PROGRAM AND FISH CODES

FLAC is a two-dimensional explicit finite difference program and is a continuum stress analysis code. It has a range of nonlinear models available for soil or rock material, interfaces and structural elements for modelling such as rock bolts and tunnel linings. Elements or zones represent materials, and a grid formed by elements or zones is adjusted by the user to fit the shape of the object to be modeled. Each element behaves according to a prescribed linear or nonlinear stress-strain law in response to the applied forces or boundary restraints.

FISH, a powerful built-in programming in FLAC, enables the user to define new variables and functions. These functions may be used to extend FLAC's usefulness and implement new constitutive models. For instance, new variables may be plotted or printed, special grid generators may be implemented, servo-control may be applied to a

numerical test, unusual distributions of properties may be specified, and parameter studies may be automated (Itasca, 2005).

5.3 NUMERICAL SIMULATION OF DIRECT SHEAR TEST RESULTS

5.3.1 Simulation of stress-strain relationships

The stress-strain relationships were characterized using simple elastic and elastic-perfectly plastic constitutive soil models. Values of equivalent Young's modulus, E, and Poisson's ratio, ν, in combination with shear strength parameters are required to compute the stresses and deformations. A rigorous elasto-plastic model such as the Modified Cam Clay model suitable for high plastic clays requires more elaborate testing. To define the appropriate Young's modulus E, results from large-scale direct shear tests were used to estimate the shear modulus, G, of rockfill materials. Rough estimates for the shear modulus can be obtained using the equation given below (Davis and Selvadurai 1996):

$$[5.1] \quad \text{Shear modulus} \approx \frac{\Delta\tau}{\Delta s} h$$

where:

$\Delta\tau$ = shear stress along the shear band

Δs = horizontal displacement

h = the height of a shear box

For isotropic and elastic materials, the shear modulus is related to the Young's modulus, E and bulk modulus, K, and Poisson's ratio, ν:

$$[5.2] \qquad G = \frac{E}{2(1+\nu)} \qquad K = \frac{E}{3(1-2\nu)}$$

where:

G = shear modulus (MPa)

E = Young's modulus(MPa)

ν = Poisson's ratio

Poisson's ratio for rockfill material and undisturbed clay were assumed to be about 0.25 and 0.4, respectively. Mobilized friction angles were also estimated at a shear strain of 3%. Dilation angles for the rockfill materials were estimated by the slope of a line drawn from the point, B shown in Figure 4.7 and intersecting the curve at a shear strain of 3%. Cohesion of the undisturbed lacustrine clay was determined from both large-scale and conventional direct shear tests.

Another method of estimating the shear modulus is done following the recommendation of Thornton and Zhang (2001). The thickness of the sheared zone as opposed to the whole thickness of the sample is considered. The sheared zone, h, can be estimated as 10 times the average grain size, D_{50}, of the rockfill material ($h = 10 \times D_{50}$), where D_{50} is the grain size corresponding to 50% finer. With the given relationship, the shear strain can be estimated by dividing the horizontal displacement by the thickness of the sheared zone ($\gamma_{zx} = \Delta s/h$). Given the large average grain size, the results of estimating the G value is very similar to that estimated using Equation 5.1.

Elastic parameters taken from direct shear tests must be used with caution given the fact that the tests create nonuniformity of both stress and strain fields in the soil sample. The triaxial test may be the best tool for estimating elastic constants but large triaxial test equipment required for testing rockfill-clay composite material is not available in our laboratory.

5.3.2 Numerical simulation of direct shear test of rockfill material

It should be understood that the numerical model developed for shear resistance mobilization of rockfill material would be also used for the numerical simulation of shear mobilization of rockfill-clay composite. Figure 5.1 shows the finite difference grid and the boundary conditions used. The effect of assigning interfaces between materials was examined in Figure 5.2. As shown in Figure 5.3, results indicate that there was no significant influence of assigning interface on the stress-strain behaviour between two simulations. For simplicity further simulations were performed in the small scale without any interface.

FLAC has an option to apply velocity at any surface of the problem domain in addition to applying surface stress or load. Therefore, the velocity shown in Figures 5.1 and 5.2 corresponds to the applied rate of horizontal displacement. This is important as the direct shear test is strain controlled, which means that the rate of horizontal (shear) displacement of the upper box relative to the fixed lower box is controlled during the test with shear load being measured during shearing. The measured shear load and known shear area provide the mobilized shear resistance at any given shear strain. The calculated shear resistance can be estimated from the summation of the shear forces of

all elements along the predetermined shear band divided by the summation of the shear area. The parameters used in the numerical simulation are shown in Table 5.1.

Loosely compacted rockfill material

Figure 5.4 shows the shear stress-displacement relationships for both the results from numerical simulations and experiments at applied normal stresses of 50 and 100 kPa. It can be seen that the numerical simulation fitted well with the results from the laboratory tests, except at much larger shear displacements where the numerical simulation slightly underpredicted the shear resistance. This will be explained later when the results from densely compacted material are discussed. Comparisons of vertical displacements during shearing are presented in Figure 5.5 where the measured vertical displacements are taken from the element in the middle column and top row of the grid. The numerical model also reasonably simulated the dilatant behaviour of rockfill materials during shearing. As mentioned in Section 4.2.1, dilatancy is dependent on the applied normal stress and a degree of density. Figure 5.6 shows the velocity vectors at applied normal stresses of 50 and 100 kPa. Dilatancy is suppressed at higher applied normal stresses as generally understood. It should be noted that experimental results exhibited small dilatant behaviour at large shear strain levels even though for loosely compacted material. The most likely reason for this unusual behaviour has been discussed earlier in Chapter 4.

Densely compacted rockfill material

Simulation for the densely compacted rockfill material was conducted in the same manner as in loosely compacted material. The parameters used in the numerical

simulation are also shown in Table 5.2. The numerical results faired well with the experiment results at smaller shear displacement, but underestimated the shear resistance at larger shear displacements as depicted in Figure 5.7.

The above-indicated discrepancy between simulated and measured mobilization of shear resistance may be attributed to the test set up where the shearing plane has circular cross-section that behaves like a three-dimensional (3-D) condition while the simulation assumed plane strain condition and thus two-dimensional (2-D) condition as illustrated in Figures 5.8a and b, respectively. Because of the circular geometry of the shear plane, the middle portion already experiences significant shearing and therefore dilation, while the edges experience little or no shear deformation (i.e., $\delta_{hm} > \delta_{he}$). This has significant implication particularly for densely compacted rockfill that are inherently dilatant. Recall that densely compacted materials initially compress and then dilate with shear displacements. The consequence of a 3-D condition in shearing is the effect of restrained dilatancy that can mobilize dilatant stresses on and near the edge of the plane of shearing.

Explanation of the effect of restrained dilatancy has originated from the work of Alfaro and Pathak (2005) on the mobilization of dilatant stresses at the interface of granular fills and geosynthetic reinforcements. Figure 5.9 is a schematic diagram taken from Section A - A of Figure 5.8. As shown in Figure 5.9, the no-sheared area is the non-dilating zone that functions as a restraint against dilatancy in the dilating zone. This generates shear stresses at the border between the dilating and non-dilating zone and results in an increase in normal stresses at both edges. A 3-D condition develops at edges while the middle section experiences 2-D behaviour. The resulting effect of generating increase in

normal stress (dilatant stress) on the plane of shearing is the enhancement of shear resistance.

Attempts were made to investigate what increase in normal stress constituted a reasonable fit to the measured shear resistance. Figure 5.10 shows that an increase of 45 kPa for the applied normal stress of 50 kPa (90% increase) and 60 kPa for the applied normal stress of 100 kPa (60%) gives a reasonable fit. There is no attempt in this study to verify these mobilized dilatant stresses. But they seem reasonable given the fact that they decrease with increasing applied normal stresses, consistent with the fact that dilatancy is suppressed with increasing applied normal stress. Also, an increase in normal stresses due to restrained dilatancy on sand and gravel materials in the range of 30% to 80% have been reported, depending on the applied normal stress (Alfaro *et al* 1995).

Simulated and measured vertical displacements during shearing are compared in Figure 5.11. It should be noted that vertical movements were measured at the middle of the sample, and so there is no restrained dilatancy at this location. The numerical simulation agrees fairly well with the measured values.

5.3.3 Numerical simulation of direct shear test of undisturbed clay

Two large-scale undrained direct tests were conducted at 50 and 100 kPa applied normal stresses. Parameters used in the numerical simulation are given in Table 5.3. Figure 5.12 demonstrated acceptable results by the numerical simulation, although the peak behaviour was not properly captured.

5.3.4 Numerical simulation of direct shear test of composite soil

Direct shear tests on rockfill-clay composite were simulated for different applied normal stresses. It was recognized that dense compaction of rockfill material cannot be achieved in tests on composite samples. Therefore, the parameters used in the rockfill columns corresponded to those of medium-densely compacted material.

Figure 5.13 shows the typical numerical model of the rockfill-clay composite. The results from both the FLAC simulations and experiments were plotted in Figure 5.14. The numerical simulations underpredicted the measured values. This again may be attributed to the 3-D geometry of the column material.

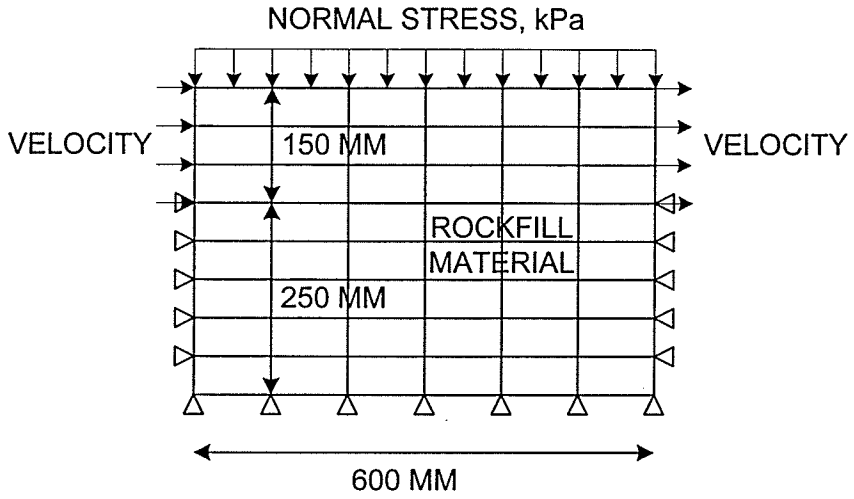

Figure 5.1 Finite difference grid with boundary conditions used in the numerical simulation

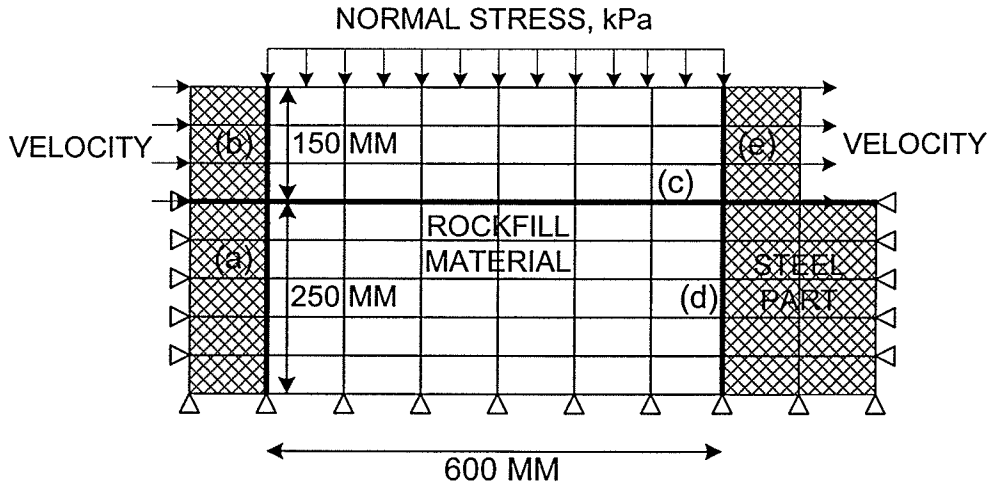

Figure 5.2 Finite difference grid with boundary conditions and interfaces used in the numerical simulation

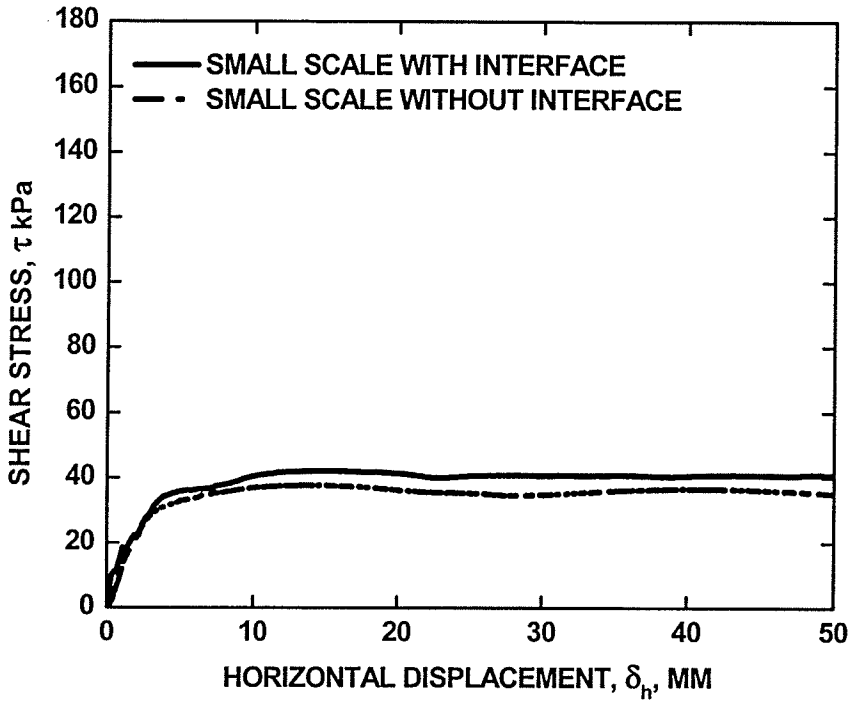

Figure 5.3 Comparison of the results from small scale numerical simulations with and without interfaces

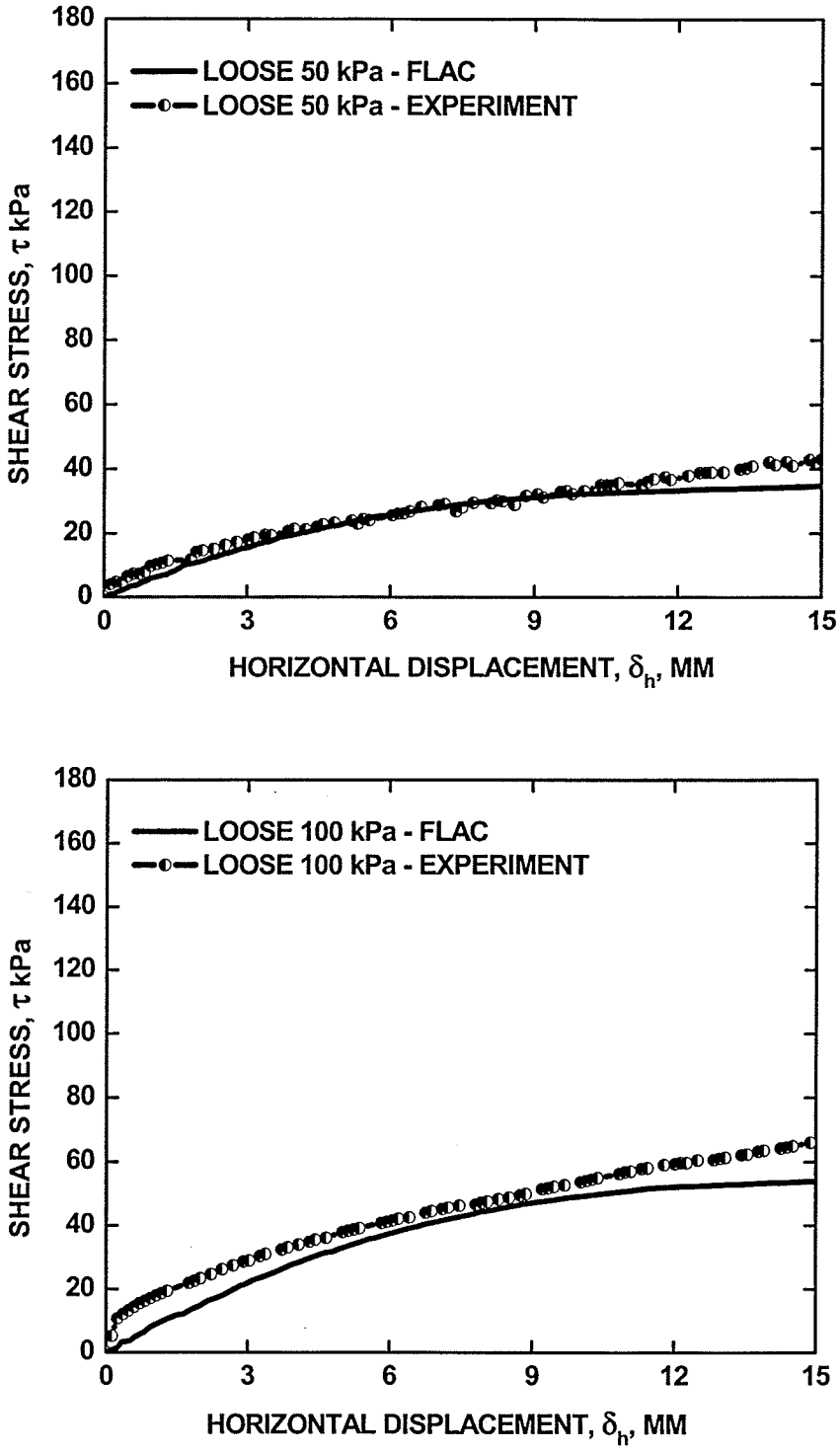

Figure 5.4 Comparisons of the results obtained from numerical simulations and experiments for loosely compacted rockfill material

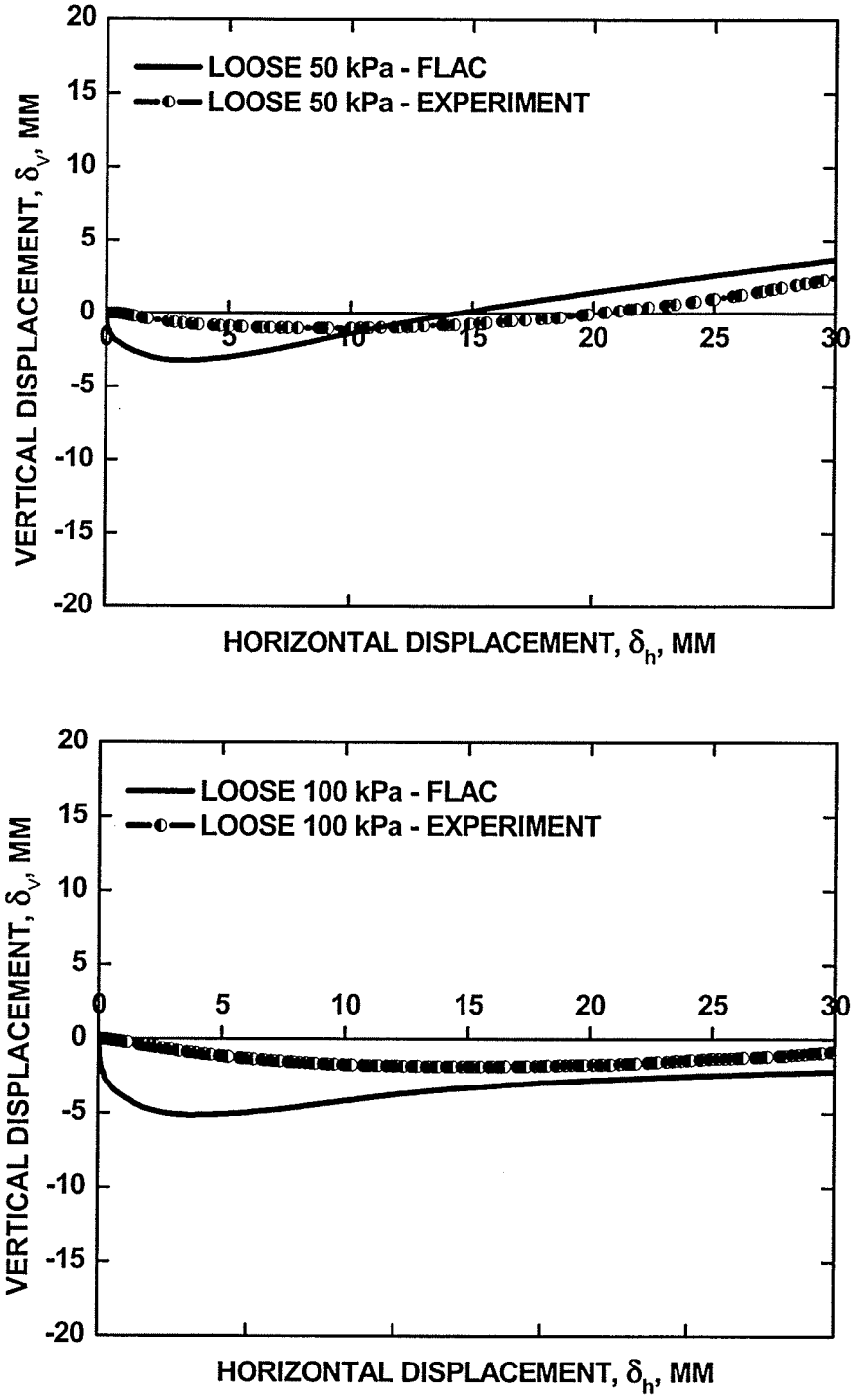

Figure 5.5 Plots of vertical displacement against horizontal displacement for loosely compacted rockfill material

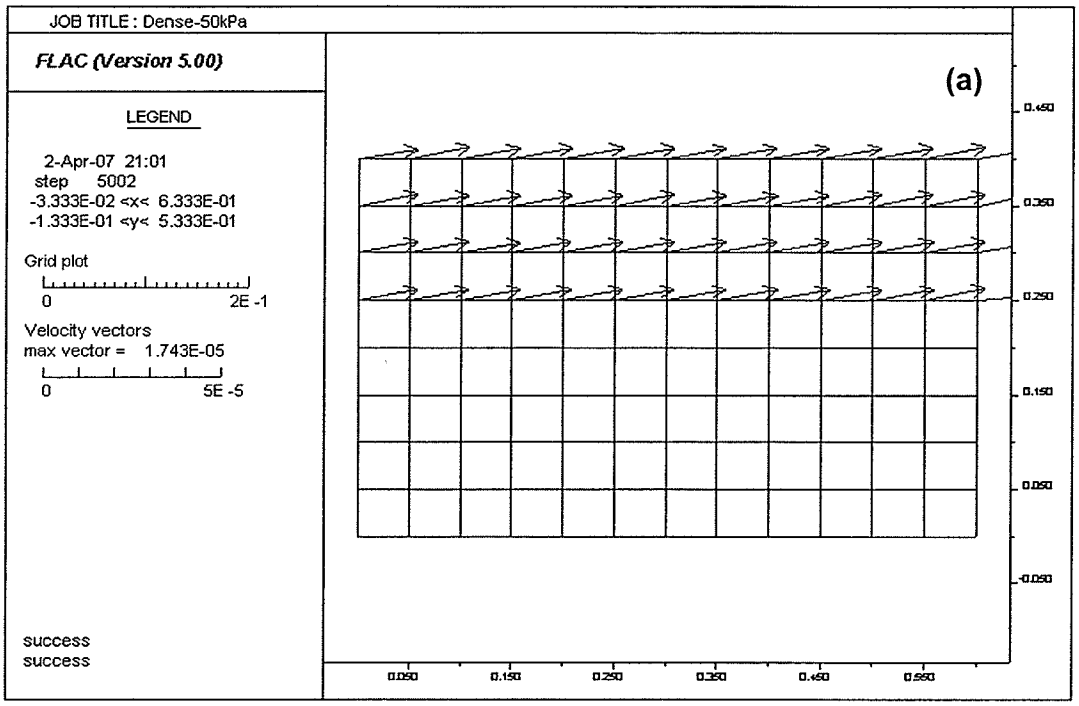

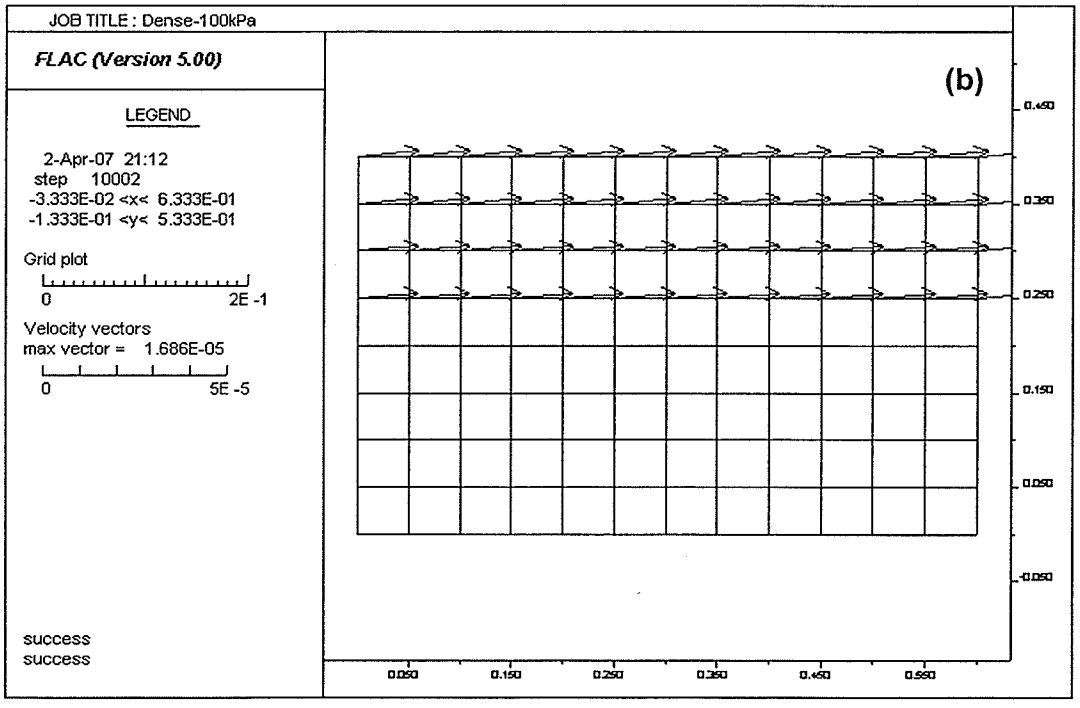

Figure 5.6 Different degrees of velocity vectors for loosely compacted rockfill material under the applied stresses of 50 and 100 kPa

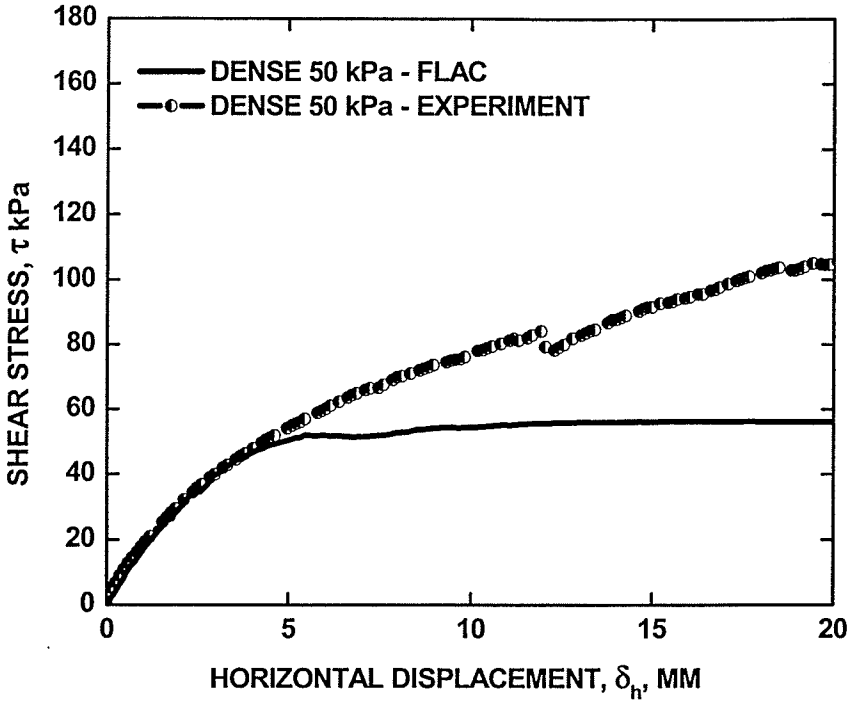

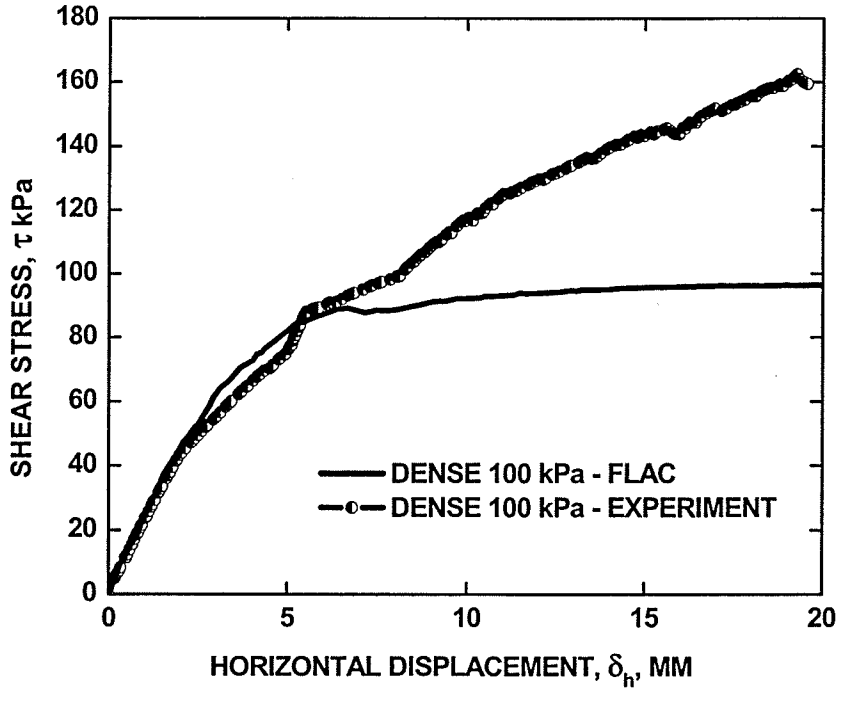

Figure 5.7 Comparisons of the results obtained from numerical simulations and experiments for densely compacted rockfill material

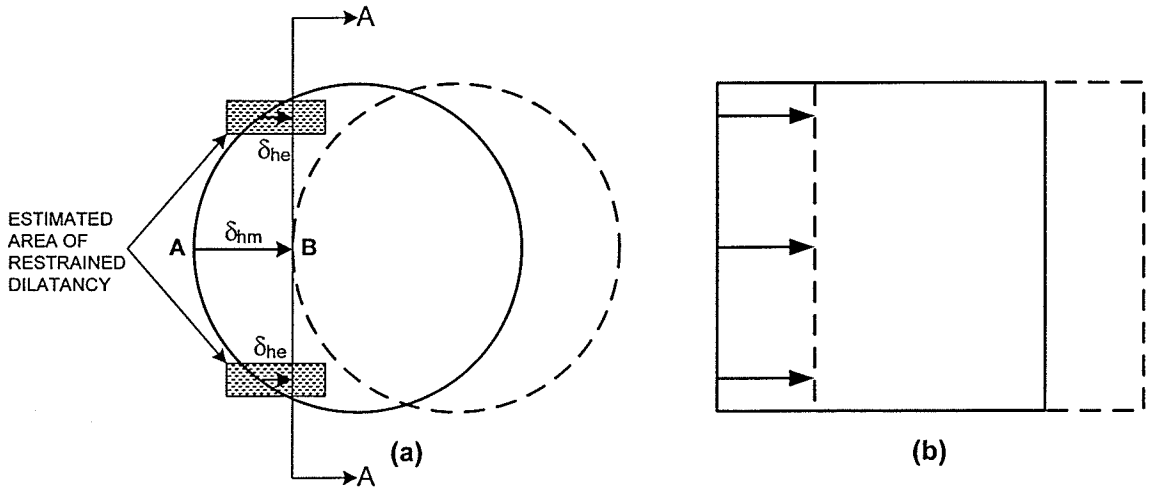

Figure 5.8 Difference between laboratory test and numerical simulation in terms of shear strain

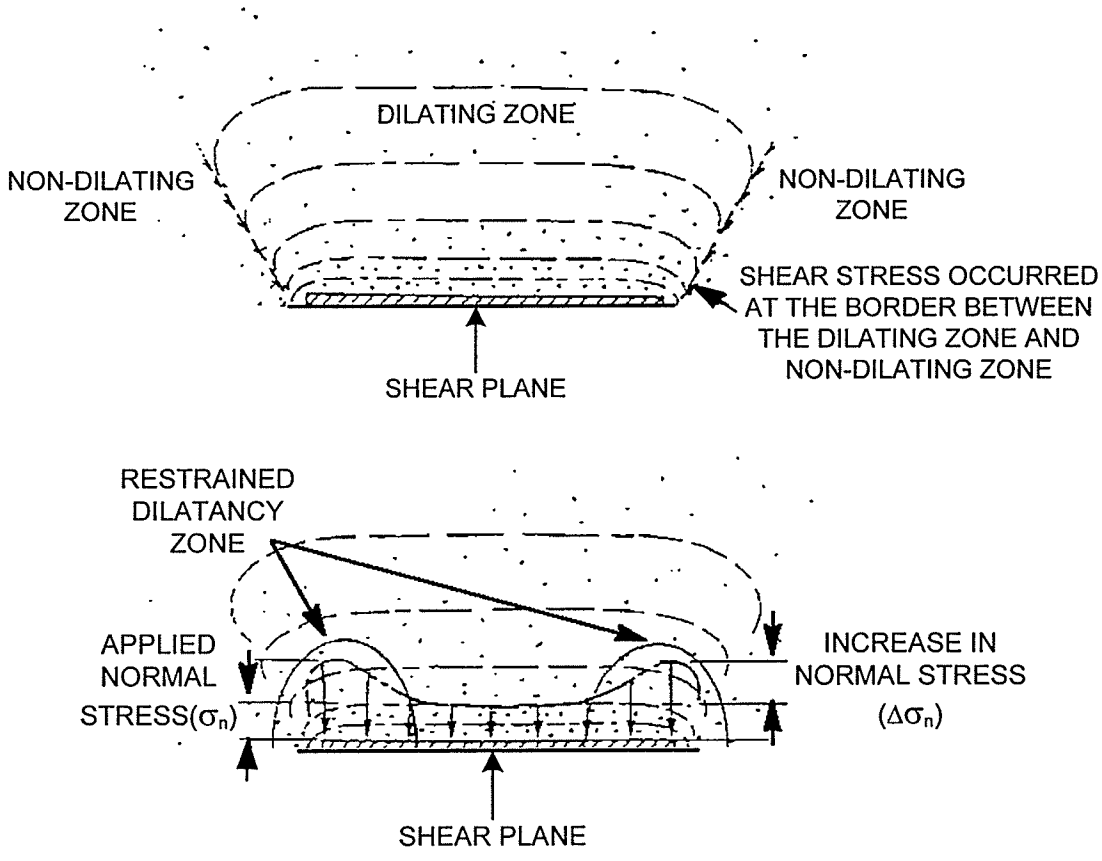

Figure 5.9 Conceptualized mobilization of increase in normal stress on the shear failure plane at Section A-A of Figure 5.8 (after Alfaro and Pathak 2005)

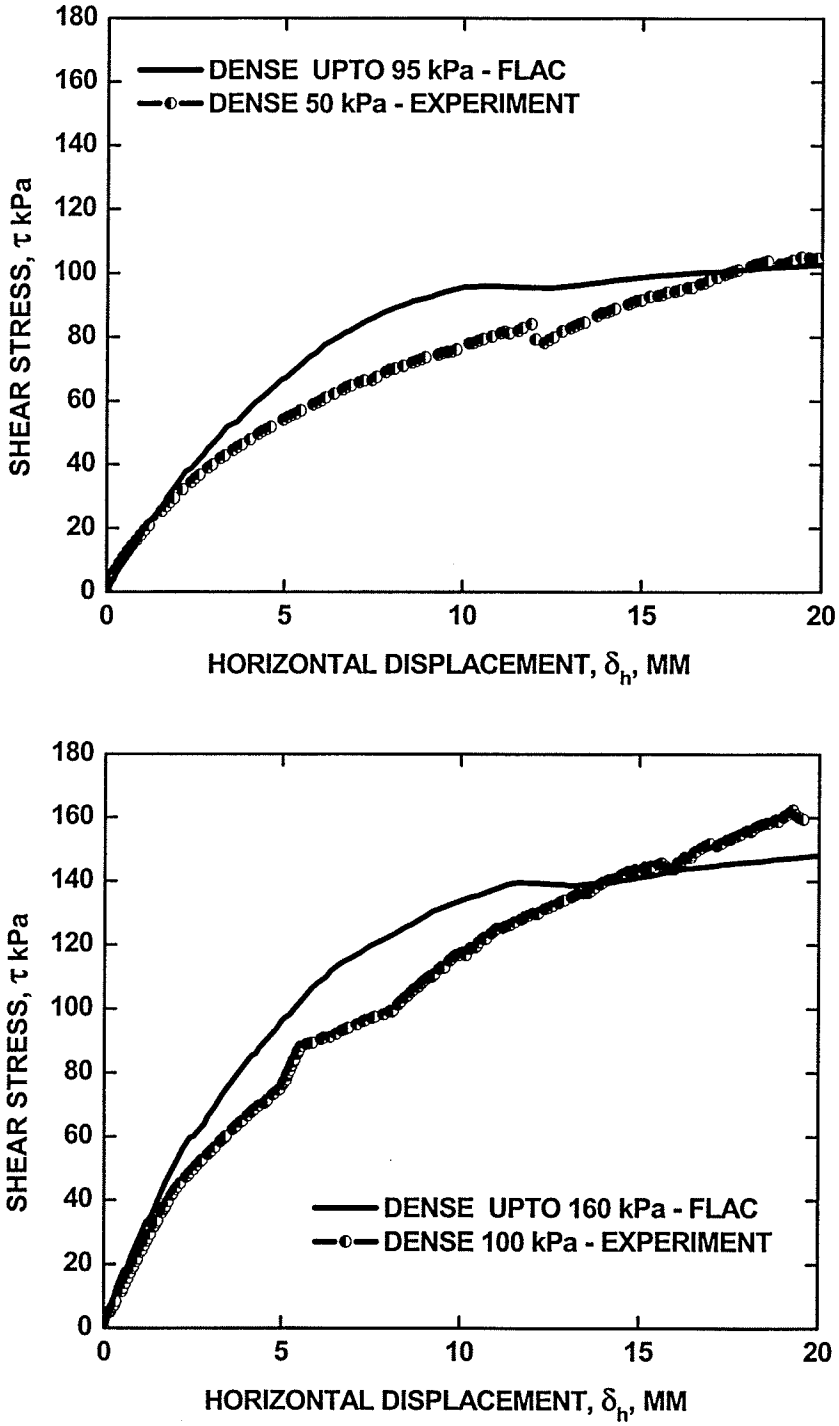

Figure 5.10 Comparisons of the results obtained from numerical simulations after increase of the normal stress and experiments for densely compacted rockfill material

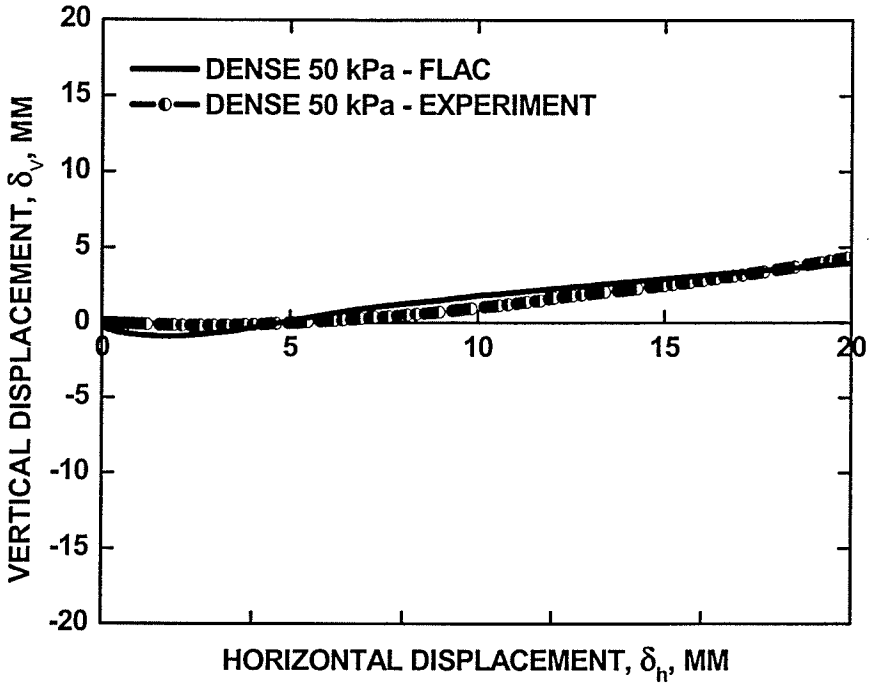

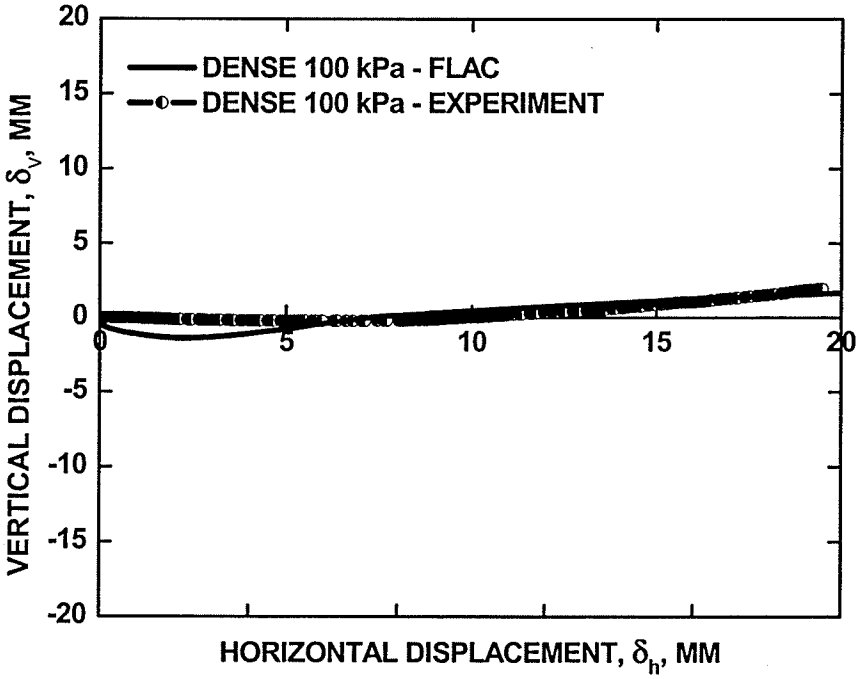

Figure 5.11 Plots of vertical displacement against horizontal displacement for densely compacted rockfill material

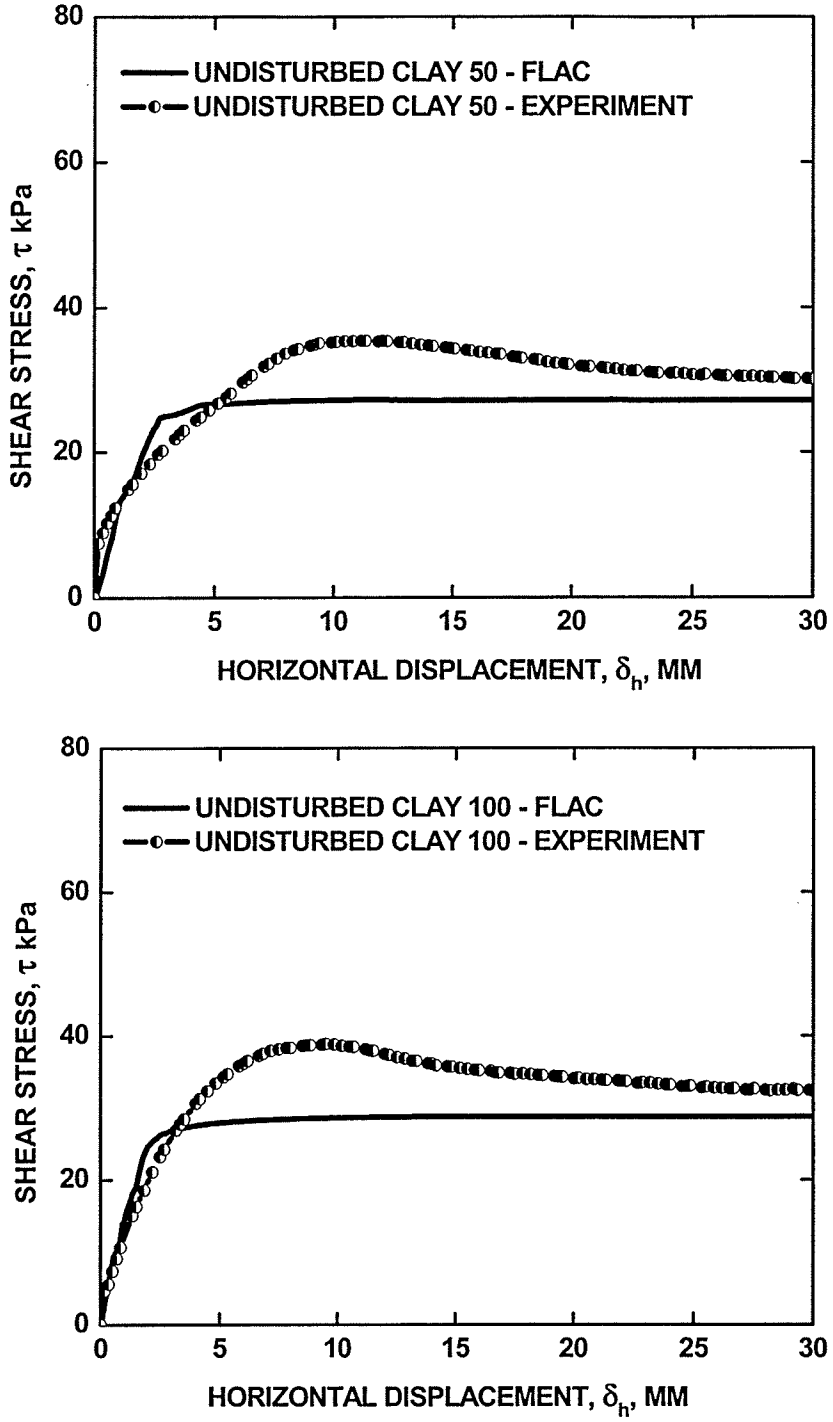

Figure 5.12 Comparisons of the results obtained from the FLAC and experiments

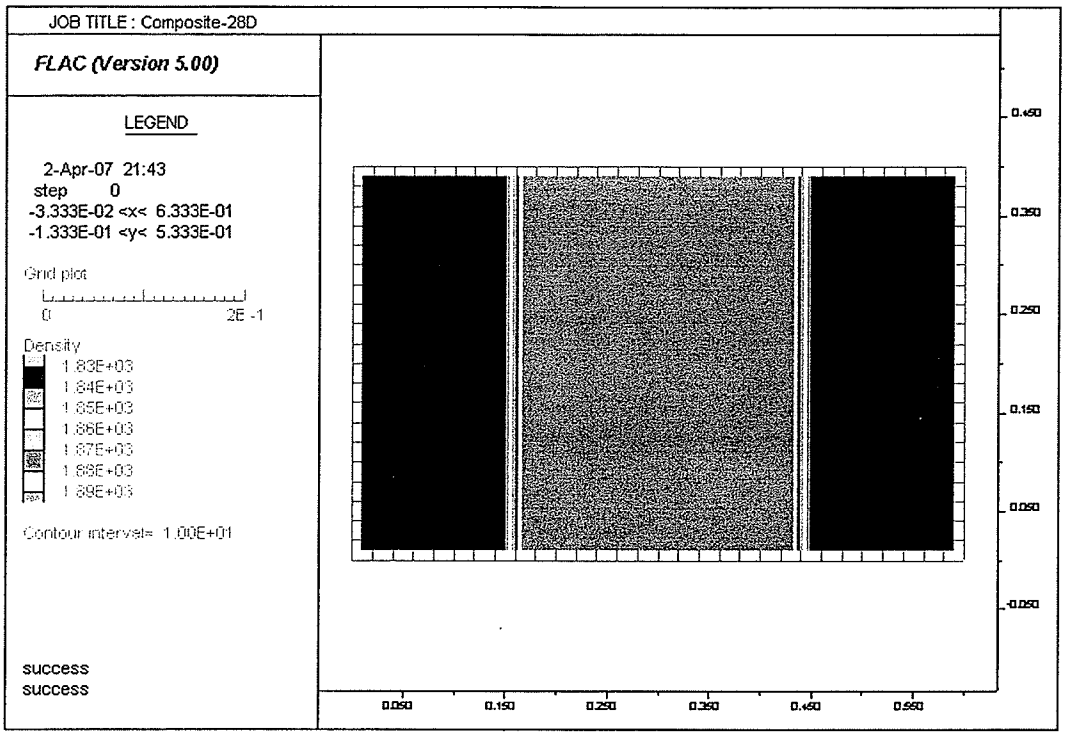

Figure 5.13 Rockfill-clay composite soil model with a 28 diameter rockfill column

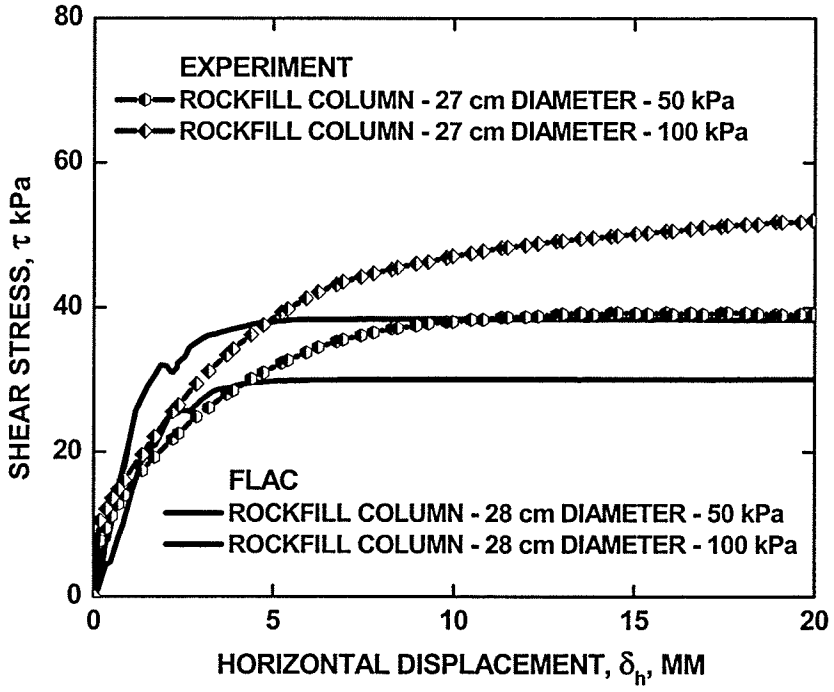

Figure 5.14 Comparison of the results obtained from the FLAC and experiments

Table 5.1 Parameters for the rockfill material in each density

Density	$\sigma'_{N\ applied}$	E, MPa	G, MPa	K, MPa	ν	ϕ_{mob}, °	ψ, °
Loose	50	4.75	1.9	3.17	0.25	42.6	10.6
	75	5.75	2.3	3.83	0.25	36.3	2.5
	100	6.25	2.5	4.17	0.25	35.0	1.7
Medium	50	8	3.2	5.33	0.25	62.2	12
	75	10	4	6.67	0.25	52.4	3.5
	100	14	5.6	9.33	0.25	50.4	4.0
Dense	50	15.0	6.0	10.0	0.25	63.4	11.9
	75	13.0	5.2	8.67	0.25	61.8	5.71
	100	21.0	8.4	14.0	0.25	56.7	5.43

Table 5.2 Parameters for the undisturbed clay

Type	$\sigma'_{N\ applied}$	E, MPa	G, MPa	K, MPa	ν
Clay	50	4.12	1.47	6.87	0.4
	100	7.42	2.65	12.4	0.4

CHAPTER 6

NUMERICAL ANALYSIS OF RIVERBANK STABILIZED WITH ROCKFILL COLUMNS

6.1 INTRODUCTION

The performance of a typical riverbank stabilized with rockfill columns was assessed by carrying out numerical analysis using the same numerical simulation described in Chapter 5. This was done by assessing the mobilized shear resistance, and therefore the 'mobilized' factors of safety for the stabilized riverbank corresponding to some degree of displacements either at the crest or toe of the riverbank. It will help address the issue as to how much movement is required to mobilize shearing resistance in the stabilized riverbank. This is a very important issue to address as recent observations have shown that movements may occur following installation of rockfill columns. Accordingly, there is a need to improve our understanding regarding the magnitude of riverbank movement required to mobilize shear resistance in the stabilized riverbank.

Two major numerical simulations were performed. The first one is on a natural riverbank without rockfill columns. This will allow checking the reasonableness of the numerical model for application in the field setting. The other simulation is on a riverbank stabilized with rockfill columns. For simplicity in the numerical simulations, it is assumed that the failure and hence movements in the riverbank are initiated either at the crest or at the toe of the riverbank. In simulating the riverbank movements, the option in the FLAC program to apply external velocity at any surface of the problem domain was used as opposed to

applying external stresses or loads. This option was also used in Chapter 5 in simulating the direct shear testing results.

Inclined and vertical velocities were applied on areas near the crest or the toe of the riverbank. Given the applied velocity and an assigned period (or time steps) of the analysis, displacement can be imposed in the designated areas and subsequently the mobilized shear stresses in the riverbank are calculated. It should be noted this approach in determining stresses from given displacements is similar to that in structural engineering applications. For example, with specified differential movements in the foundations, shear stresses, axial stresses, and bending moments in beams and columns of a multi-storey building are calculated using displacement-based finite element analysis.

The main advantage of the displacement-based numerical analysis for stabilized riverbank problem is that one can have an idea as to the amount of riverbank movements to mobilize certain degree of shear resistance in the native clay and rockfill columns. This will allow the user to first set up the in-situ stress of the riverbank before the installation of rockfill columns and subsequently allow the stabilized riverbank to move mobilizing the shear resistance of the clay and rockfill. The mobilized shear resistance would provide an estimate of the 'mobilized' factor of safety and the approximate movement in the riverbank.

6.2 GEOMETRY OF A TYPICAL RIVERBANK IN WINNIPEG

The cross-section of a typical riverbank analyzed in this study consisting of three sections, the upper bank, mid-bank and toe is shown in Figure 6.1. Each section of the

riverbank has a slope of 6H:1V, 10H:1V and 4H:1V, respectively, and also represents its own characteristics associated with initial formation in the soft lacustrine sediments, influenced from regulating river levels and effects of erosion and slope instabilities (Tutkaluk 2000). Elevations of the crest range from 230 to 232 m while toe elevations range from 218 to 220 m. Slope height from the crest to the horizontal ground surface at the toe was 12 m, which was also used in earlier studies by Baracos and Graham (1981).

Mishtak (1964) reported that the majority of the riverbanks which had failed became stable at slopes of 4.5H to 6.75H:1V. This indicated that the geometry of the upper bank section was probably the steepest slope at which the riverbank becomes stable. The mid bank section is less steep and is affected by regulating river levels. The toe section is much steeper than the mid bank due to both year-round submergence and continued erosion (Tutkaluk 2000). For simplicity in the numerical simulation, the entire riverbank has a slope of 6H:1V. This slope was used in the slope stability studies for the Winnipeg Floodway (Tutkaluk 2000) and was generally the slope of most riverbank sections observed by the City of Winnipeg (2000) based on its survey for riverbanks along the Red River within the city.

6.3 PERFORMANCE OF THE NATURAL RIVERBANK

6.3.1 Grid generation and boundary conditions

A finite difference grid for the typical riverbank was generated similar to the geometry mentioned above. It has 130 m length and 19 m height with riverbank slope of 6H:1V. The riverbank consists of three different layers: lacustrine clay, weak clay and glacial till.

Mohr-Coulomb plasticity constitutive model was assigned and each element had 1m length per unit width.

Gravity of 9.81 m/s^2 was applied on the elements to establish in-situ stress conditions in the riverbank. Establishing in-situ stress conditions is important as soil materials are very independent to their initial stresses. Both X and Y directions at the bottom were constrained while X directions on both sides of the domain were constrained. The grid was then adjusted by the program to obtain a reasonable grid generation.

6.3.2 Material properties and water table location

Material properties were assigned to each layer as shown in Table 6.1. The soil properties were determined from the laboratory large scale direct shear tests, except the properties of weak clay, which were taken from numerical analysis performed by Tatkaluk (2000). The strength parameters for the lacustrine clay layer were assigned their post-peak values. For the purpose of this analysis, the water table was assumed on the ground surface as a worst case scenario. A saturated density or wet density must be assigned to carry out effective stress analysis following the formula that was incorporated through a FISH function in FLAC program:

$$[6.1] \qquad \rho^{WET} = \rho + n\rho_W$$

where ρ^{WET} is the wet in-situ density, ρ is the in-situ density above the water table, n is the porosity, and ρ_w is the water density. Porosity of each material was assigned 0.5 for lacustrine clay, 0.5 for weak clay, and 0.2 for till material. When the water table is

assigned to the model, FLAC program assumes that all zones below the water table will be fully saturated and automatically be assigned the value for wet density. Water pressures were calculated in zones submerged below the water table.

6.3.3 Applying vertical velocity on the failed soil mass

As mentioned earlier, simulation of riverbank movements was conducted using the option in the FLAC program where the external velocity can be applied at any surface of the problem domain. Given the applied velocity and assigned time steps in the analysis, displacement can be imposed in designated areas and subsequently the mobilized shear stresses in the riverbank are calculated.

Prior to the application of velocity, FLAC/Slope, which is an add-on program to the main FLAC program, was run to estimate the factor of safety of a slope using the shear strength reduction (SSR) technique. Running FLAC/Slope will allow the determination of the location of the potential failure plane (slip plane) and subsequently provide an idea where the surface velocity can be applied.

Figure 6.2 shows the failure slip surface through the contours of shear strains. It can be seen that the maximum shear strain occurred near the crest of the riverbank. Sequential analysis of the formation of slip surface indicated that the slip surface initiated near the crest for the condition being analyzed. This potential failure slip surface initiated approximately 10 m within the crest as shown in Figure 6.2 with a factor of safety close to unity, indicating failure of the natural riverbank. Therefore, velocities were applied on the crest within this area. Question arose as to what direction these velocities could be applied. It was decided to apply velocities at the crest that had inclination parallel to the

inclination of the slip surface at the crest as shown in Figure 6.3. The inclined angle was estimated to be about 35° from the horizontal. Vertical velocity was also applied on the crest to simulate any movement following a tension crack at the surface as shown in Figure 6.4. A velocity of 0.1678e-4 m/s was applied throughout all simulation, similar to that used in the large-scale direct shear tests. As mentioned in Section 6.1, the desired movement can be obtained by the relationship between time steps and velocity.

6.3.4 Results and discussion

Figures 6.5 and 6.6 show the magnified displacement vectors corresponding to the application of inclined and vertical velocities, respectively that resulted in about 5 cm displacement. As expected, the application of inclined velocities led to inclined displacement vectors near the crest while the application of vertical velocities led to vertical displacements at the crest. It is interesting to see that both applications of velocity reflect the slip surface shown in Figure 6.2, with the exception of a small part near the toe where the slip surface tends to exit higher in the riverbank with the application of velocities compared to that using the FLAC/Slope option. This may be attributed to the non-uniform mobilization of shear resistance in the case of the former compared to a uniform mobilization of shear resistance assumed in the latter.

The displacement patterns shown in Figures 6.5 and 6.6 are considered to indicate failure in the riverbank, which means the 'mobilized' factor of safety should be about unity. To verify if this is so, the factor of safety is estimated following the same format as in the limit equilibrium method but with slight modification to accommodate the non-uniformity of the mobilization of shear resistance in the riverbank and the shear stress-

strain relationships of the materials. The 'mobilized' factor of safety (FS_{mob}) will now come in the form as follows:

$$[6.2] \qquad FS_{mob} = \frac{\sum_{i=1}^{n} \tau_{i,mob}}{\sum_{i=1}^{n} \tau_{i,app}}$$

where i = location number, n = total number of locations, $\tau_{i,mob}$ = mobilized shear resistance at a location, and $\tau_{i,app}$ = applied or driving shear stress at a location. Note that the denominator of Equation 6.2 is the same as in the usual limit equilibrium formulation, which is the applied or driving shear stress at a point along the slip surface due to the weight of the sliding mass and external load if any. The numerator of Equation 6.2 is a similar form to that in the usual limit equilibrium formulation except that it is now representing the 'mobilized' shear resistance based on the shear stress-strain relationship of the material as opposed to the shear strength of the material, $\tau_{i,max}$ or $\tau_{i,failure}$. In other words, if the riverbank fails, $\Sigma\tau_{i,app} = \Sigma\tau_{i,max}$ or FS = 1. (Having established the usage, quotes '—' will no longer be used around subsequent references to 'mobilized'.)

Equation 6.2 requires calculation of the values of $\Sigma\tau_{i,app}$ and $\Sigma\tau_{i,max}$ along the slip surface that require slope angles of the slip surface at selected points to determine the applied shear and normal stresses. Making use of the AutoCAD software, the results of the numerical simulations were exported into AutoCAD to determine the values of inclination of slip surface, vertical and horizontal normal stresses and shear stresses in each element along the failure slip surface. Theses values were then imported to a Microsoft

Excel spreadsheet to calculate the mobilized factor of safety. It was found that the mobilized factors of safety for these cases shown in Figures 6.5 and 6.6 were indeed close to unity indicating unstable natural riverbank, consistent with what was found in FLAC/Slope simulation. Figure 6.7 shows how the grid was deformed with the application of 5 cm movement in the crest.

SEEP/W and SIGMA/W incorporated in SLOPE/W were used to verify the location of potential failure surface and the factor of safety. Figure 6.8 shows the failure slip surface and factor of safety from SLOPE/W supporting the results of the FLAC numerical simulation. Shear stress distributions determined from the two aforementioned analyses were comparable as well as depicted in Figure 6.9. Another computer program, Phase 2.0 (RockScience Inc. 2004) which uses the shear strength reduction technique to determine the factor of safety and slip surface was also employed to verify the FLAC simulation results. Figure 6.10 shows the shear strain for a natural riverbank from Phase 2.0 demonstrating a similar slip surface as that found in the FLAC simulation. The factor of safety in Phase 2.0 is also close to unity and consistent with that calculated in FLAC simulation.

6.4 PERFORMANCE OF RIVERBANK STABILIZED WITH ROCKFILL COLUMNS

6.4.1 Grid generation for rockfill columns

Based on the same geometry and boundary conditions used in an earlier simulation on natural riverbanks, zones for 5 rows of rockfill columns were added in the model. The discrete installation of rockfill columns results in a three-dimensional problem. However,

the available FLAC program and other geotechnical computer programs at the University of Manitoba are capable only of simulating two-dimensional problems. Therefore, the rockfill columns were converted into a strip material in the plane-strain (two-dimensional) model following the equivalent area concept (Bergado et al 1994). Rockfill columns with diameter of 2 m and spacing of 4 m between center of columns are used in the numerical simulation. These are installed in the middle third of the slip surface to provide optimum efficiency (see Abdulrazaq et al 2006).

6.4.2 Rockfill material properties and water table location

Properties of the rockfill material used in the analysis are shown in Table 6.1. The porosity of the rockfill material was used 0.4. The location of water table was the same as that in the natural riverbank simulations.

6.4.3 Applying vertical velocity on the crest and steps

It was assumed that slip surface for natural and stabilized riverbanks were the same. This assumption may not be valid but was made for simplicity in the analysis and for comparison purposes, the velocities and hence displacements were applied in two locations. In one, the velocity was applied in the crest similar to that simulated in the natural riverbank. This simulates the condition where movements of the stabilized riverbank are due mainly to the weight of the failed mass of soil. In the other, the velocity was applied at a selected area near the toe. This simulates potential toe erosion and therefore the movement of the riverbank initiated at the toe. Figures 6.11 and 6.12 show the configurations of the riverbank stabilized with rockfill columns, indicating the application of the velocities on the crest and at the toe, respectively.

6.4.4 Results and discussion

Figure 6.13 shows the displacement vectors in the stabilized riverbank. The overall displacement of the stabilized riverbank was much less than that of the natural riverbank (see Figure 6.6). Note that the application of the same velocity (therefore displacement) would result in the same movements at the crest. However, the installation of rockfill columns significantly reduced the displacements near the toe of the riverbank as well as in locations where rockfill columns were installed. The mobilized factor of safety of the stabilized riverbank was calculated in the same manner as that of the natural riverbank. It was found that the stabilized riverbank has a mobilized factor of safety of about 1.26 corresponding to a vertical displacement of 5 cm at the crest.

Applying velocity at the toe led to shallower slip surface near the crest compared to that where velocity was applied at the crest as shown in Figure 6.14. This observation is also demonstrated when comparing the shear strain contours shown in Figures 6.15 and 6.16 and the slight difference in deformation patterns shown in Figures 6.17 and 6.18. The factor of safety corresponding to the displacement of 5 cm at the toe was found to be lesser as well, which is about 1.21. This may be attributed to slightly different displacement patterns between the two cases, and therefore the mobilization of shear resistance. Whether the displacement applied in the crest is vertical or inclined, the results seem to be not so different. Both displacements may have resulted in almost full mobilization of shear resistance in both native clay and rockfill materials as will be discussed in the next paragraph.

It is expected that the mobilization of shear resistance of the stabilized riverbank will differ with different amount of movements at the crest. One can estimate how much

shearing resistance in the stabilized riverbank is mobilized and therefore achieve a certain level of factor of safety using the definition of mobilized factor of safety established in Equation 6.2 for a given movement in the crest. Estimation of movements at the crest corresponding to a mobilized factor of safety is important for serviceability aspect of the design. This means that engineers need information about the possible movements expected in the riverbank for a designed factor of safety to ensure that these movements are acceptable to infrastructure at the vicinity of the riverbank. Figure 6.19 shows the shear stress distributions along the slip surface for two vertical displacements at the crest. As vertical displacements increased, the mobilized shear stresses also increased. It can be seen that movement in the crest of about 5 cm almost be mobilized the full shearing resistance of native clay but the rockfill columns are yet to be sheared to reach their full shear resistance.

The mobilized safety factors are calculated to be about 1.19 and 1.26 at vertical displacements of 2.5 and 5.0 cm, respectively. The factor of safety obtained from SLOPE/W in association with SIGMA/W and SEEP/W (Geo-Slope International 2004) is about 1.31 as shown in Figure 6.20. The corresponding value from Phase 2.0 is about 1.35 as depicted in Figure 6.21. Both SLOPE/W and Phase 2.0 used the customary definition of factor of safety which is the available strength divided by the applied shear stress. The values of safety factors from both SLOPE/W and Phase 2.0 calculations are expected to be higher than the value calculated from FLAC simulation because these two programs assumed full mobilization of shear resistance of the materials in the riverbank.

Attempts have been made to verify the numerical simulations carried out in this study in estimating the movements of stabilized riverbank corresponding to mobilized factor of

safety. In spite of difference in soil profile and number of rockfill columns installed, long-term monitoring data of stabilized riverbank in Winnipeg compiled by UMA-AECOM (2006) were used to at least verify the reasonableness of riverbank movements calculated in the numerical simulations. Figures 6.22 and 6.23 show the comparison between the observed horizontal displacements from slope indicators installed at the site and those from numerical simulations. It can be seen that the horizontal displacements have been reasonably simulated for both vertical and inclined displacement applications at a location within the columns near the middle portion of the riverbank. The simulated horizontal displacements have underpredicted the measured displacements with depths at the location near the crest. This may be due to the fact that the numerical simulation does not have the capability of simulating large localized slippage as shown in the data from the slope indicator (such as noticeable slippage at Elevation 220 m). Also, the numerical simulation does not have capability of simulating any potential of tension cracking that may have occurred in the field.

It is realized that the application of displacements either at the crest or at the toe of the riverbank in the numerical simulation is arbitrary. The numerical simulation will provide engineers with a tool to relate movements in the stabilized riverbank and the factor of safety that can be mobilized with a given movement.

A separate research project is on-going to install rockfill columns in a fully-instrumented section along the riverbank and subsequently load it to failure. This will further validate and fine-tune the combined results from the large-scale laboratory testing, numerical simulations and the assumptions made.

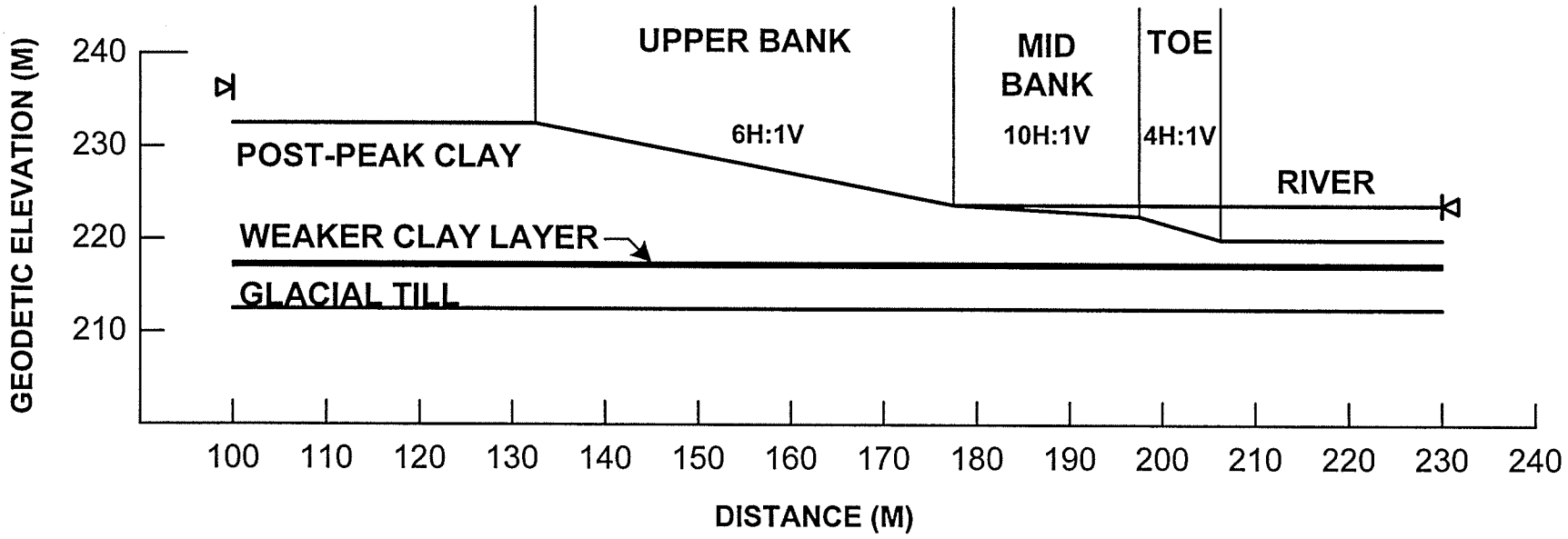

Figure 6.1 Cross section of a typical riverbank used in the numerical simulation (after Tutkaluk 2000)

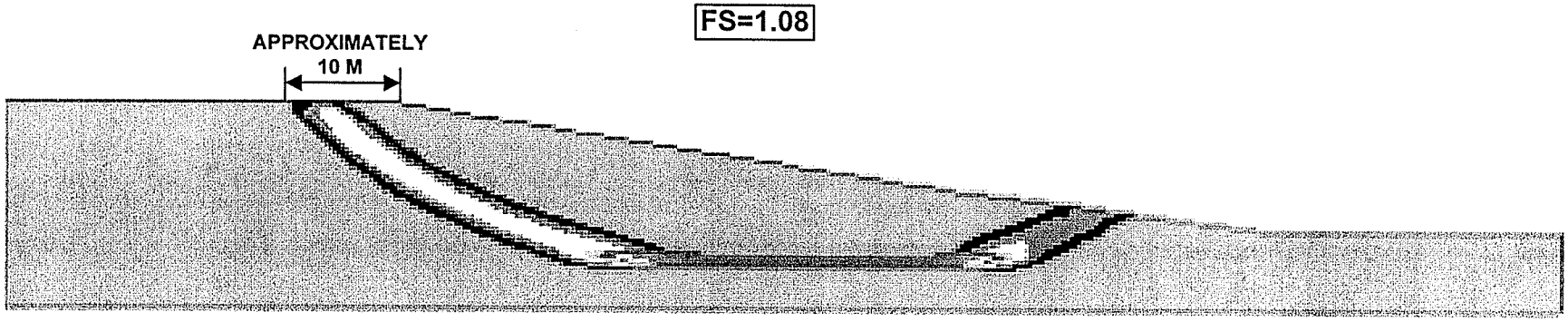

Figure 6.2 Shear strain contours showing the potential failure slip surface from FLAC/Slope simulation

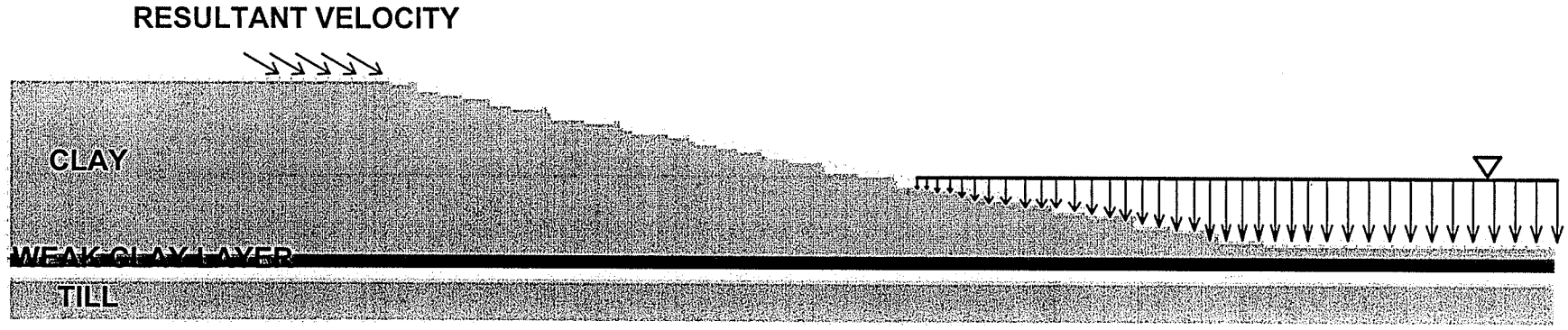

Figure 6.3 FLAC model of a natural riverbank after assigning material properties, vertical velocity and river water level

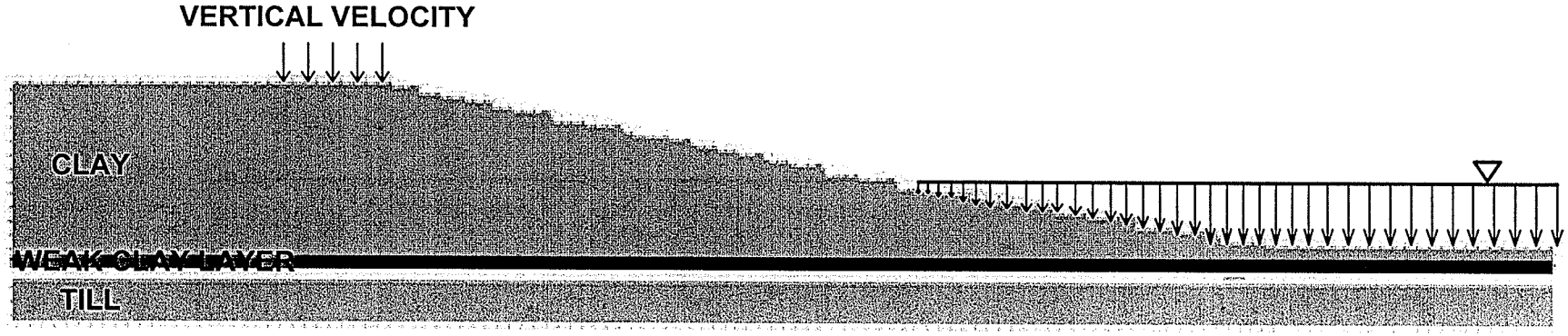

Figure 6.4 FLAC model of a natural riverbank after assigning material properties, vertical velocity and pressure

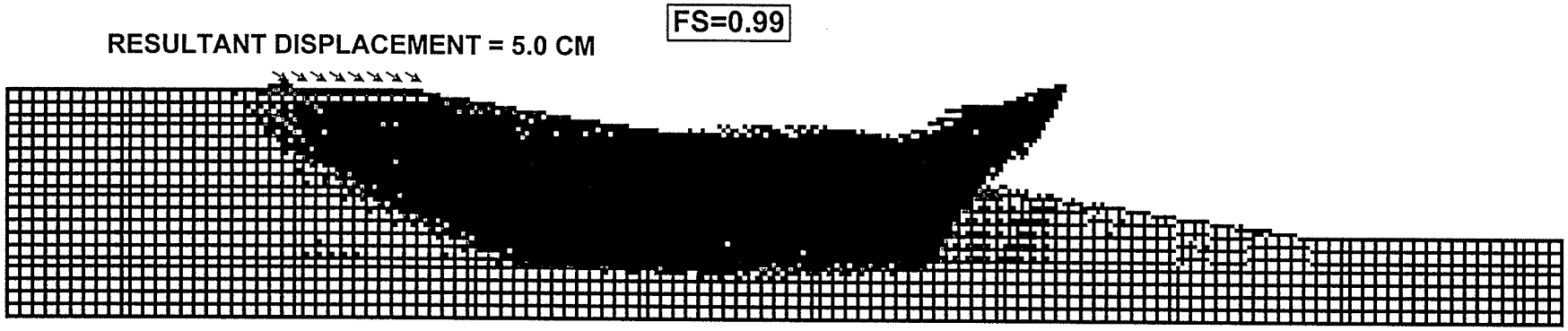

Figure 6.5 Magnified displacement vectors in a natural riverbank for applied inclined displacement equivalent to 5 cm using FLAC model

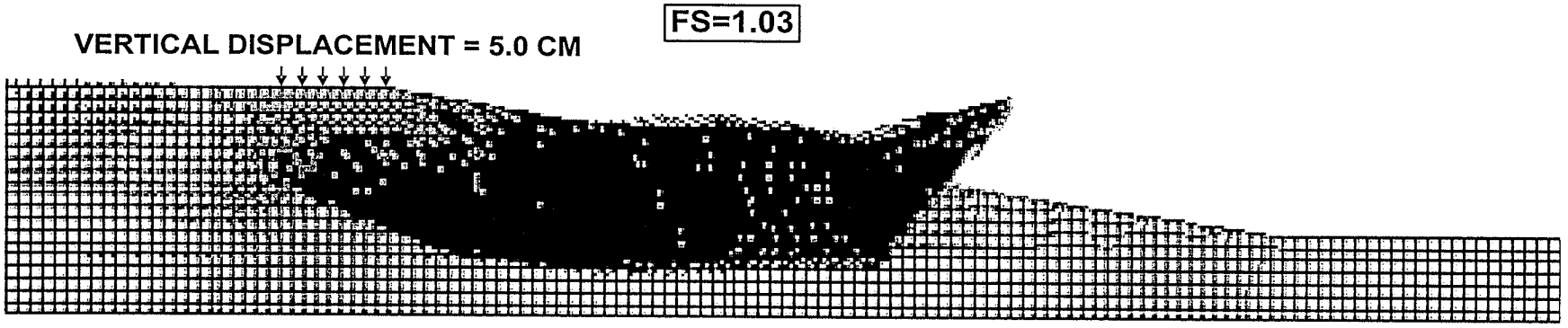

Figure 6.6 Magnified displacement vectors in a natural riverbank for applied vertical displacement equivalent to 5 cm using FLAC model

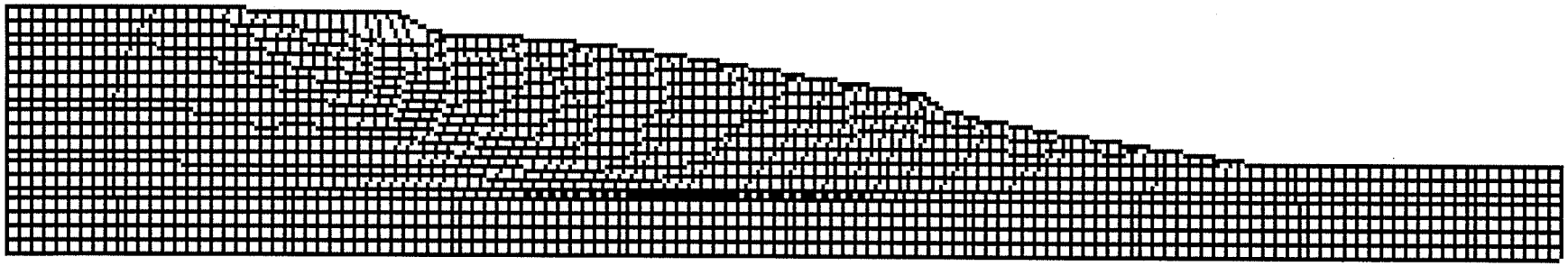

Figure 6.7 Deformed mesh for a natural riverbank at vertical displacement of 5 cm in FLAC model (magnification 20)

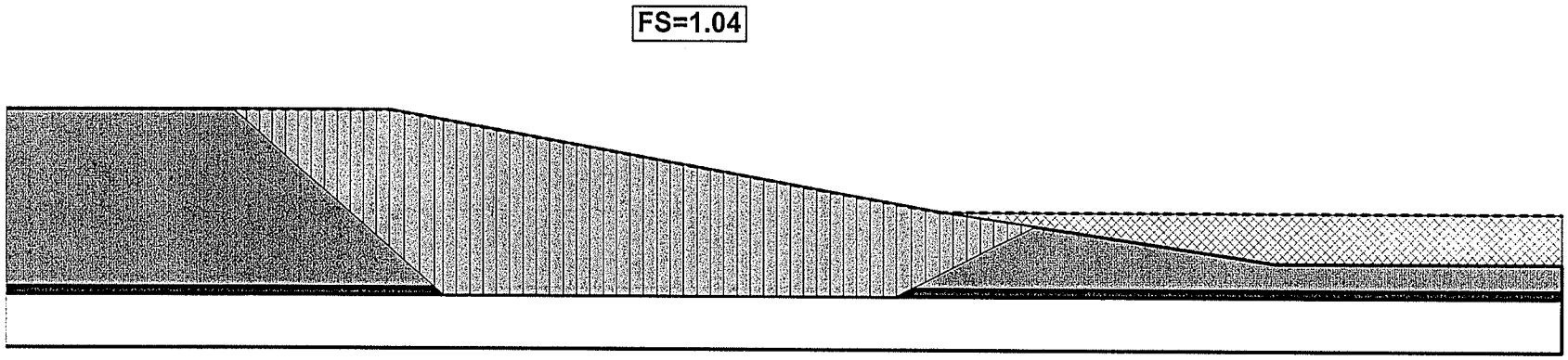

Figure 6.8 Location of slip surface from SLOPE/W associated with SEEP/W and SIGMA/W computer programs

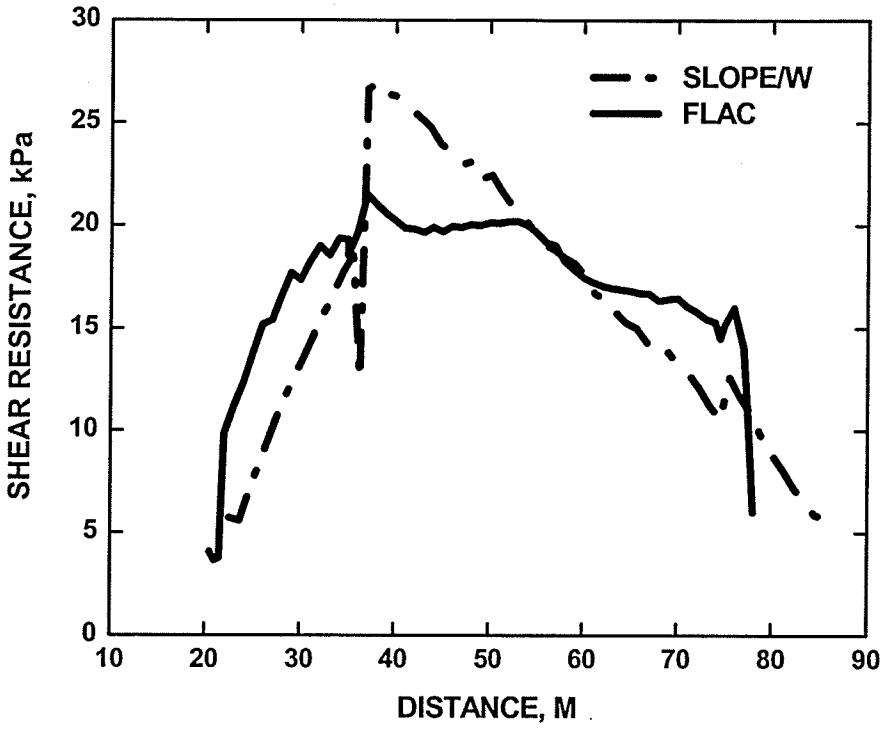

Figure 6.9 Comparison of shear stress distributions derived from FLAC and SLOPE/W programs

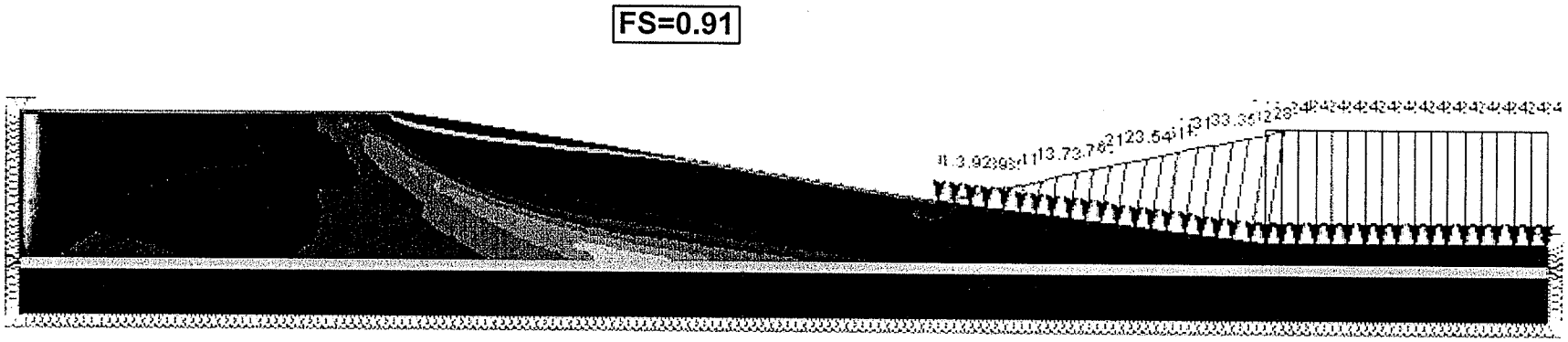

Figure 6.10 Shear strain contour and factor of safety obtained from Phase 2.0 model for a natural riverbank

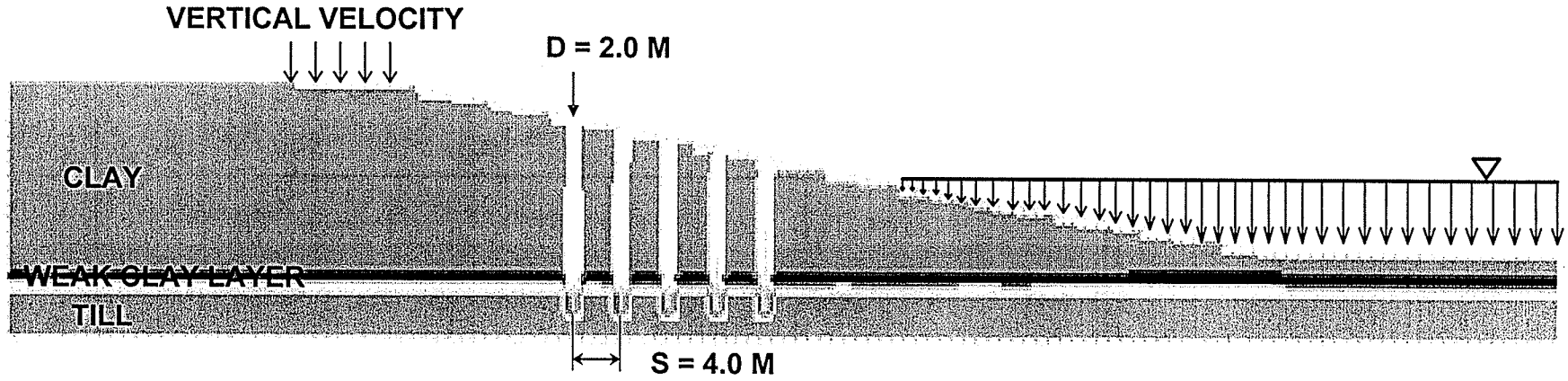

Figure 6.11 FLAC model of a stabilized riverbank showing the applied velocity at the crest (vertical displacement = 5 cm)

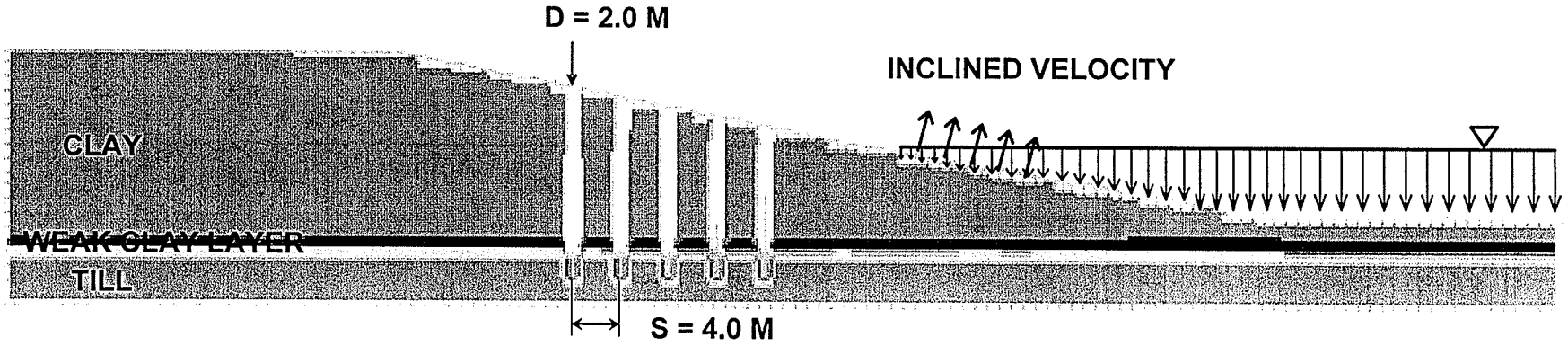

Figure 6.12 FLAC model of a stabilized riverbank showing the applied velocity at the toe (vertical displacement = 5 cm)

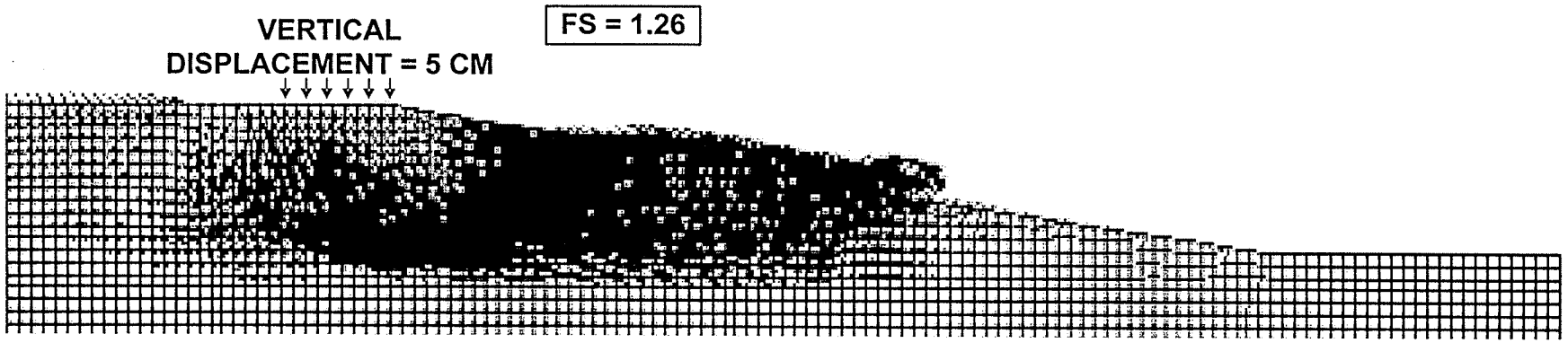

Figure 6.13 Magnified displacement vectors in stabilized riverbank for applied vertical displacement at the crest equivalent to 5 cm using FLAC model

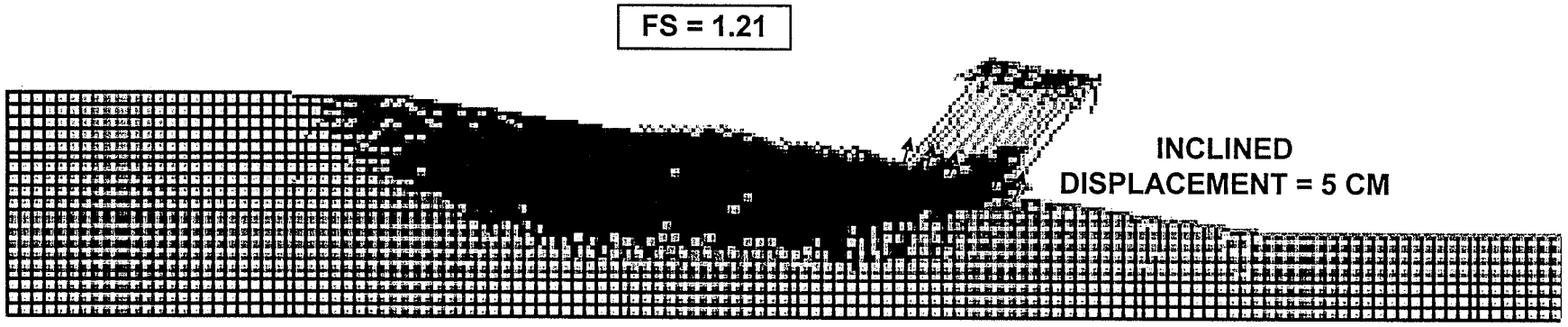

Figure 6.14 Magnified displacement vectors in stabilized riverbank for applied inclined displacement at the toe equivalent to 5 cm using FLAC model

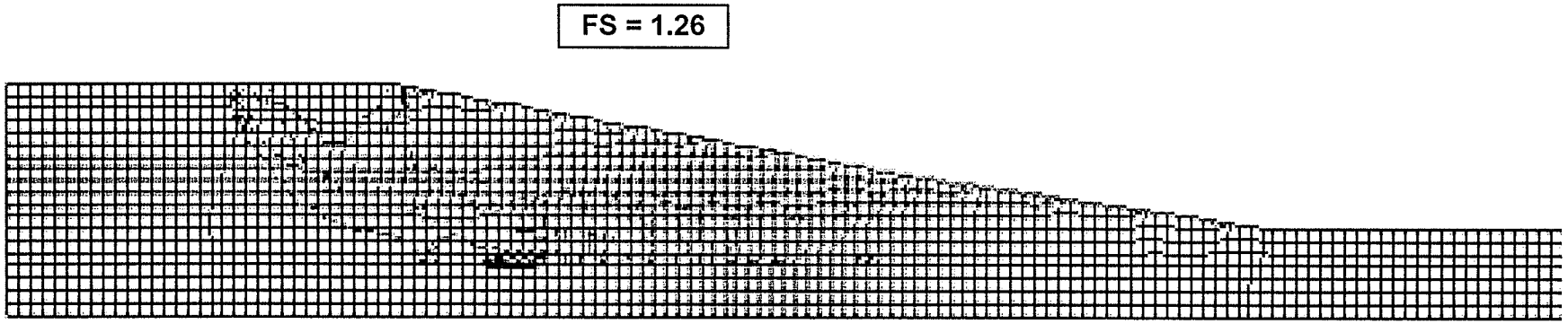

Figure 6.15 Shear strain contours indicating failure slip surface at vertical displacement at the crest equivalent to 5 cm in FLAC model for stabilized riverbank

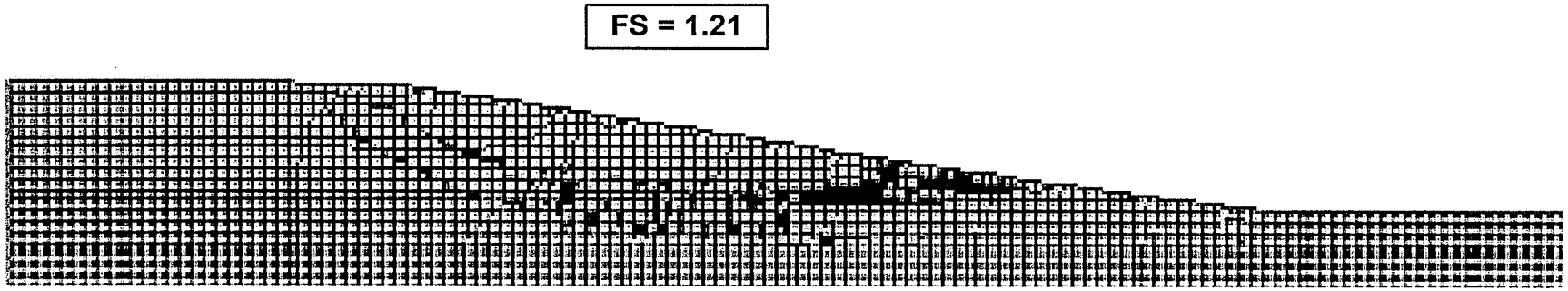

Figure 6.16 Shear strain contours indicating failure slip surface at vertical displacement at the toe equivalent to 5 cm in FLAC model for stabilized riverbank

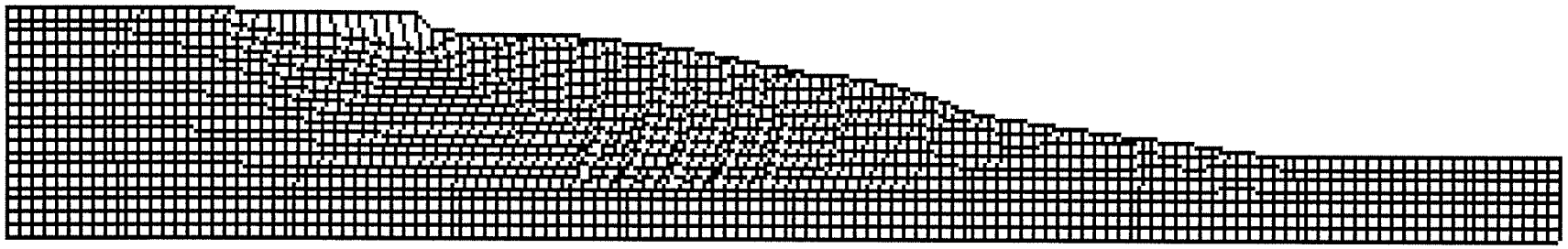

Figure 6.17 Deformed mesh of a stabilized riverbank for vertical displacement at the crest of 5 cm in FLAC model (magnification 20)

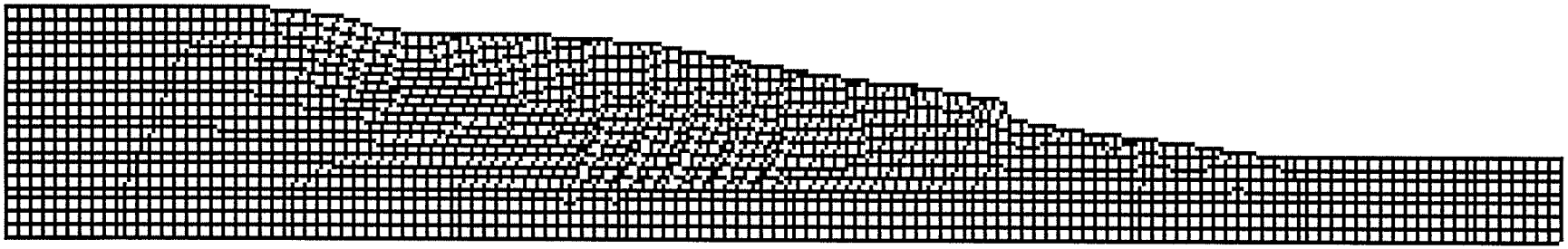

Figure 6.18 Deformed mesh of a stabilized riverbank for inclined displacement at the toe of 5 cm in FLAC model (magnification 20)

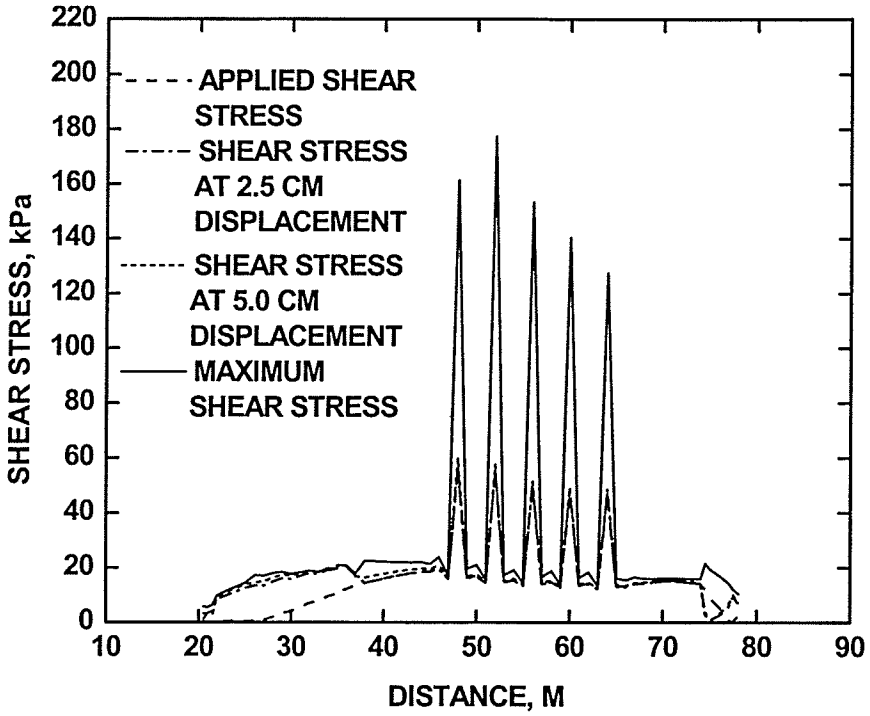

Figure 6.19 Comparison of shear stress distribution for a stabilized riverbank at different vertical displacements along the failure slip surface in FLAC

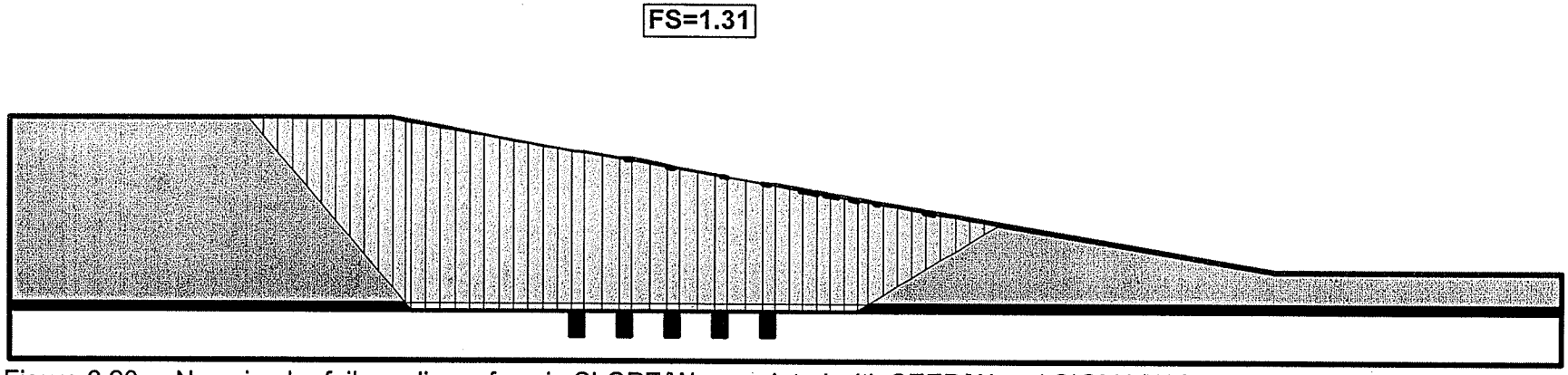

Figure 6.20 Non circular failure slip surface in SLOPE/W associated with SEEP/W and SIGMA/W for a stabilized riverbank

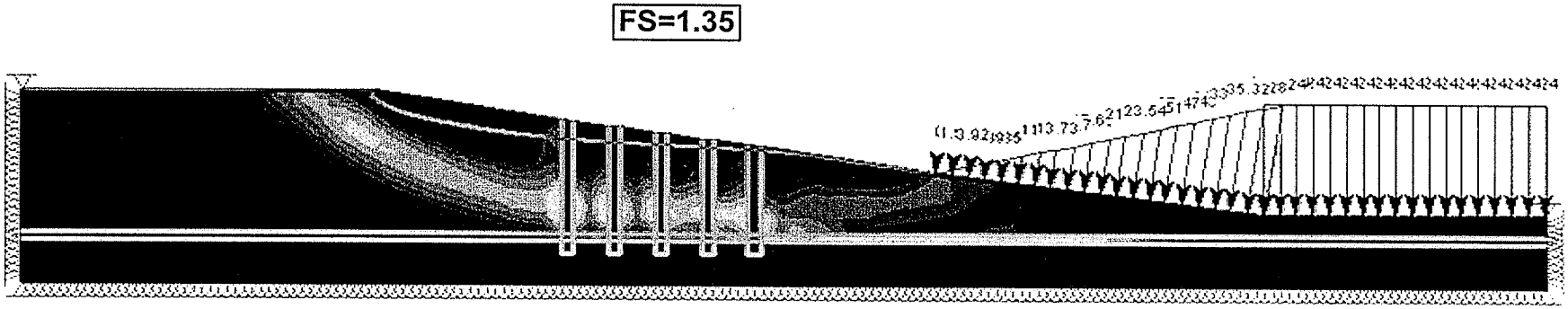

Figure 6.21 Shear strain contour obtained from Phase 2.0 model for a stabilized riverbank

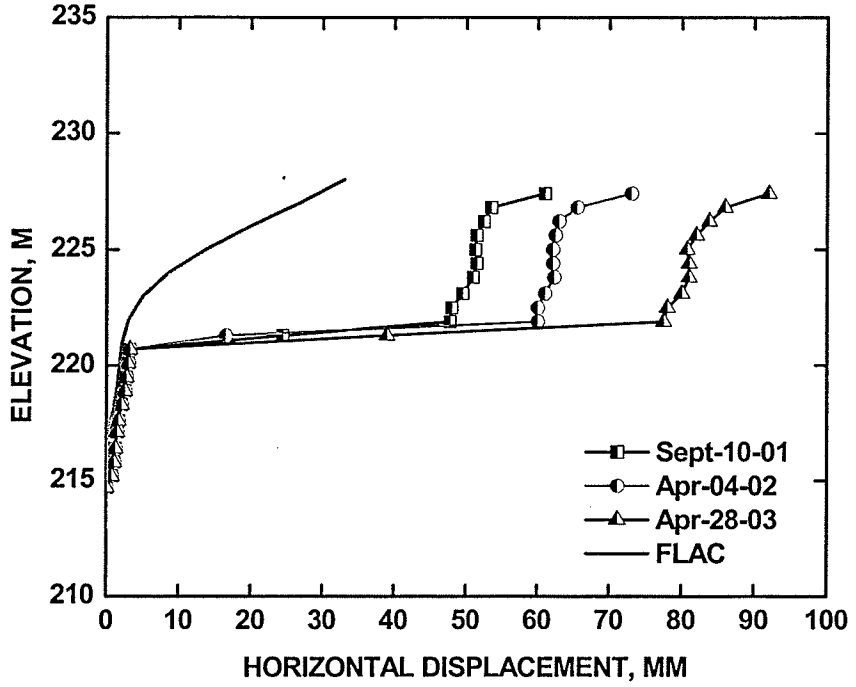

(a) Comparison of horizontal displacements from slope indicators at the site (after UMA-AECOM 2006) and from FLAC simulation (vertical velocity)

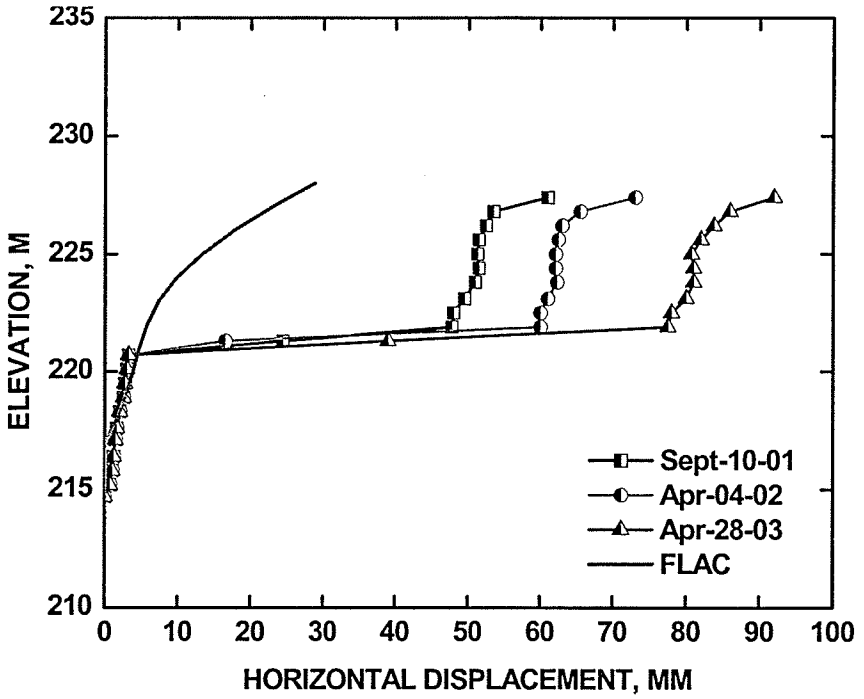

(b) Comparison of horizontal displacements from slope indicators at the site (after UMA-AECOM 2006) and from FLAC simulation (inclined velocity)

Figure 6.22 Horizontal displacements at riverbank crest with the application of 5 cm vertical displacement

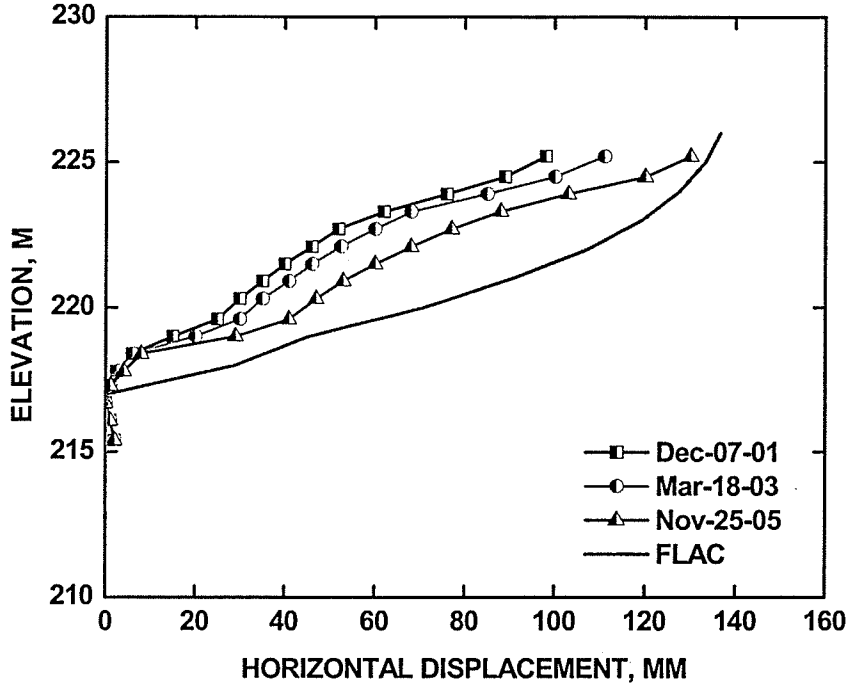

(a) Comparison of horizontal displacements from slope indicators at the site (after UMA-AECOM 2006) and from FLAC simulation (vertical velocity)

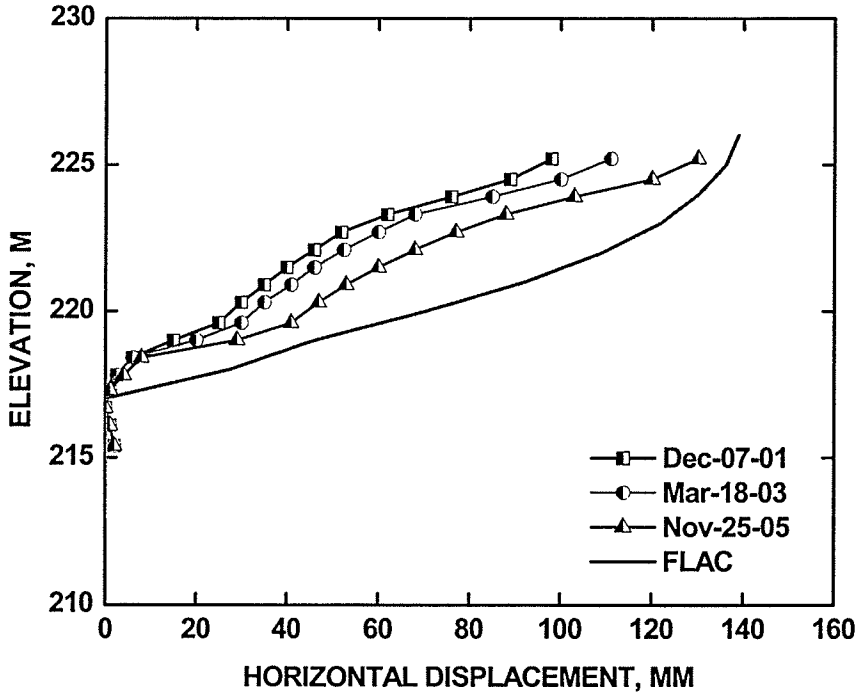

(b) Comparison of horizontal displacements from slope indicators at the site (after UMA-AECOM 2006) and from FLAC simulation (inclined velocity)

Figure 6.23 Horizontal displacements between rockfill columns with the application of 5 cm vertical displacement

Table 6.1 Material properties used in numerical simulation

Soil	Density, ρ, kg/m^3	Shear modulus, G, kPa	Bulk modulus, K, kPa	Cohesion, c, kPa	Friction, ϕ', °
Lacustrine clay	1733	3.57e3	16.7e3	4.0	15
Weak clay	1600	1.79e3	8.33e3	3.0	12
Till	2242	1e7	1e7	0	70*
Rockfill material	1898	8.4e3	14e3	0	50

* *Note:* This material was intentionally given high value of ϕ to force the slip surface not to pass through this layer.

CHAPTER 7

CONCLUSIONS, DISSCUSSION AND RECOMMENDATIONS

7.1 CONCLUSIONS

The main objective of this research was to provide an improved understanding about how much movement a stabilized riverbank has to undergo to obtain a desired shear resistance of the rockfill column. This was done by assessing the displacements required to mobilize shear resistance in rockfill columns, native clay and the rockfill-clay composite soil. The mobilization of shear resistance in cemented rockfill and different layouts of rockfill columns was also assessed. Finally, numerical simulations were carried out to asses the performance of the riverbank stabilized with rockfill columns.

Large-scale direct shear tests were conducted on rockfill materials, undisturbed clay, rockfill-clay composite soil samples including cemented rockfill columns, rockfill columns, and rockfill materials placed as shear key and rib layouts.

By using the FLAC computer program as a modelling platform, a numerical model was developed to simulate the experimental results obtained from large-scale direct shear tests. The model was then used to assess the performance of a typical riverbank stabilized with rockfill columns.

7.2 CONCLUSIONS FROM THE LABORATORY TESTING PROGRAM

1. Mobilization of shear resistance in rockfill columns is highly dependent on the relative density of the material and the applied normal stress.
2. During shearing, dilatancy of the rockfill material is greater at the backside of the shear box compared to the front in the direction of movement due to the progressive mobilization of shearing along the shear plain. This has implications in the comparison of the measured and simulated shear resistance with shear displacement (see Section 7.3.1, Item 2).
3. For rockfill materials, higher relative densities lead to higher shear resistances. The shear resistance in dense condition is almost twice as high as the loose condition at the same normal stress of 100 kPa.
4. Test results of both the native clay and composite soils show that mobilization of shear resistance in the rockfill column does not start until the peak strength of the clay is mobilized at about 2% shear strain.
5. The results for treated rockfill materials shows that the peak shear strength of the rockfill column using 0.5% cement content is increased, but the ultimate strength is almost the same as that of the untreated rockfill material. The shear stiffness for both 0.5% cemented and untreated rockfill columns is close at relatively small shear strain.
6. Tests on composite soils show that adding 5% of cement by weight to the rockfill column will increase the shear stiffness, but this has no effect on the ultimate shear resistance compared to an untreated rockfill column. This was due to the fact the former resulted in a different failure mechanism.
7. Tests on composite remolded soils show that increasing the area replacement ratio increases shear strength of the reinforced soils proportionally as expected. However, it has little impact on the shear stiffness.

8. For the same area replacement ratio, closed spacing of rockfill columns leads to slightly higher shear resistance compared to the opened spacing pattern. It even has a higher resistance than the shear key layout, probably due to the three-dimensional effect of the columnar layout. Rib layout of rockfill materials provides the highest shear resistance mobilization.
9. Installation of rockfill columns with and without casing has no significant difference on the stress-strain behaviour of the clay-rockfill composite.

7.3 CONCLUSIONS FROM THE NUMERICAL SIMULATION

7.3.1 Simulation of large-scale direct shear tests

1. For the loosely compacted rockfill material, the numerical simulation results fitted well with the results from the laboratory tests, except at much larger shear displacements where the numerical simulation slightly underpredicted the shear resistance.
2. For the densely compacted rockfill material, the numerical results faired well with the experiment results at smaller shear displacement, but underestimated the shear resistance at larger shear displacements due to the testing set up. The three-dimensional (3-D) geometry effect of the testing set up may have resulted in dilatancy being restrained near the edge due to the 3-D nature at the plane of shearing. This may be also true for Item 1 above where at large shear strains dilatancy was observed even for loose condition.

7.3.2 Simulation of typical riverbank stabilized with rockfill columns

1. The application of inclined and vertical velocities resulting in about 5 cm displacement on the crest of a natural riverbank was used to calculate the 'mobilized' factor of safety. Based on the conditions assumed in the numerical simulation, the safety factors are calculated as 0.99 and 1.03 for inclined and vertical displacements, respectively. With those displacements, the factor of safety is close to unity indicating failure in the riverbank or the shear resistance having been fully mobilized. The failure slip surfaces and factors of safety from other computer programs such as SLOPE/W in association with SEEP/W and SIGMA/W using limit equilibrium method of analysis and Phase 2.0 using the shear strength reduction method of analysis support the results of the FLAC numerical simulation.
2. The overall movement of the stabilized riverbank with the installation of 5 rows of rockfill columns was much less than that of the natural riverbank, particularly near the toe of the riverbank as well as in locations where rockfill columns were installed.
3. The stabilized riverbank has a mobilized factor of safety of about 1.26 corresponding to a vertical displacement of 5 cm at the crest, slightly less than that calculated by those assuming full mobilization of shear resistance. The factor of safety obtained from SLOPE/W in association with SIGMA/W and SEEP/W is about 1.31, and the corresponding value from Phase 2.0 is about 1.35.

7.4 RECOMMENDATIONS FOR FURTHER WORK

In this research, laboratory tests and numerical simulations were performed. This research has provided an improved understanding about the shear mobilization of

rockfill materials in the stabilized riverbank. There are areas identified that would probably benefit from additional study.

1. Triaxial tests for rockfill materials or composite samples can be conducted to obtain parameters that include information about pore water pressures during shearing. They will also provide a more accurate determination of shear stress-strain relationships.
2. For numerical simulation, seasonal piezometric conditions should be considered to investigate the effect on slope stability and see how the results would differ from the conclusions stated in the previous Section.
3. The loss of riverbank material at the toe due to erosion as opposed to only applying displacements should be simulated to assess how much loss would decrease the mobilized factor of safety.

REFERENCES

Abdulrazaq, W., Alfaro, M.C. and Blatz, J. 2006. *Effects of rock column geometry and layout for stabilizing natural riverbanks.* Sea to Sky Geotechnique, 415-421.

Alfaro, M.C., Miura, N. and Bergado, D.T. 1995. *Soil-geogrid reinforcement interaction by pullout and direct shear tests.* Geotechnical Testing Journal 18, (2), 157-167.

Alfaro, M.C. and Pathak, Y. (2005). *Dilatant Stresses at the Interface Between Granular Fills and Geogrid Strip Reinforcements*. Geosynthetics International 12:5, 239-252.

ASTM D421–85, 2000. *Standard practice for dry preparation of soil samples for particle-size analysis and determination of soil constants.* ASTM, Philadelphia, Pa., pp. 8-9.

ASTM D422–63, 2002. *Standard test method for particle-size analysis of soils*. ASTM, Philadelphia, Pa., pp. 10-17.

ASTM D4253–00, 2002. *Standard test methods for maximum index density and unit weight of soils using a vibratory table*. ASTM, Philadelphia, Pa., pp. 532-546.

ASTM D4254–00, 2002. *Standard test method for minimum index density and unit weight of soils and calculation of relative density.* ASTM, Philadelphia, Pa., pp. 547-555.

Atkinson, J. 1992. *An introduction to the mechanics of soils and foundations.* McGraw-Hill, Berkshire, England.

Baracos, A. 1960. *The stability of River Banks in the Metropolitan Winnipeg Area.* Proc. 14th Canadian Soil Mechanics Conference. NRCC Technical Memo. No. 69. 185-198.

Baracos, A. 1977. *Compositional and structural anisotropy of Winnipeg soils - a study based on scanning electron microscopy and X-ray diffraction analysis.* Canadian Geotechnical Journal, 14, 125-137.

Baracos, A. 1978. *The effects of River Levels, Groundwater and Other Seasonal Changes on River Banks in Winnipeg.* 31st Canadian Geotechnical Conference, Winnipeg, Manitoba.

Baracos, A. and Graham, J. 1981. *Landslide problems in Winnipeg.* Canadian. Geotechnical Journal, 18, 390-401.

Baracos, A., Graham, J. and Domaschuk, L. 1980. *Yielding and rupture in a lacustrine clay.* Canadian Geotechnical Journal, 17, 559-573.

Baracos, A., Graham, J., Kjartanson, B.H., and Shields, D.H. 1983b. *Geological Engineering Maps and Report for Urban Development of Winnipeg.* Geological Environment and Soil Properties. ASCE Convention, Houston, TX, October 1983, 39-56.

Bergado, D.T., Chai, J.C., Alfaro, M.C. and Balasubramaniam, A.S. 1994. *Improvement techniques of soft ground in subsiding and lowland environment.* A.A. Balkema, Brookfield, VT, USA.

British Standard BS 1377 1990. *Methods of test for soil for civil engineering purposes.*

Budhu, M. 2001. *Soil Mechanics & Foundations.* John Wiley & Sons, New York, NY, USA.

City of Winnipeg 2000. *Riverbank stability characterization study for city owned riverbanks.* Planning, Property and Development Department, City of Winnipeg, Winnipeg, MB, Canada.

Crawford, C.B. 1964. *Some Characteristics of Winnipeg Clay.* Canadian Geotechnical Journal, 1(4), 227-235.

Cala, M. and Flisiak, J. 2001. *Slope stability analysis with FLAC and limit equilibrium methods.* Proceedings of the 2nd international FLAC Symposium on Numerical Modeling in Geomechanics, 29(10), 113-114.

Duncan, J.M. and Wright S.G. 2005. *Soil strength and slope stability.* John Wiley & Sons, New York, NY, USA.

Dawson, E., Motamed, F., Nesarajah, S., and Roth, M. 2000. *Geotechnical Stability Analysis by Strength Reduction.* Slope Stability 2000, ASCE Geotechnical Special Publication, No.101. 99-103.

Duncan, J. M. 1996. *State of The Art: Limit Equilibrium and Finite-Element Analysis of Slopes.* Journal of Geotechnical Engineering, 122(7), 577-596

Fredlund, D.G. and Krahn, J. 1977. *Comparison of slope stability methods of analysis.* Canadian Geotechnical Journal, 14,429-439.

Freeman, W.S. and Sutherland, H.B. 1974. *Slope stability analysis in anisotropic Winnipeg clays.* Canadian Geotechnical Journal, 11(1), 59-71.

Goughnour, R.R., Sung, J.T. and Ramsey, J.S. 1990. *Slide correction by stone column. Deep Foundation Improvements: Design, Construction and Testing.* Bachus, R.E., Editor, ASTM STP 1089: 131-147.

Graham, J. 1979. *Embankment stability on anisotropic soft clays.* Canadian Geotechnical Journal, 16, 295-308

Graham, J. 1986. *Slope Stability Analysis: Applications in plastic clays.* 34th Annual Soil Mechanics and Foundation Engineering Conference, Minneapolis, MN.

Graham, J. and Au, V.C.S. 1985. *Effects of Freeze-Thaw and Softening on a Natural Clay at Low Stresses.* Canadian Geotechnical Journal, 22, 69-78.

Graham, J., Noonan, M.L. and Lew, K.V. 1983. *Yield states and stress-strain relationships in a natural plastic clay.* Canadian Geotechnical Journal, 20, 502-516.

Griffiths, D.V. and Lane, P.A. 1999. Slope Stability Analysis by Finite Elements. Geotechnique, 49,387-403.

Gupta, K. K., Ramamurthy, T. and Venkatachalam, K. 1995. *Stress-strain response and volume changes of rockfills.* Water and Energy 2001, International R&D Conference, New Delhi, India: pp. 416-427.

Itasca. 2005. *FLAC – Fast Lagrangian Analysis of Continua*. Minneapolis, USA.

Loh, A.K. and Holt, R.T. 1974. *Directional Variation in Undrained Shear Strength and Fabric of Winnipeg Upper Brown Clay*. Canadian Geotechnical Journal, 11, 430-437.

Matsui, T. and Ka-Ching, San. 1992. Finite *Element Slope Stability Analysis by Shear Strength Reduction Technique.* Soils and Foundations, 32(1), 59-70.

Mesri, G. and Huvaj, N. 2004. *Residual shear strength mobilized in Red River slope failures.* Proc. of the Ninth International Symposium on Landslides, Rio de Janeiro, Brazil.

Mishtak, J. 1964. *Soil mechanics aspects of the Red River Floodway*. Canadian Geotechnical Journal, 1(3), 133-146.

Quigley, R.M. 1968. Soil mineralogy, Winnipeg swelling clays. Canadian Geotechnical Journal, 5: 120-122.

Ramamurthy, T, T., and Gupta, K. K. 1980 *Prediction of the Behaviour of Rockfill Materials.* Environmental Conference. Proceedings of the Technical Association of the Pulp and Paper Industry, 1, p1.13 - 1.18.

Swan, C.C. and Seo, Young-Seo. 1999. *Slope Stability Analysis Using Finite Techniques.* 13th Iowa ASCE Geotechnical Conference, Williamsburg, Iowa.

Tallin, J., 2006. *Branch 1 Aqueduct Seine River Siphon Riverbank Monitoring.* Unpublished report to Water and Waste department, The City of Winnipeg, MB.

Teller, J.T. 1976. *Lake Agassiz deposits in the main offshore basin of southern Manitoba.* Canadian Journal of Earth Sciences, 13, 27-43.

Tutkaluk, J. M. 2000. *The effect of seasonal variiations in the Red river and upper carbonate aquifer on the riverbank stability in Winnipeg.* M.Sc. thesis, Department of Civil Engineering, University of Manitoba, Winnipeg, MB.

Tweedie, R., Clementino, R., Papanicolas, D., Skirrow, R. and Moser, G. 2004. *Stabilization of a highway embankment fill over an arch culvert using stone columns.* Proceedings of the 57th Canadian Geotechnical Conference , Quebec, Quebec, Canada.

Yarechewski, D. and Tallin, J. 2003. Riverbank *stabilization performance with rock-filled ribs/shear key and columns.* Proceedings of the 56th Canadian Geotechnical Conference, Winnipeg, Manitoba, Canada.

Varadarajan, A, A., Sharma, K.G., Venkatachalam, K., and Gupta, A. K. 2003. *Testing and Modeling Two Rockfill Materials.* Journal of geotechnical and geoenvironmental engineering, 129, No 3, 206-218.